UCLA
UCLA Electronic Theses and Dissertations

Title
Characterization of Rheb Signaling in Cancer and Disease

Permalink
https://escholarship.org/uc/item/9717z2w8

Author
Heard, Jeff Heard

Publication Date
2017

Peer reviewed|Thesis/dissertation

eScholarship.org Powered by the California Digital Library
University of California

UNIVERSITY OF CALIFORNIA

Los Angeles

Characterization of Rheb Signaling in Cancer and Disease

A dissertation submitted in partial satisfaction of the

requirements for the degree Doctor of Philosophy

in Microbiology, Immunology, and Molecular Genetics

by

Jeffrey James Heard

2017

ABSTRACT OF THE DISSERTATION

Characterization of Rheb Signaling in Cancer and Disease

by

Jeffrey James Heard

Doctor of Philosophy in Microbiology, Immunology, and Molecular Genetics

University of California, Los Angeles, 2017

Professor Fuyuhiko Tamanoi, Chair

Ras homolog enriched in brain (RHEB) is a member of the Ras superfamily of small GTPases that are responsible for the activation of numerous diverse cellular pathways in the cell. Rheb directly activates mTORC1, a crucial signaling pathway that stimulates protein synthesis and cell proliferation. Aberrant Rheb/mTORC1 signaling has been linked to many diseases including cancer. Unfortunately, mTORC1 inhibitors often display only partial antitumor activity, with tumor regrowth upon discontinuation of the drugs. Some reports suggest Rheb may have mTORC1-indpendent functions, but studies to identify additional Rheb effector proteins are lacking.

The aim of this dissertation is to identify new effector proteins of Rheb, and characterize the signaling pathways affected by Rheb interaction with these proteins. To accomplish this, I employ various biochemical techniques. The main approach in identifying new effector proteins is to look for proteins that do not interact with Rheb effector domain mutants, show similar co-localization with Rheb, and whose function is altered upon Rheb interaction.

In this dissertation I present results identifying four different effector proteins of Rheb, and explore the biological relevance of these interactions. First I confirm Rheb interaction with mTOR

and TSC. Second, I show a novel interaction between Rheb and CAD, the protein responsible for carrying out the first three enzymatic steps in *de novo* pyrimidine biosynthesis. In this section I present results demonstrating Rheb stimulates pyrimidine biosynthesis through CAD. Third, I show Rheb interaction with AMPK, a kinase complex that shuts down cell growth and proliferation. Fourth, I show RHEB interaction with BRAF that results in the inhibition of the MAPK pathway. In this section I identify a RHEB mutation from cancer genome database analysis, and demonstrate its ability to transform normal cells into cancer cells through stimulation of the RAF/MEK/ERK signaling pathway.

In conclusion, this dissertation identifies new effector proteins of Rheb and significantly expands our current knowledge of Rheb signaling.

The dissertation of Jeffrey James Heard is approved.

Donald B. Kohn

April D. Pyle

Daniel T. Kamei

Fuyuhiko Tamanoi, Committee Chair

University of California, Los Angeles

2017

DEDICATION

I dedicate this dissertation to my incredible wife Lindsey, my loving and supportive parents Bryan and Cheryl, my brother Kyle, my sister Kelly, my grandparents Janice, Lynn, Julia, and Jim, and to the most loyal and happy dog Willow.

TABLE OF CONTENTS

LIST OF FIGURES

ACKNOWLEDGEMENTS

First and foremost, I would like to thank my wife, Lindsey, for all of her love and support. I would have never been able to complete this dissertation without her patience, guidance, and infectious sense of humor. She has provided me with a happy and stable home that has made my life as a graduate student so much more enjoyable. I also have to thank her for allowing me to get a dog, in Los Angeles, while living in an apartment. Willow brings a smile to my face every time I come home and has been excellent therapy on tough scientific days.

I also must thank my family for the advice and wisdom they have provided me throughout my life. My parents, Bryan and Cheryl, have been extremely patient listeners. They have listened to me through my most exciting and my most stressful times in graduate school. Their calm and wise guidance is a big reason why I am able to be as successful as I am today. I also blame them for my passion for science, as my Dad is an engineer and my Mom a biologist. My brother, Kyle, has been my go to source for distractions, including long discussions on Game of Thrones, the newest superhero movies, and the best Netflix shows. I have also been fortunate enough to have weekly lunches with my sister, Kelly, who is an undergraduate at UCLA. She is always a blast to hang out with and keeps me up-to-date on what undergraduates think is “cool.”

I would also like to thank my friends, who have supported me throughout my life. I have been fortunate enough to be surrounded by loyal, loving, and supportive friends, many of which I have had since childhood. Whether we were camping, snowboarding, or hanging out a bar, my friends have provided me with many wonderful memories and much-needed distractions from work life.

I would like to thank my mentor, Dr. Fuyuhiko Tamanoi for his advice and support throughout my graduate school career. He encouraged my ideas and let me explore different areas of signal transduction. He guided and pushed me when needed, but also provided me with the opportunity to become an independent scientist and allowed my critical thinking skills to flourish. I would not have been able to complete this dissertation without him. I would also like to

thank my committee, Dr. Donald Kohn, Dr. April Pyle, Dr. Joseph Loo, and Dr. Daniel Kamei for their advice and ideas that helped strengthen and improve the work in this dissertation.

Next I would like to thank the other members of the Tamanoi laboratory, both past and present, for providing me with help, suggestions, and answers to all questions ranging from experiments to graduate school to life. In this laboratory, I have had the unique opportunity to make relationships with people from all over the world including Japan, Vietnam, Taiwan, and Iran. This has strengthened my skills as a scientist by opening my eyes to alternative ways of thinking from around the world.

I would also like to thank the UCLA Biotechnology Training Grant, as it provided me with two years of funding and several unique opportunities not available to most graduate students. These opportunities included organizing and leading a conference at UCLA for the Biotechnology Training Grant, as well as the chance to work as a summer intern at a biotechnology company for one quarter. This helped confirm my aspirations of entering industry research, gave me an incredible opportunity to network, and added new techniques to my toolbox. I would also like to thank the UCLA Dissertation Year Fellowship, as it provided me with the funding to complete my final year of research.

VITA

Education

B.S., Molecular, Cellular, and Developmental Biology — Seattle, WA
University of Washington — June 2010

Research Experience

Doctoral Research – University of California, Los Angeles — 2012 – Present
Graduate Student with Dr. Fuyuhiko Tamanoi
Thesis title: Characterizing Rheb, an important member of the Ras superfamily of oncoproteins

R&D Internship – Kite Pharma, Santa Monica CA — June – September 2016
Intern under Dr. Ruben Rodriguez, Principal Scientist

Research Scientist – University of Washington, Seattle — 2010 – 2012
Researcher with Dr. Michael Bamshad

Undergraduate Researcher - University of Washington, Seattle — 2009-2010
Researcher with Dr. Lee Ann Campbell

Leadership Experience

UCLA Biotechnology Symposium Coordinator — June 2nd 2016

Head Teaching Assistant – Intro to Molecular Biology (Life Sciences 3), UCLA — Spring 2015

Teaching Assistant – Introductory Microbiology (MIMG 101), UCLA — Fall 2013

Awards

Dissertation Year Fellowship — September 2016 – June 2017

NIH-UCLA Biotechnology Training Grant — June 2014 – June 2016
NIH# T32 GM067555-11: $40,000 in external funding

MIMG Teaching Assistant of the Year Nomination — 2014-2015

Publications & Presentations

J.J. Heard, I. Phung, M. Potes, and F. Tamanoi. “Rheb Y35N cancer mutation drives oncogenic transformation through increased B-Raf dimerization.” Manuscript in preparation.

J. J. Heard and F. Tamanoi, “GTP-Binding Protein Rheb,” in *Encyclopedia of Signaling Molecules*, S. Choi, Ed. New York, NY: Springer New York, 2017, pp. 1–6.

J.J. Heard, I. Phung, M. Potes, and F. Tamanoi. “Rheb GTPase Mutation Drives Cancer Transformation.” Presented at UCLA Molecular Biology Institute Annual Symposium. Ventura, CA. April 2017.

J.J. Heard. “Identification of a New Target for RHEB GTPase - AMPK.” Presented at UCLA Biotechnology Training in Biomedical Sciences and Engineering Symposium. Los Angeles, CA. June 2, 2016

T. Sato, H. Akasu, W. Shimono, C. Matsu, Y. Fujiwara, Y. Shibagaki, **J. J. Heard**, F. Tamanoi, and S. Hattori, “Rheb protein binds CAD (carbamoyl-phosphate synthetase 2, aspartate transcarbamoylase, and dihydroorotase) protein in a GTP- and effector domain-dependent manner and influences its cellular localization and carbamoyl-phosphate synthetase (CPSase) activity,” J. Biol. Chem., vol. 290, no. 2, pp. 1096–1105, Jan. 2015.

J. J. Heard, V. Fong, S. Z. Bathaie, and F. Tamanoi, “Recent progress in the study of the Rheb family GTPases.,” Cell. Signal., vol. 26, no. 9, pp. 1950–1957, May 2014.

L.A. Campbell, M.W. Berry, **J.J. Heard**, M.E. Rosenfeld, and C.-C. Kuo. “*Chlamydia pneumoniae* induces expression of the scavenger receptor LOX-1 and proatherogenic factors in C56BL/6H mice.” pp. 161-164. *Chlamydial Infections: Proceedings of the Twelfth International Symposium on Human Chlamydial Infection.* Schachter, J. et al. eds. Hof bei Salzburg, Austria. June 2010.

CHAPTER 1:

BACKGROUND

Ras homolog enriched in brain (Rheb)

Ras homolog enriched in brain (Rheb) was first discovered as a gene induced by increased synaptic activity in neuronal cells and after seizures in the hippocampus [1]. Although originally identified as being enriched in brain tissue, it has since been shown to have a ubiquitous expression profile across all mammalian tissues [2]. Rheb shares strong homology with the Ras superfamily of small GTPases. These proteins act as molecular switches in the cell, alternating between GTP-bound ("on") and GDP-bound ("off") states in response to environmental signals (Figure 1.1).

Rheb is highly conserved in eukaryotes from yeast to human, although it is not found in plants. Lower eukaryotes from yeast to Drosophila contain only one Rheb gene, however, mammalian cells contain two different Rheb genes, Rheb1 and Rheb2 (RhebL1). They share 50% amino acid similarity, but their tissue expression profiles appear different. Rheb1 is expressed ubiquitously while Rheb2 expression is more limited to the brain [3]. To date, most studies have looked at Rheb1. While similar functions are suggested, lack of Rheb2 characterization diminishes our knowledge of any potential differences between Rheb1 and Rheb2.

Figure 1.1: Rheb Acts as a Molecular Switch

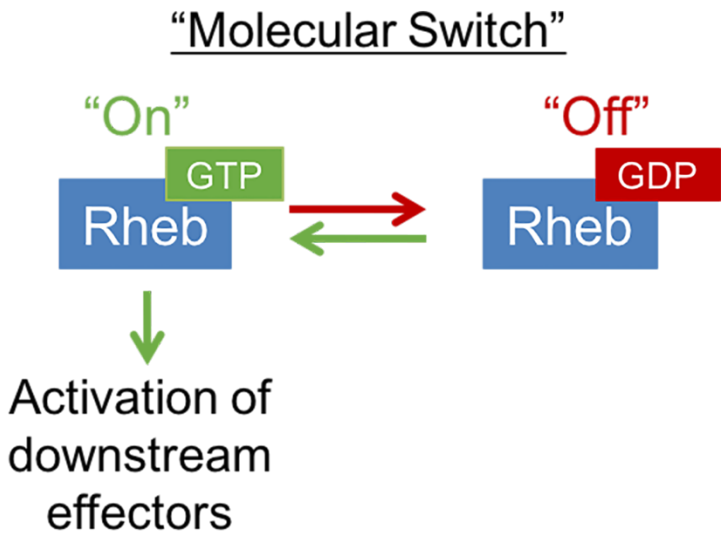

Rheb is a member of the Ras superfamily of small GTPases. They are termed "molecular switches" in the cell because they switch between GTP-bound "on" state and GDP-bound "off" state. When GTP-bound "on", they activate downstream effectors.

Structure of Rheb

RHEB is a 184 amino acid, 21kDa protein. The N-terminal 169 amino acids make up the GTPase domain. This region contains five G-boxes, nucleotide sequences that interact with guanine nucleotides (Figure 1.2). This region also contains two switch regions (Switch I and Switch II), surface loops that undergo significant conformational changes between GDP and GTP bound states. These shifts in conformation control the affinity of RHEB towards effector proteins. The Rheb effector domain lies within the Switch I region, and is the site where Rheb interacts with its downstream proteins. The 15 remaining C-terminal residues make up a highly variable region ending in a -CAAX domain (where C is cysteine, A is amphipathic amino acid, and X is any amino acid). Post-translational modification of this CAAX domain is required for proper RHEB localization in cells, as discussed in later sections.

Despite strong similarities in amino acid sequence, Rheb has low intrinsic GTPase activity compared with Ras, and exists at predominantly higher GTP-bound levels [4]. The crystal structures of Rheb bound GTP and bound GDP reveal several important differences between Rheb and other small GTPases [5]. The important difference in both amino acid sequence, and structure, involves the switch II region. The switch II region of Rheb is in an unraveled conformation rather than the usual α-helical conformation of Ras, and the structure undergoes little change between GTP bound and GDP bound states. In addition, there are major differences between Rheb and Ras in the orientation of two highly conserved amino acids. A conserved glutamine residue (Gln64 in Rheb and Gln61 in Ras) participates in GTP hydrolysis in Ras, however this residue is buried in a hydrophobic core in Rheb. This prevents glutamine interaction with either GTP or the catalytic active site. Another unique element to Rheb, is that a conserved tyrosine residue (Tyr35 in Rheb, Tyr32 in Ras) blocks access to the GTP from a possible GAP (GTPase-Activating Protein) arginine finger [6]. These two structural elements provide possible explanations for why Rheb has low intrinsic GTPase activity and has higher GTP bound levels in the cell to compare other small GTPases.

Figure 1.2: RHEB Structure

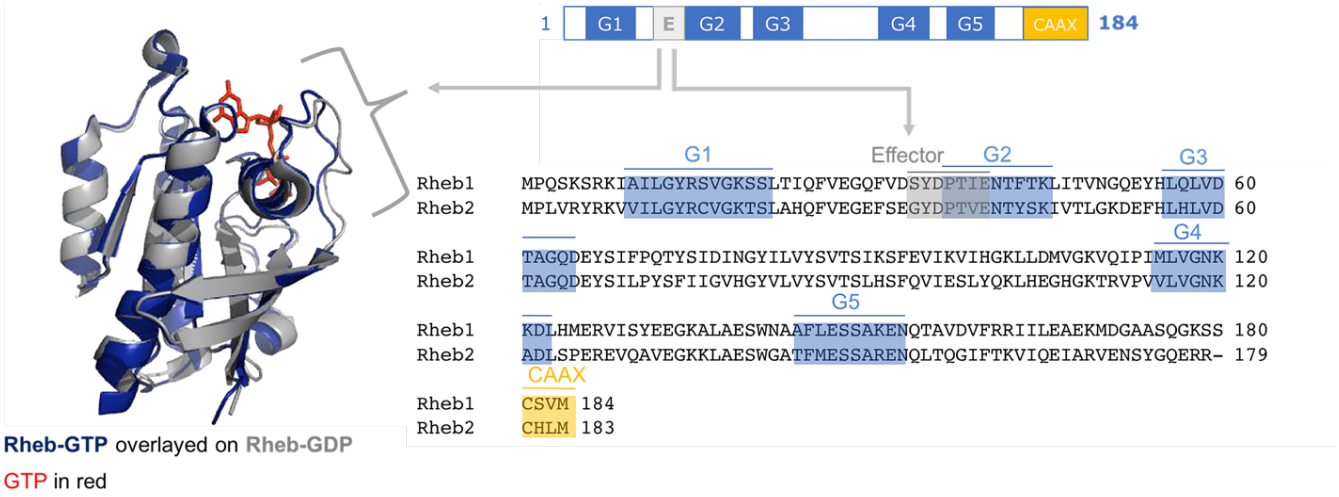

(*Left*) The crystal structure of RHEB bound GTP (blue) is structurally aligned with RHEB bound GDP (gray). The location of GTP (red) is shown in the guanine nucleotide binding pocket of Rheb crystal structure. (*Right*) Amino acid sequences from RHEB1 (184 AA) and RHEB2 (183 AA) are aligned, with highly conserved regions highlighted (G-boxes in blue, effector domain in gray, and CAAX box in yellow). Arrows point to the effector domain (E) on the crystal structure and on the amino acid sequences.

Rheb activates the mTORC1 signaling pathway

Rheb stimulates cell growth and proliferation through direct activation of the mechanistic target of the rapamycin complex 1 (mTORC1) signaling pathway (Figure 1.3) [7], [8]. mTORC1 is a protein complex consisting of the serine/threonine kinase target of rapamycin (mTOR), regulatory-associated protein of mTOR (RAPTOR), mammalian lethal with SEC12 protein 8 (MLST8), proline-rich AKT1 Substrate 1 (PRAS40) and DEP domain-containing mTOR-interacting protein (DEPTOR). mTORC1 is activated through insulin binding its receptor at the cell surface, resulting in activation of PI3K and subsequent activation of AKT. AKT phosphorylates and inhibits the GTPase-Activating Protein (GAP) for Rheb (see TSC section below), thus keeping Rheb GTP-bound and activating mTORC1. mTORC1 then phosphorylates several downstream targets, most notably pS6K and 4E-BP1, resulting in an increase in protein synthesis and progression of the cell cycle [9]. This pathway is one of the most important pathways for increasing cell proliferation in response to increased growth factors, and has been linked to many diseases.

Tuberous sclerosis complex (TSC) is the GAP protein for Rheb

Rheb has relatively low intrinsic GTPase activity, and therefor requires the help of a GTPase-Activating Protein (GAP) to switch from a GTP to GDP bound state. The GAP for Rheb was identified as the tuberous sclerosis complex (TSC) [10], [11]. TSC is a trimeric protein consisting of the proteins TSC1, TSC2 and TBC1D7. TSC is named after the disease tuberous sclerosis, which arises from inactivating mutations in *TSC1* or *TSC2* genes and resulting in high Rheb-GTP levels and over-activation of mTORC1 [12]. TSC is controlled by several upstream kinases in response to nutrient levels in the cell. Growth factors activate AKT, which in turn phosphorylates and inhibits TSC. In contrast, low energy in cells (i.e. a high ratio of AMP to ATP) activates AMPK, which in turn phosphorylates and activates TSC to shutdown Rheb/mTORC1 activity.

Figure 1.3: Rheb Signaling

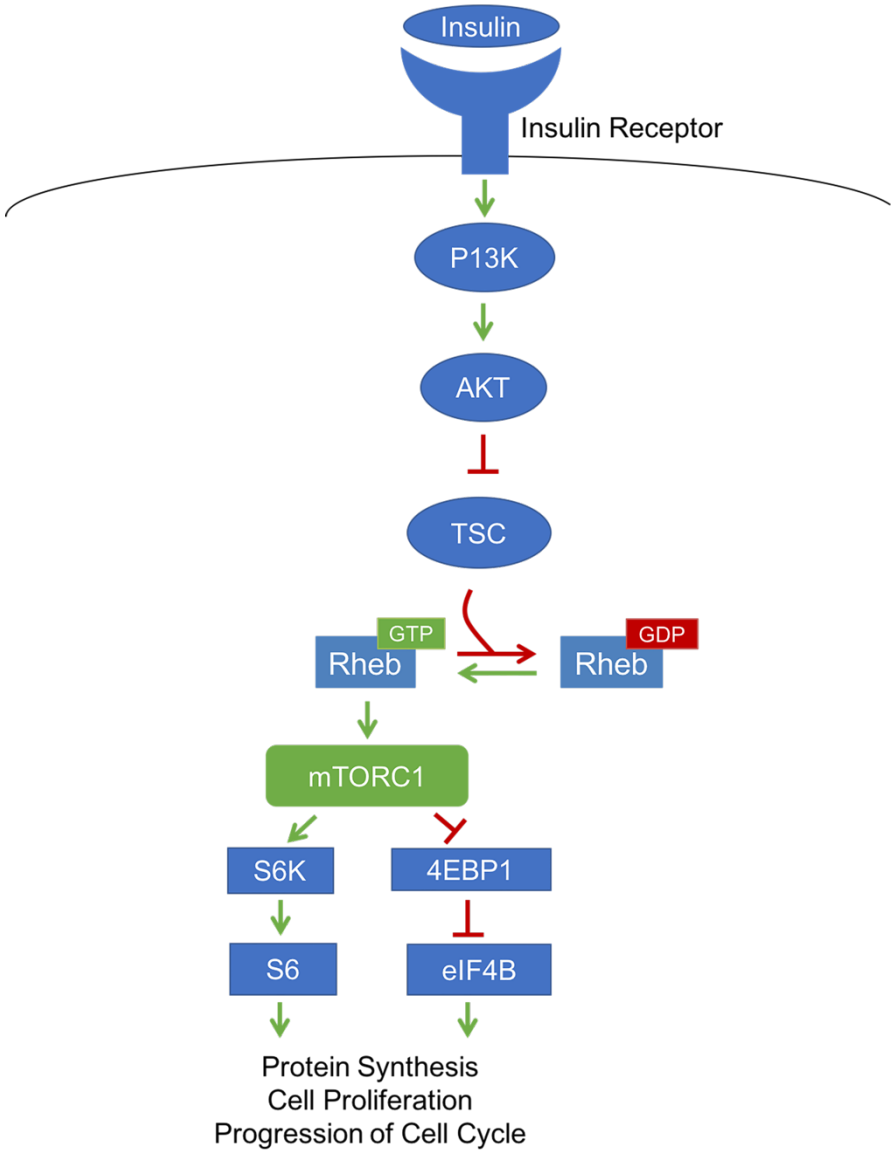

Canonical Rheb signaling activates mTORC1 pathway. Insulin binding the insulin receptor on the cell membrane begins the signal transduction pathway by activating the PI3K kinase, which phosphorylates and activates AKT kinase, which in turn phosphorylates and inhibits TSC. This results in higher Rheb GTP levels, which stimulates mTORC1 activity, and a subsequent increase in protein synthesis, cell proliferation and progression of cell cycle.

Rheb in Disease

Many proliferative diseases have been linked to overactived Rheb/mTORC1 signaling, including Peutz-Jeghers syndrome (PJS), Lymphangioleiomyomatosis (LAM), and Tuberous Sclerosis (TS). Symptoms of these disease involve appearance of benign tumors all over the body which can result in dangerous complications including bowl obstruction, lymphatic obstruction, and seizures [13]–[15]. These diseases arise when mutations in TSC1 or TSC2 result in inactivation of TSC function, leading to overactivation of Rheb/mTORC1. However, treatment of these diseases with mTORC1 inhibitors have only limited antitumor effects, indicating that Rheb may play a role in these diseases independent of, or in addition to, mTORC1 activation [16], [17].

Rheb has also been linked to cancer. Analysis of cancer genomic databases has revealed that amplification of Rheb is associated with the development of skin epithelial carcinogenesis including breast cancer and head and neck cancer [18]. In addition, a reoccurring mutation in Rheb (Y35N) has been found in three patients with clear cell renal cell carcinoma and two patents with endometrial cancers [19].

Important Rheb mutations

A variety of Rheb mutants have been identified that result in both activation and loss-of-function of Rheb (Table 1.4). The most well studied and utilized activating mutant is Q64L, as it has been reported to exhibit increased basal GTP levels and more strongly activate mTORC1 [11]. Another activating mutant, G63A, was discovered through systematic amino acid mutations in the G3-box [20]. The G63A mutant results in decreased GTPase activity and shows decreased sensitivity towards TSC2-GAP mediated GTPase activity. These attributes correspond with higher GTP-bound Rheb and stronger activation of mTORC1.

Recently an important functional mutation in Rheb was discovered at Tyr35 [6]. A mutation of this residue to alanine (Y35A) results in the increase of intrinsic GTPase activity and a decrease in RHEB-GTP levels. GTP hydrolysis in Rheb requires Asp65 from the switch II region, and it was

discovered that Tyr35 normally blocks access of Asp65 to the nucleotide binding pocket. The Y35A mutation results in increased accessibility of Asp65 to the nucleotide binding pocket, thus increasing GTP hydrolysis. As mentioned previously, a reoccurring Y35N mutation was discovered in cancer genomic databases. Interestingly, the Y35N mutant was found to have the opposite effect as Y35A, by showing increased activation of the mTORC1 pathway [21].

A previous publication reported additional key Rheb mutants by carrying out random mutagenesis of Rheb in fission yeast [22]. Using this method several strong activating mutants were identified including V17G, S21G, K120R and N153T/S. Researchers have also identified Rheb loss-of-function mutants through mutating residues in Rheb and testing their ability to activate mTORC1 using an *in vitro* mTORC1 activation assay [23]. From these experiments the T38A mutation was identified as a strong loss-of-function mutant for Rheb due to decreased ability to bind effector proteins and activate mTORC1. Additionally, dominant negative mutants for Rheb, including S20N and D60I/K/V, have been identified [24]. The various important mutants of Rheb are listed in Table 1.4.

Table 1.4: Rheb Mutants

This table lists *Rheb1* mutations that have been confirmed to exert an effect on Rheb function. This table was adapted from my first author review paper in *Cellular Signaling* [2].

Mutation type	Amino acid position	Mutation(s)	Reference(s)
Activating	16	S16H	[25]
	17	V17A/G	[22]
	21	S21G/I	[22]
	35	Y35N/C/H	[21]
	63	G63A	[20]
	64	Q64L	[4]
	120	K120R	[22]
	153	N153T/S	[22], [25]
Activating mutations found in cancer database	35	Y35N (5x)	[19], [21]
	139	E139K/D/G/* (2X)	[21]
Loss of function	35	Y35A	[6], [22]
	36	D36A	[23]
	37	P37A	[22], [23]
	38	T38A	[22], [23], [26]
	39	I39A, K	[22], [26]
	41	N41A	[23], [26]
	65	D65A	[6]
	67, 69	Y67A/I69A	[27]
	76, 77	I76A/D77A	[27]
Dominant negative	20	S20N	[23], [24]
	60	D60I/K/V	[23], [24]
Loss of membrane association	181	C181S	[28], [29]

Lysosomal localization of Rheb

Ras superfamily of small GTPases contain a highly conserved –CAAX motif (A is an aliphatic amino acid, X is the C-terminal amino acid) on their carboxy-terminus. A lipid group (farnesyl group in the case of Rheb) is added onto the terminal cysteine, followed by cleavage of the –AAX motif by RCE1, and then carboxylmethylation by ICMT1 [28], [29]. These post translational modifications target GTPases to membranes [29], [30]. Additionally, Ras GTPases (H-, K-, and N-Ras) are often found on the plasma membrane due to a polybasic domain just upstream of the -CAAX motif. However, Rheb lacks this polybasic domain and is therefore associated with endomembranes and not the plasma membrane.

Studies revealed that Rheb strongly co-localizes with the lysosomal marker LAMP2 [31], [32]. Rheb, mTORC1, and TSC come together at the lysosome, and that localization of these proteins influences important signaling events in response to amino acids and growth conditions [31], [32]. Rheb-LAMP2 colocalization is not affected by changes in amino acid or insulin stimulation, and is believed to be required for proper localization of the TSC complex to the lysosome [32]. SiRNA mediated Rheb knockdown disrupted colocalization of TSC2 and LAMP2, as well as decreased mTORC1 signaling [32]. However, similar results were not found when observing Rheb knockdown effects on mTORC1 localization, which suggests that Rheb is only needed for localization of the TSC complex, and not mTORC1, to the lysosome [32]. In contrast, other studies using siRNA-mediated Rheb knockdowns in $TSC2^{-/-}$ MEF cells, provided evidence that full dissociation of mTORC1 from the lysosome cannot be achieved in the presence of Rheb. This suggests a direct relationship between Rheb and mTORC1 localization to the lysosome [33]. A proposed "dual anchoring mechanism" is suggested by models in which Rag proteins may be involved in recruiting mTORC1 to the lysosomal surface while Rheb is critical to retaining it there [33].

CHAPTER 2:

AIMS AND APPROACHES

2.1 Aims of the dissertation

The Rheb/mTORC1 pathway continues to be thoroughly studied as a potential target for cellular proliferative diseases like cancer. However, most of these studies focus on inhibiting mTORC1 directly, with relatively few studies exploring the impact Rheb has on cell signal transduction independently of mTORC1. The few studies focusing on Rheb function and signaling have provided strong evidence for the need to further characterize Rheb signaling. The aim for this dissertation is to identify new Rheb effector proteins, investigate Rheb alterations in cancer, and define Rheb effects on signaling pathways indpenednet of mTORC1.

1. To identify new Rheb effector proteins

Rheb is a member of the family of Ras GTPases, which is a highly-conserved family of signaling proteins responsible for the activation of countless diverse cellular pathways including control of the cytoskeleton, vesicle transport, cell division, and nutrient sensing. Studies have revealed multiple downstream effector proteins for a number of these small GTPases including members from the Ras, Ral, and Rho families [34]. To date, mTORC1 is the only universally accepted effector protein for Rheb, but it is highly unlikely to be the only one. In this aim I set out to identify new Rheb effector proteins through genetic engineering and biochemical techniques. Specifically, I express Rheb activating and effector domain inactivating mutants in cells, and perform a combination immunoprecipitation, liquid chromatography, mass spectrometry, and western blotting techniques to identify novel Rheb-binding proteins.

2. To investigate Rheb alterations in cancer

With the advancement of genetic sequencing technologies, there has been an enormous influx in genetic data available for researchers to analyze. This has been particularly useful in studying cancer genetics, as several large cancer genomic datasets, including TCGA and COSMIC, have been made publically available. Several important cancer-driving mutations have

been identified in Ras proteins, however there are limited analysis performed on Rheb. In this aim I analyze cancer genomic datasets to identify important alterations in Rheb. Through this analysis, I identified a reoccurring cancer mutation (Y35N), and generated a cell line stably expressing Rheb Y35N. In this cell line I observed cancer transformative properties similar to strong cancer-driving mutant KRAS G12V.

3. To analyze Rheb signaling

While Rheb activation of mTORC1 has been well examined, studies on Rheb signaling independent of mTORC1 are lacking. Previous publications have suggested Rheb could play a role in controlling other nutrient sensing pathways including MAPK and AMPK, but the physiological relevance of these have yet to be confirmed. In this aim I set out to characterize Rheb signaling pathways I uncover through my experiments in aims 1 and 2, in addition to those previously reported. Together, these studies provide a solid foundation for the discovery of new Rheb signaling pathways, and solidify the importance for continuing the study of Rheb GTPase.

2.2 Approach

2.2.1 RHEB Immunoprecipitation

The schematic in Figure 2.1A shows our general scheme for identifying potential new Rheb effector proteins. The first step in identifying new RHEB-binding proteins is immunoprecipitation (IP) of RHEB protein. However, due to the relatively low abundance of endogenous RHEB in cells, I transiently overexpressed RHEB in HEK 293T cells under the control of the strong CMV promoter. In addition, I included a FLAG tag on the N-terminus of Rheb for two reasons: 1. to differentiate between plasmid-expressed RHEB and endogenous RHEB (important when expressing RHEB-mutants), and 2. to facilitate strong immunoprecipitation of RHEB by using an anti-FLAG antibody and FLAG peptide elution. After transfecting plasmids expressing FLAG-RHEB, I collect cell lysates, and perform a FLAG-RHEB IP (Figure 2.1A). SDS-PAGE is run to denature and separate any RHEB-protein complexes and for easier visualization of proteins present in the IP (Figure 2.1B). Both Rheb1 and Rheb2 were used and show similar results.

Figure 2.1 Rheb Immunoprecipitation Method

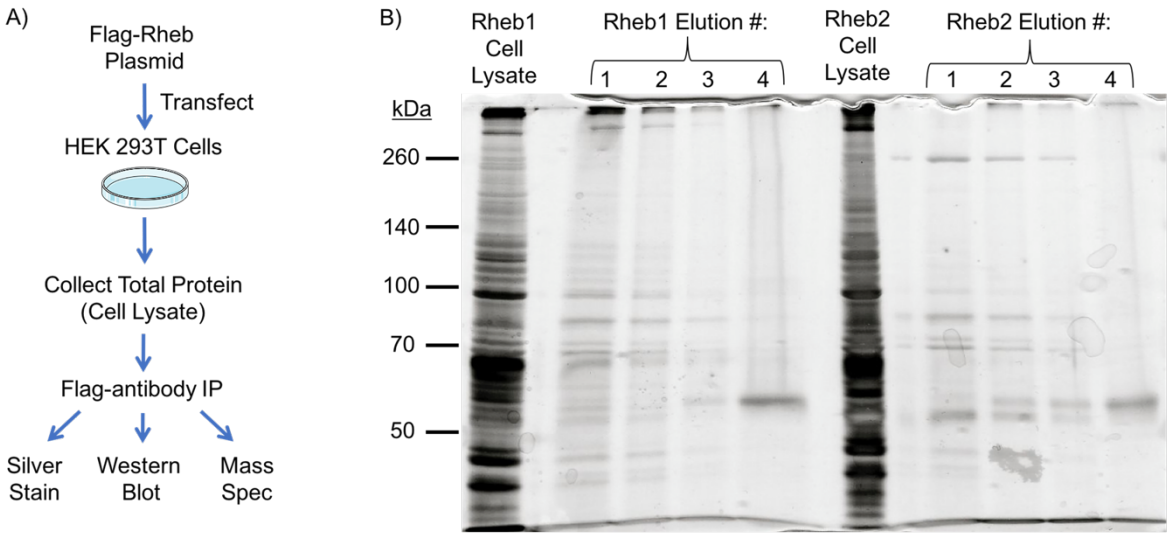

A) Schematic of Rheb immunoprecipitation method for identifying new Rheb effectors. B) Silver stain of SDS-PAGE of Rheb1 and Rheb2 pull downs. FLAG-tagged Rheb1 and Rheb2 were overexpressed in HEK 293T cells, total cell lysate were collected, and Rheb was immunoprecipitated using anti-FLAG antibody. After a series of washes, Rheb samples were eluted from antibody using FLAG peptide. Total cell lysate and elutions were run on SDS-PAGE and proteins were stained with silver nitrate for visualization.

2.2.2 Rheb effector mutants

Rheb contains many of the important structural domains that define small GTPases, including five G-boxes, a C-terminal CAAX motif, and an effector domain. In their active GTP-bound states, GTPases transmit signals through proteins called effectors. The structural basis for determining GTPase-effector interaction involves a region on the GTPases called the effector domain. This region undergoes significant structural changes between GDP and GTP bound states, thus when a GTPase is bound to GTP, the effector domain displays increased affinity towards effector proteins [35], [36].

In order to identify new Rheb effectors, I looked for proteins whose interaction with Rheb depends on an intact effector domain. To accomplish this, I utilized a previously identified mutant of Rheb that alters the effector domain, T38A. Tyrosine 38 is located in the effector domain and the T38A mutation has been previously shown to prevent Rheb from activating downstream effector mTORC1 [23]. In this approach I transiently overexpress RHEB WT or RHEB T38A, and perform immunoprecipitation experiments as in section 2.2.1. True RHEB effector proteins will interact less effectively with RHEB T38A than RHEB WT.

2.2.3 Colocalization

Previous research suggests an important aspect of Rheb regulation of downstream signaling involves recruiting proteins to the lysosome [31]–[33]. This was shown to be the case with mTORC1, as Rheb was required for TSC localization to the lysosome and retaining mTORC1 at the lysosome. Failure of Rheb to properly localize to the lysosome resulted in loss of insulin mediated shut down of mTORC1, and decreased mTORC1 activation [31]–[33].

For most proteins, spatial localization in the cell greatly affects their function, and thus it is critical to determine the effects Rheb has on the localization of its effector proteins. In this approach, I use fluorescent microscopy to monitor the localization of Rheb and Rheb-interacting proteins in cells. I use several methods to accomplish this. I overexpress FLAG-Rheb in the cell

and use anti-FLAG antibody combined with secondary antibody conjugated to a fluorescent molecule. As a control, I use a mutant Rheb that is unable to localize to the lysosomes. This Rheb mutant has the terminal cysteine of the CAAX motif mutated to a serine (RHEB C181S), which prevents the addition of a lipid moiety required for membrane association of Rheb. This causes Rheb to localize in the cytoplasm rather than its normal location on the lysosomal membrane (Figure 2.2).

To determine localization within the cell, I can stain various organelles including lysosomes, and nucleus. For localization to the lysosome I use a lysotracker fluorescent dye because I find that this gives the best signal compared to the commonly used LAMP2 antibody. The nucleus is easily stained with DAPI. The fluorescent microscope I utilized can see three colors, red, green, and blue. Because DAPI is always stained in blue, I use red and green to stain the proteins and organelles. This way the colocalization of proteins and organelles can be easily observed by the intensity of yellow pixels, as an overlap between green and red pixels. Figure 2.2 shows the fluorescent results of RHEB WT and RHEB C181S colocalized with lysosomes.

In this dissertation I will use Rheb when talking about the gene and RHEB when talking about the protein. As stated previously, there are two Rheb genes in mammalian cells, Rheb1 and Rheb2. When I mention Rheb I am referring to Rheb1.

Figure 2.2: RHEB Localization

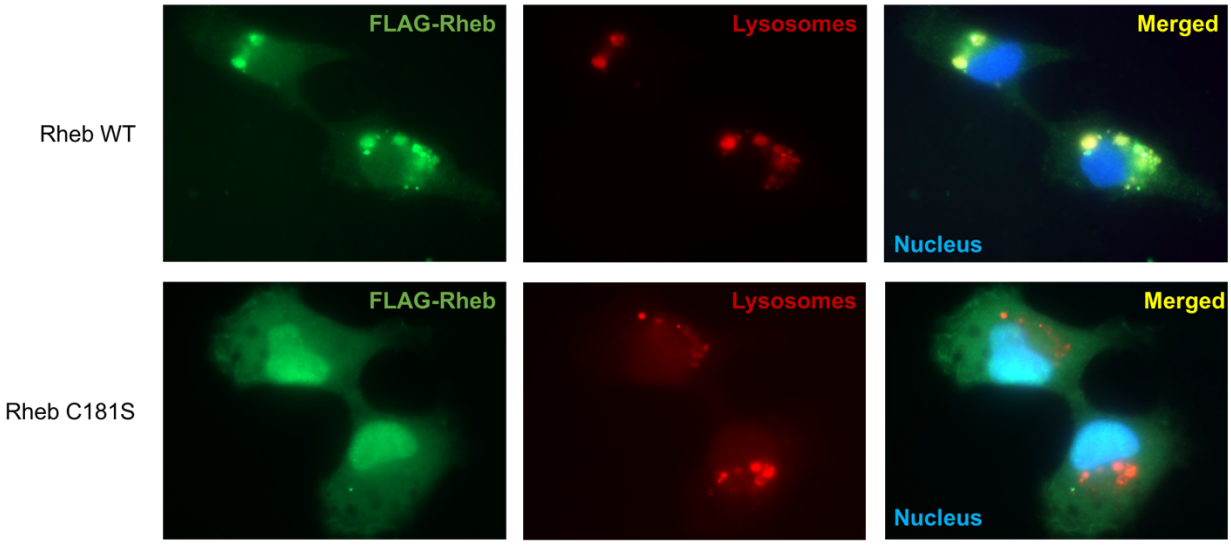

FLAG-RHEB WT, and C181S were overexpressed in HeLa cells grown on glass slides. Cells were treated with 1uM Lysotracker Red prior to fixation. Cells were stained with antibodies against FLAG, followed by incubation with green-fluorescently tagged secondary antibodies. Cells were imaged using fluorescent microscope. Blue indicates DAPI-stained nucleus.

CHAPTER 3:

RESULTS

3.1 MTOR/TSC

mTORC1 as a Rheb downstream effector

Canonical Rheb signaling involves activation of mTORC1, a multi-protein complex consisting of the kinase mTOR (mechanistic target of rapamycin), Raptor (regulatory associated protein of mTOR), mLST8 (mammalian lethal with SEC13 protein 8), DEPTOR (DEP-domain-containing mTOR-interacting protein) and PRAS40 (proline-rich Akt substrate 40kDa). mTORC1 is responsible for increasing cell proliferation and protein synthesis in response to nutrients and growth factors [37]. *Drosophila* studies provided genetic evidence for the idea that Rheb functions to promote cell growth and cell cycle progression through the TORC1 signaling pathway [7], [8].

The idea that mTORC1 is a direct downstream effector of Rheb began with the discovery that only the active form of Rheb (Rheb bound GTP) can stimulate mTORC1 activity *in vitro* [23], [38]. This observation was further solidified when it was shown that mutations in the Rheb effector domain decreased Rheb's ability to interact with and activate mTORC1 [23].

I performed a western blot for proteins previously known to interact with RHEB, mTOR and TSC2 as outlined in the IP approach. We see that both mTOR and TSC2 bands are present in Rheb IP sample, and not in our control IP sample (FLAG IP from cells not expressing any FLAG-tagged proteins) (Figure 3.1.1A). Additionally, I observed less mTOR binding with a Rheb effector domain mutant, Rheb T38A, compared with Rheb WT (Figure 3.1.1B). This confirms previous publications and, more importantly, that our approach can be used to identify effector proteins.

To ensure that mTOR interaction is specific to Rheb, I expressed and immunoprecipitated other small GTPases. Because Rheb is known to exist in a high GTP-bound state in cells compared with other GTPases, I used active mutant forms of these GTPases. I observed that mTOR interacts with both Rheb1 and Rheb2, but does not come down with the other active small GTPases (Figure 3.1.1C).

Figure 3.1.1: RHEB Interacts with mTOR and TSC2

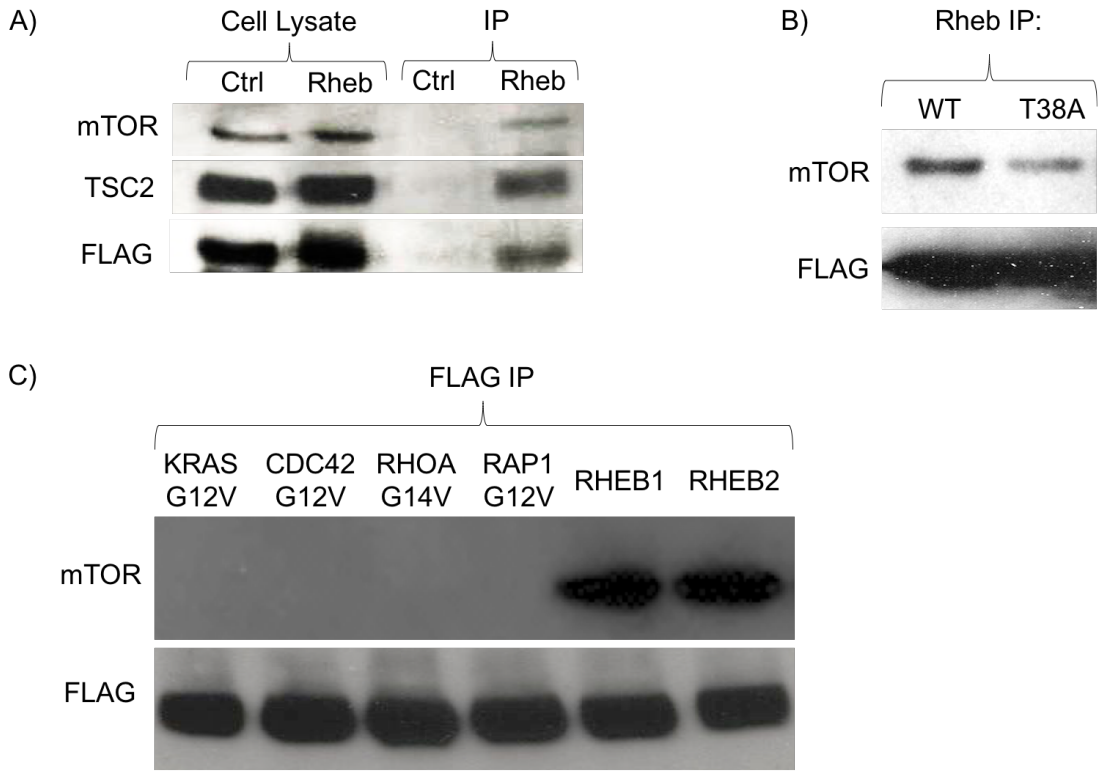

A) FLAG-Rheb1 was transiently transfected and expressed in HEK 293T cells. Cell lysates were collected, immunoprecipitation using anti-FLAG antibody was performed, proteins were resolved by SDS-PAGE, and western blot against mTOR, TSC2, and FLAG was carried out. B) FLAG-Rheb1 WT or FLAG-Rheb1 T38A were expressed in HEK 293T cells and immunoprecipitation was carried out as in *A.* Western blot against mTOR and FLAG is shown. C) FLAG-tagged active mutants of KRAS, CDC42, RHOA, and RAP1 were expressed in HEK 293T cells and immunoprecipitation was carried out as in *A* and *B.* Western blot for mTOR and FLAG is shown.

3.2 CAD

Need to identify other downstream Rheb effectors

Outside of mTORC1, few studies have attempted to identify additional Rheb effectors. Many GTPases have been shown to interact with multiple downstream effectors, including Ras, Ral, Rho, and Rab [34]. Further identification of effector proteins should uncover additional Rheb functions. In this dissertation I set out to identify new Rheb effectors based on two criteria; (i) the effector protein binds active Rheb-GTP, and (ii) the protein requires an intact Rheb effector domain. Through these experiments I was able to identify a novel Rheb effector protein, CAD, that has important biological effects in cells.

RHEB-CAD Interaction

To identify novel Rheb effector proteins I expressed an active RHEB mutant, Q64L, and an effector domain RHEB mutant, T38A, in HEK 293T cells. I collected cell lysates and immunoprecipitated RHEB mutants from these cells. Proteins in the IP samples were separated by SDS-PAGE and visualized using silver nitrate staining. As a control, I also performed a GFP IP. A clear band around 250kDa was observed in the RHEB Q64L lane, but was absent in the RHEB T38A lane (Figure 3.2.1A). This implies the presence of a protein whose interaction is dependent on an intact Rheb effector domain. Using liquid chromatography coupled with tandem mass spectrometry (LC-MS/MS), we identified the protein as CAD. Western blot analysis using antibodies for CAD from both RHEB1 and RHEB2 IPs confirm a RHEB-CAD interaction (Figure 3.2.1B). It appears CAD binds RHEB2 stronger than RHEB1, thus I decided to use RHEB2 expression and IP for the remaining experiments.

Rheb is known to interact with mTORC1, and CAD has been previously shown to be regulated by mTORC1 [39], [40]. I tested whether mTOR-RHEB-CAD form a complex by performing an mTORC1 IP. In western blots for CAD and Rheb we see that CAD does not appear

in the mTORC1 IP, while Rheb does (Figure 3.2.1C). This suggests that RHEB-CAD forms a complex independently of the RHEB-mTORC1 complex.

CAD enzyme in *de novo* pyrimidine nucleotide biosynthesis

Carbamoyl-phosphate Synthetase 2, Aspartate Transcarbamoylase, and Dihydroorotase (CAD) is a multifunctional enzyme responsible for carrying out the first three steps in *de novo* pyrimidine nucleotide biosynthesis. Nucleotide synthesis is crucial for cellular growth and proliferation in rapidly dividing cells, thus this pathway is an exciting candidate to target for cancer therapy. The rate limiting step in pyrimidine synthesis pathway is catalyzed by the carbamoyl phosophate synthetase II (CPSase) of CAD [41], [42]. CPSase acts in the second step of pyrimidine biosynthesis and converts bicarbonate, glutamine, and two ATP molecules into carbamoyl phosphate. CAD activity is controlled by a multitude of signals including phosphorylation by several kinases and allosteric regulation by substrate/product binding. CAD activity is up-regulated through phosphorylation by mitogen activated protein kinase (MAPK) and protein kinase C (PKC) during S-phase of cell growth [43]. Additionally, binding of 5-phosphoribosyl-1-pyrophosphate (PRPP), a substrate for subsequent steps in pyrimidine biosynthesis, increases CAD activity. CAD is down-regulated in stationary growth cells by phosphorylation through cAMP-dependent protein kinase a (PKA), resulting in decreased sensitivity to PRPP [44], [45]. Additionally, binding of UTP, a downstream product of the pathway, decreases CAD activity as part of a negative feedback loop [45]. Recently it was shown that CAD is phosphorylated by S6K via activated mTORC1 pathway, resulting in increased CAD activity [39], [40]. To date, no non-kinase protein has been identified as playing a role in regulating CAD activity.

Figure 3.2.1: Identification of RHEB-CAD Interaction

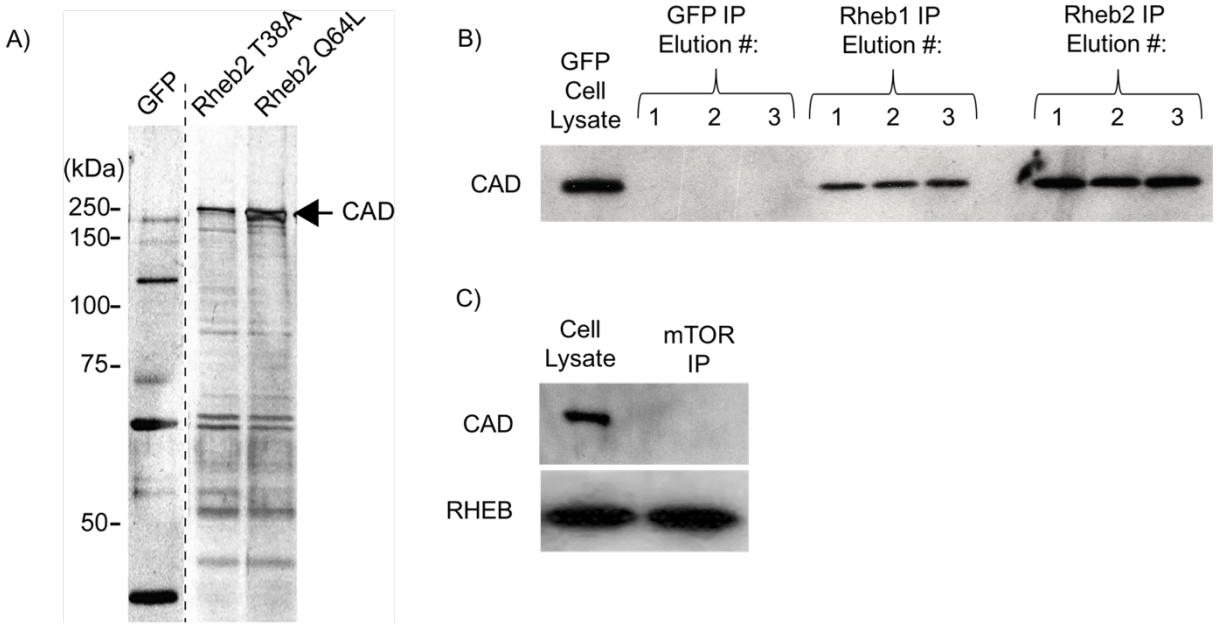

A) Rheb2 T38A, Rheb2 Q64L, and GFP were overexpressed in HEK 293T cells. Cell lysates were collected, FLAG-RHEB immunoprecipitation was performed, and proteins were resolved by SDS-PAGE and visualized with silver stain. CAD was identified by LC-MS/MS. B) Rheb1 WT, Rheb2 WT and GFP were overexpressed in HEK 293T cells. Cell lysates were collected, FLAG-RHEB immunoprecipitation was performed, and proteins were eluted from the FLAG column three separate times. The samples were resolved by SDS-PAGE and western blot of CAD was performed to look at CAD-protein interaction. C) HEK 293T cells overexpressing AU1-mTOR were subjected to AU1-IP. CAD and RHEB western blots were performed to look for co-immunoprecipitation with mTOR.

Rheb-CAD interaction is specific to Rheb and depends on GTP binding

To see if CAD-Rheb interaction was specific among small GTPases, I performed FLAG-IP from HEK 293T cells expressing FLAG-H-Ras, FLAG-RalA, and FLAG-Rac1. Western blot for CAD reveals no CAD protein in the IPs of these other small GTPases, indicating this interaction is specific to Rheb (Figure 3.2.2A). True effector proteins exhibit enhanced binding to GTP-bound GTPases. To test whether CAD interaction is dependent on the GTP-bound status of Rheb, I loaded His6-tagged RHEB proteins with non-hydrolysable GTPγS, GDP, or treated with EDTA to generate a nucleotide-free RHEB. These RHEB proteins were incubated with HEK293T cell lysates, followed by immunoprecipitation of CAD. Western blot for His6-Rheb showed that the Rheb-CAD interaction was strongest with RHEB-GTP and was significantly reduced with both RHEB-GDP and nucleotide-free RHEB (Figure 3.2.2B). This indicates the CAD interaction is enhanced by active RHEB, consistent with effector protein interactions with Ras family GTPases.

Figure 3.2.2: Rheb-CAD Interaction Specificity and GTP-Binding Dependency

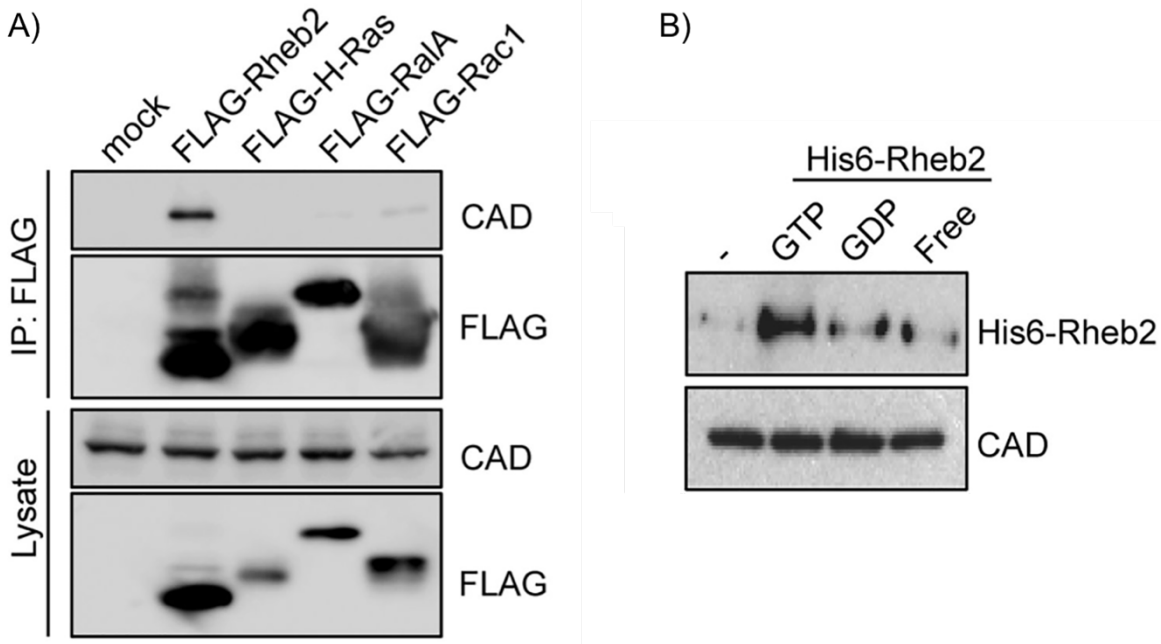

A) FLAG tagged -RHEB2, HRAS, RALA, and RAC1 were overexpressed in HEK 293T cells. FLAG IP was performed and western blot for CAD was used to detect CAD co-immunoprecipitation. B) His6-Rheb2 was loaded with GTPγS, GDP, or EDTA (nucleotide free) and incubated with cell lysates from HEK293T cells. Anti-CAD immunoprecipitation was performed, followed by Western blot using His6 antibody.

Further characterization of Rheb-CAD complex

As a result of the denaturing and reducing conditions of SDS-PAGE, native protein complexes are broken up and separated into individual proteins. To observe the native RHEB-CAD complex in cells I executed two different methods.

First, I used size exclusion chromatography to separate native Rheb-CAD complex. To accomplish this, I performed immunoprecipitation of FLAG-Rheb as done previously. Then I loaded my IP samples onto a liquid chromatography column packed with Sephacryl S-300 resin, which is used to separate mid-size proteins in the globular protein range of 10kDa to 1.5 MDa. As samples run through the column they are separated by size, with the smaller protein complexes coming out in the earliest fractions and the larger protein complexes coming out in later fractions. I collected and ran all the excluded fractions on an SDS-PAGE and observed strong bands for Rheb and CAD appearing in overlapping fractions, indicating that they form a complex together in the cell (Figure 3.2.3A). To further confirm this result, I collected the fractions that contained both CAD and Rheb (Fractions 11-14 from Figure 3.2.3A) and ran them through the column a second time. Silver stain and western blot confirmed the presence of CAD and Rheb in these same fractions (Figure 3.2.3B,C), indicating that RHEB-CAD form a strong and stable complex in cells.

Second, I ran my samples on a blue native gel. Blue native PAGE differs from SDS-PAGE because it is run without SDS or denaturing conditions like heating [46]. In blue native PAGE coomassie dye is used to induce a slight negative charge shift on the proteins, and protein complexes are separated by their intrinsic charge and 3D size. Western blot for FLAG-RHEB reveals several bands at around 20, 66, 200, 400, and 750 kDa (Figure 3.2.3D). Western blot for CAD reveals two bands at around 400 and 750 kDa, indicating that RHEB-CAD may form a complex in this range. Because Rheb is 21kDa in size, and CAD is 250kDa, this result suggests RHEB-CAD may form multimers or complexes with additional proteins.

Figure 3.2.3: **Size Exclusion Separation of RHEB-Protein Complexes**

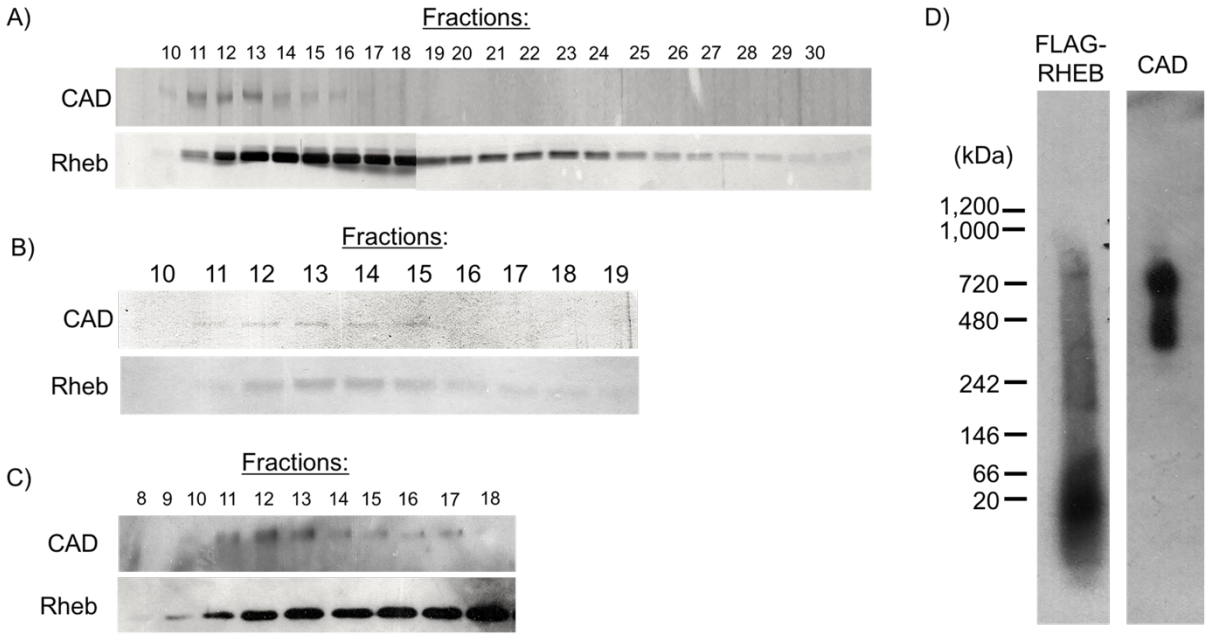

A) FLAG-RHEB immunoprecipitation was performed and samples were run through a size exclusion column packed with sephacryl S-300 resin. Every 250ul excluded from the column were collected in separate fractions and ran on SDS-PAGE. Protein bands were visualized with silver stain. B) Fractions 11-14 from *Figure 2.3A* were collected and run on size exclusion column a second time. These new fractions were collected and run on SDS-PAGE and protein bands were visualized by silver stain. C) Western blot of SDS-PAGE from *Figure 2.3B* using CAD and RHEB antibodies. D) Immunoprecipitated FLAG-RHEB samples were run on using blue native PAGE, to separate native protein complexes by size without separating the complexes into individual proteins. Western blot against FLAG-RHEB (Left) and against CAD (Rheb) was performed.

Narrowing down CAD binding site on Rheb

As mentioned previously, CAD is a large multienzymatic protein consisting of three protein domains that carryout the first three steps in pyrimidine nucleotide biosynthesis (Figure 3.2.4A). CAD protein contains three separate domains. The carbamoyl-phosphate synthetase (CPS) domain is responsible for carrying out the first step in pyrimidine biosynthesis by converting glutamine and bicarbonate to carbamoyl-phosphate. This step is the rate-limiting step in the nucleotide biosynthesis pathway. The CPS domain also contains several important regulatory sites, including a MAPK phosphorylation site at threonine 456, a PKA1 phosphorylation site at threonine 1037, and a UTP/PRPP substrate binding domain corresponding to amino acids 1265-1461 [47]. The aspartate transcarbamylase (ATC) domain carries out the second step in pyrimidine biosynthesis, converting carbamoyl-phosphate and aspartate to N-Carbamoyl-L-Aspartate. The dihydroorotase (DHO) domain carries out the third step in pyrimidine biosynthesis, converting N-Carbamoyl-L-Aspartate into dihydroorotate.

In order to identify the region on CAD where Rheb binds, we generated and expressed various fragments of CAD protein labeled with a MYC tag (Figure 3.2.4A). We co-expressed these fragments with FLAG-RHEB in HEK 293T cells and performed a FLAG-RHEB IP. Western blot against MYC-CAD revealed which CAD fragments came down with RHEB (Figure 3.2.4B). From the western blot analysis, we see that RHEB binds the CPSase.B2-B3 fragment, and does not bind any fragment lacking the CPS.B3 domain (Figure 3.2.4B). This led us to believe that Rheb binds the CPS.B3 domain. To confirm this, we generated a MYC-tagged CPS.B3 fragment and co-expressed with FLAG-RHEB in HEK293T cells. We observed this fragment coming down with RHEB in a FLAG-RHEB IP, and not appearing in the control IP (no FLAG protein expressed in cells) (Figure3.2.4C). These results suggest that this is the region for RHEB-CAD interaction.

Figure 3.2.4: Identification of Rheb Binding Site on CAD

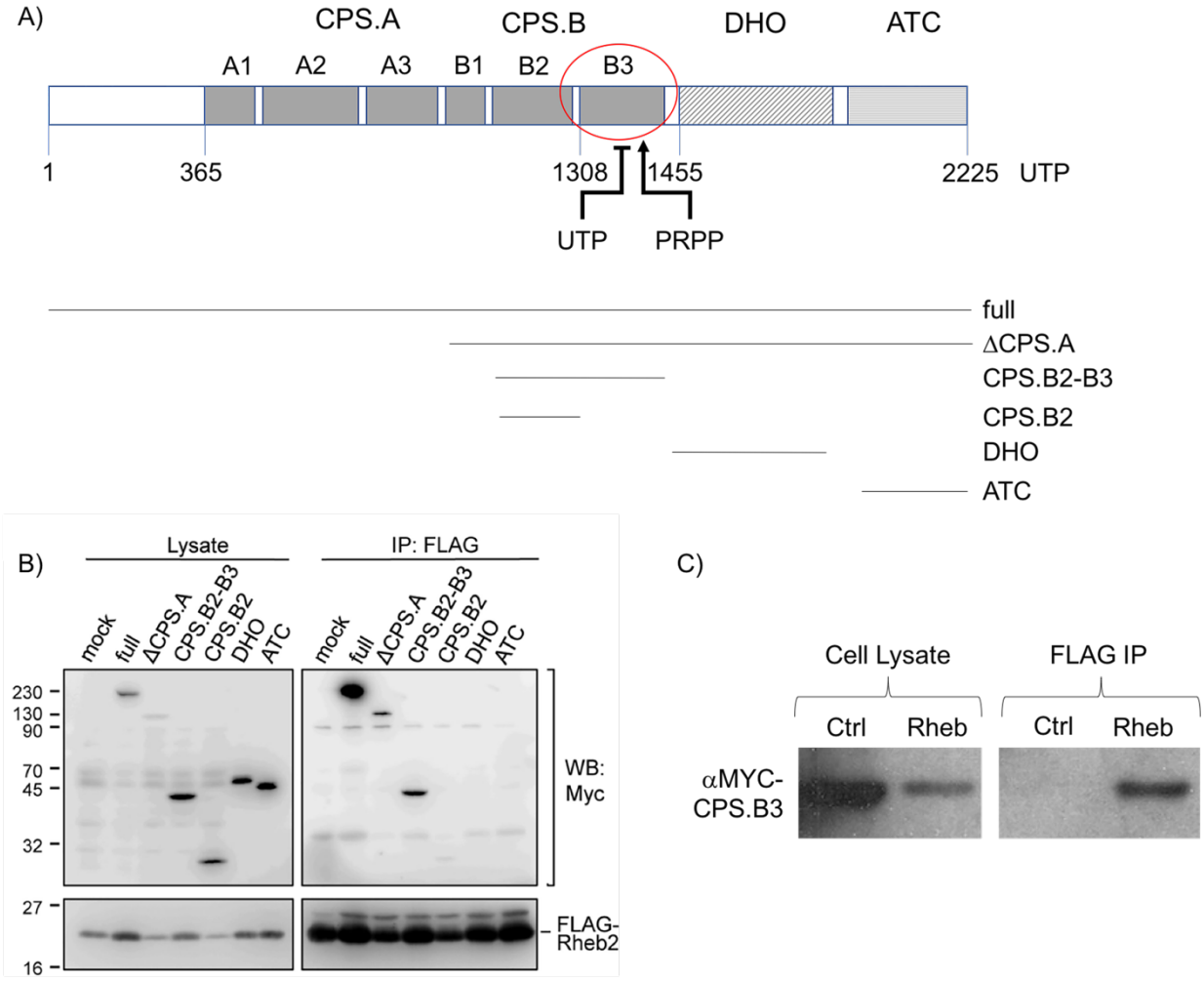

A) Diagram of the MYC-tagged CAD fragments that were generated. The region identified in *B* and *C* as the Rheb binding site is circled in Red. B) The MYC-CAD fragments from *A* were co-expressed with FLAG-RHEB in HEK293T cells. Cell lysates were collected and immunoprecipitation of FLAG-RHEB was performed. Western blot for MYC identified which CAD fragments came down with RHEB. C) A new MYC-tagged CAD fragment was generated called CPS.B3 (the red circled region in *A*) and was co-expressed in HEK 293T cells with FLAG-RHEB. Immunoprecipitation was performed as in *B*. Western blot against MYC confirmed CPS.B3 coming down with RHEB

Rheb-CAD metabolomics

The CPS.B3 domain is important for controlling CAD activity, as it contains a UTP binding site for allosteric inhibition as well as a PRPP binding site for CAD activation (Figure 3.2.4 A). We hypothesized that RHEB binding in this region would affect CAD activity in the cell. First we tested the ability of Rheb to effect CAD activity by using an *in vitro* assay for CAD activity. In this assay CAD is immunoprecipitated from HEK293T cells and incubated with glutamine, aspartate, and ^{14}C-labeled sodium bicarbonate, the three metabolites required for CAD enzyme activity. Carbon-14 metabolites were then counted as a readout of CPSase activity. To ensure this assay works we added either UTP or PRPP to the mixture and observed the effect on CPSase activity. As expected, UTP greatly inhibited CPSase activity and PRPP greatly activated CPSase activity (Figure 3.2.5A). Using this *in vitro* assay, we tested whether RHEB-GTP affects CAD activity. We loaded RHEB1 and RHEB2 with GTPγS, a non-hydrolyzable form of GTP that locks RHEB in the active GTP-bound state, and added them to our *in vitro* CAD assay. We can see that both RHEB1-GTP and RHEB2-GTP activate CAD activity *in vitro* (Figure 3.2.5B). Interestingly, addition of UTP still inhibited CAD activity *in vitro* even in the presence of Rheb-GTP (Figure 3.2.5C). This suggests that Rheb may activate CAD activity, but does not prevent CAD sensitivity towards UTP inhibition.

I sought to determine whether RHEB affects CAD activity *in vivo* by measuring CAD activity in cells where Rheb is overactive. In this experiment I used a TSC2$^{-/-}$ cell line, which results in high levels of RHEB-GTP due to the absence of TSC2 to facilitate RHEB GTPase activity. We collected metabolites from TSC2$^{-/-}$ and normal TSC2 expressing cell lines, and analyzed metabolite levels using liquid chromatography/mass spectrometry (LC/MS). We observed increased levels of N-Carbamoyl-L-Aspartate, the downstream product of CPSase enzyme. We also detected increased levels of UMP in these overactive RHEB cell lines (Figure 3.2.5D). This matches our *in vitro* assay and suggests Rheb directly stimulates CAD activity.

Figure 3.2.5: Overactive RHEB Increases CAD Activity

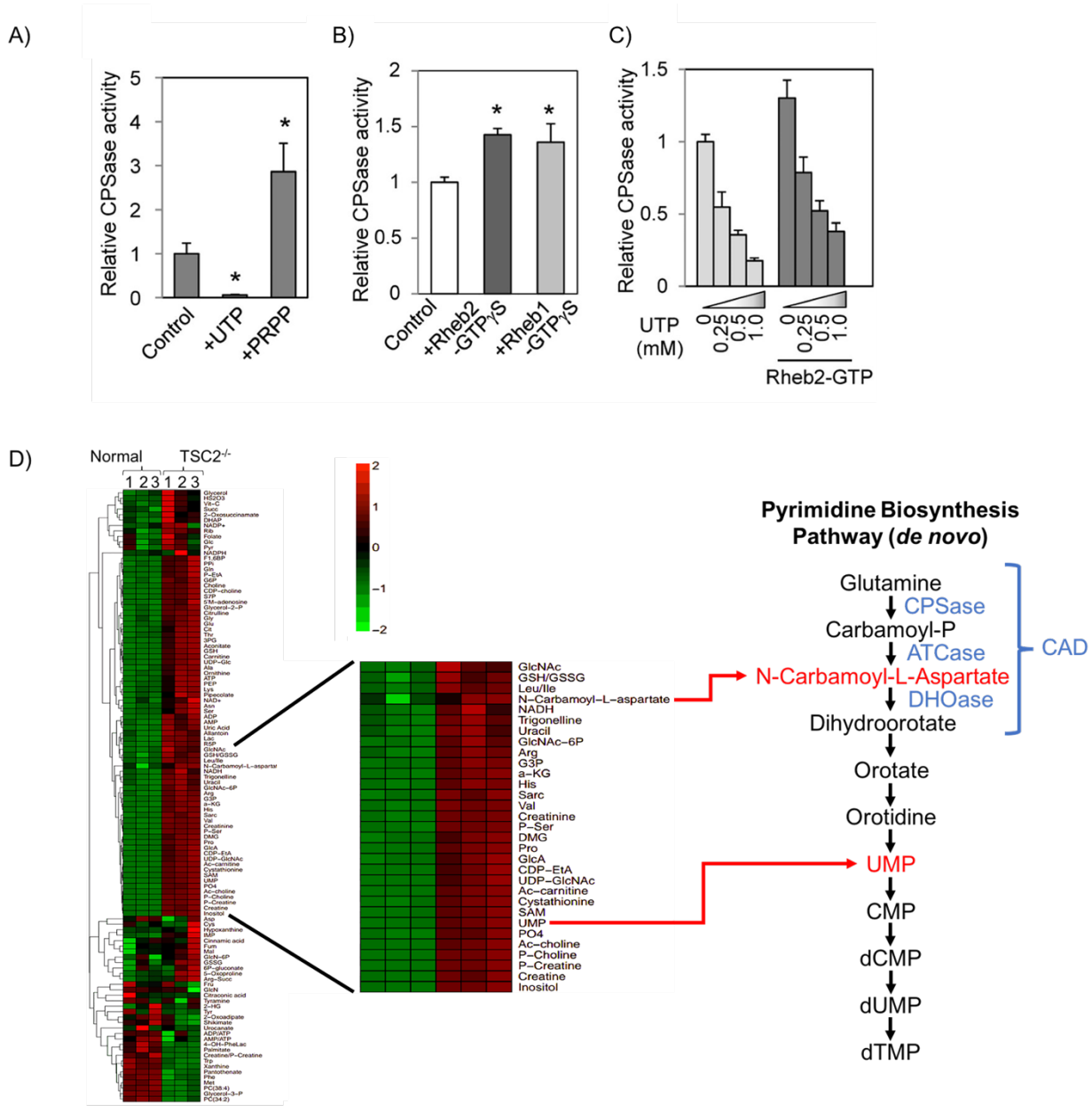

A-C) An *in vitro* assay measuring CAD activity was performed in the presence or absence of UTP, PRPP, RHEB1-GTPγS, or Rheb2-GTPγS. Bars represent results of three independent experiments with S.D.*,p<0.05 versus control. D) Metabolites were collected from WT and TSC2$^{-/-}$ MEF cells and analyzed using liquid chromatography/mass spectrometry. N-carbamoyl-L-Aspartate, an intermediate of the CAD pathway, and UMP were observed to be increased under these conditions.

Rheb-CAD co-localization

Localization studies have shown Rheb, TSC, and mTORC1 form a signaling node on the lysosomal membrane surface [31]–[33]. In these studies it was revealed Rheb is required for TSC recruitment to the lysosome in response to nutrient deprivation [32]. Additionally, while Rheb is not necessary to recruit mTOR to the lysosome, it is required to keep mTOR at the lysosome and for proper mTOR activation [33]. Rheb's influence on protein localization of the mTORC1 pathway led us to explore whether Rheb has a similar effect on CAD localization and function.

Rheb is known to reside mainly on lysosomes, so we looked to see if CAD had similar localization. We expressed Halo-CAD in HeLa cells and used immunofluorescent microscopy to observe CAD co-localization with LAMP2, a lysosomal marker. CAD appears to reside mainly in the cytosol surrounding the nucleus on all sides, but also partially overlaps with LAMP2 (Figure 3.2.6A Top). Rheb, however, appears to have a much more restricted localization that strongly overlaps with LAMP2 (Figure 3.2.6A Bottom).

Rheb influences CAD localization

To test if Rheb influences CAD localization, we co-expressed both GFP-RHEB and Halo-CAD in HeLa cells and performed immunofluorescent microscopy. When Rheb is overexpressed we see that the localization of CAD changes dramatically. We observe CAD overlapping strongly with GFP-RHEB, in a pattern consistent with strong lysosomal localization (Figure 3.2.6B). In comparison, Halo-CAD localization in the GFP control cells (no Rheb overexpression), is more dispersed (Figure 3.2.6B). These results suggest that RHEB overexpression alters CAD localization by recruiting it to the lysosomes.

To further test if RHEB affects CAD localization, we treated HeLa cells expressing GFP-Rheb and Halo-CAD with farnesyl transferase inhibitor (FTI). FTI treatment inhibits Rheb localization to lysosomal membranes by blocking the addition of a farnesyl lipid to the CAAX motif on RHEB. We observed that both CAD and RHEB become widely dispersed in the cells in

response to FTI treatment (Figure 3.2.6C). These results show that RHEB localizes a portion of CAD to the lysosomes, which may be a mechanism by which RHEB effects CAD signaling.

*****The majority of the work presented in this section, **3.2 CAD,** was published in a paper I co-authored in the *Journal of Biological Chemistry* [48].

Figure 3.2.6: Rheb and CAD Colocalize at the Lysosomes

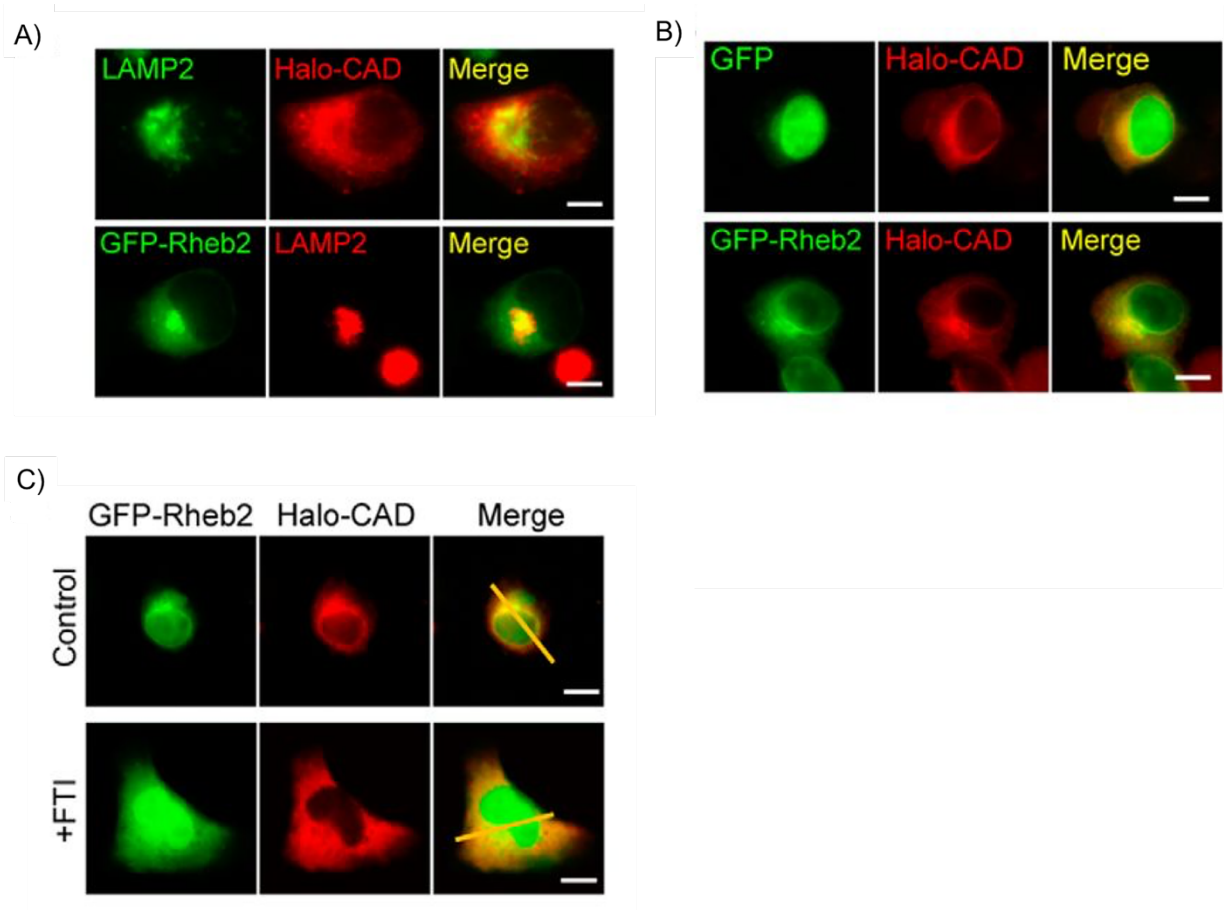

A) Halo-CAD or GFP-Rheb2 were expressed in HeLa cells. Halo was labeled with HaloTag TMR ligand 30 minutes before fixation. Lysosomes were stained with LAMP2 antibodies after cell fixation. B) HeLa cells expressing GFP and Halo-CAD, or GFP-Rheb2 and Halo-CAD, were stained with HaloTag TMR ligand 30 min before fixation. C) HeLa cells expressing GFP-Rheb2 and Halo-CAD were treated with 10μM FTI-277 for 24hr. Halo was labeled as in *A&B.*

3.3 AMPK

RHEB-AMPKα Interaction

Another protein I identified as binding Rheb is 5' AMP-activated protein kinase (AMPK). AMPK is a serine/threonine kinase responsible for maintaining energy homeostasis in the cell [49]. AMPK is a heterotrimeric complex consisting of three protein subunits, the catalytic α-subunit and regulatory β– and γ-subunits (Figure 3.3.1A). As shown in Figure 3.3.1B, immunoprecipitation of FLAG-RHEB protein expressed in HEK 293T cells identified an interaction with the AMPKα subunit. Neither of the 2 β-isoform-subunits, or the γ-subunit came down (Figure 3.3.1B). This may be due to Rheb binding AMPKα and sequestering it away from the β and γ subunits, thus breaking up the AMPK complex.

Figure 3.3.1: RHEB-AMPKα Interaction

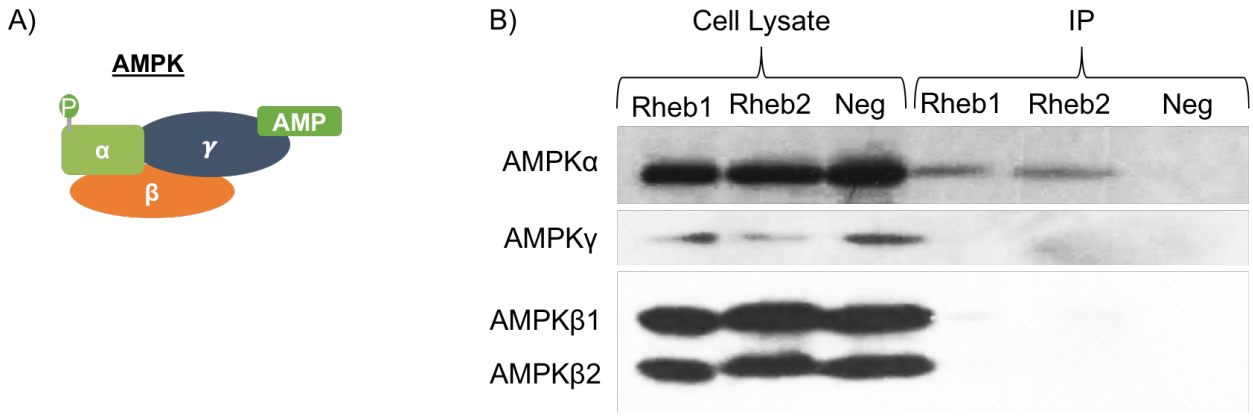

A) Diagram of AMPK complex consisting of the α, β and γ subunits. The P represents the activating LKB1/CAMKK2 phosphorylation site at Thr172 of the AMPKα subunit. B) FLAG-Rheb was expressed in HEK 293T cells and a FLAG immunoprecipitation was performed. Proteins were resolved by SDS-PAGE and western blot for AMPKα-, β–, and γ–subunits revealed a RHEB interaction with only the α subunit of AMPK.

RHEB-AMPKα Interaction is Effector Domain Dependent and Specific to Rheb

I tested whether the RHEB-AMPKα interaction was dependent on an effector domain, as is the case for effector proteins. I immunoprecipitated Rheb WT and Rheb T38A effector domain mutant from HEK 293T cells overexpressing these two proteins. We see that AMPKα interacts much less effectively with the Rheb T38A mutant compared with Rheb WT (Figure 3.3.2A). This suggests that the AMPKα interaction is an effector protein of Rheb.

I next wanted to test whether the interaction of AMPKα was specific to Rheb among other small GTPases. When compared with other small GTPases, Rheb exists in a highly activated, GTP-bound, state. To control for this, I expressed mutant active forms of RHOA, RAP1, CDC42, and KRAS in HEK 293T cells. Immunoprecipitation of these GTPases, showed that AMPKα only interacted with Rheb (Figure 3.3.2B). This suggests that AMPK interaction is specific to Rheb among small GTPases.

Figure 3.3.2: RHEB-AMPKα Interaction is Effector-Domain Dependent and Specific to RHEB

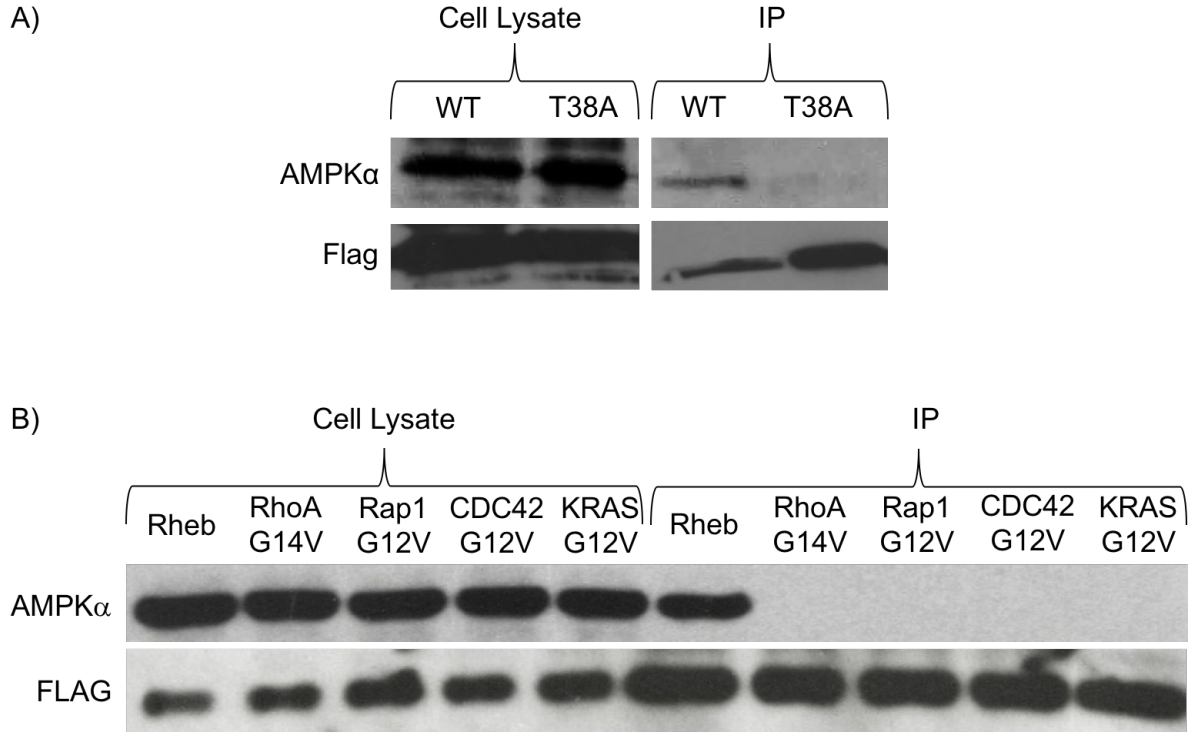

A) FLAG-Rheb WT and FLAG-Rheb T38A were expressed in HEK 293T cells followed by FLAG immunoprecipitation, SDS-PAGE and western blot of AMPKα. Results show that AMPKα interacts with Rheb in an effector domain dependent manner. B) Active mutant, FLAG-tagged, GTPases were expressed in HEKT 293T cells followed by FLAG immunoprecipitation, SDS-PAGE, and western blot for AMPKα. Results show AMPKα binds Rheb specifically among small GTPases.

Rheb and AMPKα Colocalize at the Lysosomes

Further support for the RHEB-AMPK interaction was obtained by demonstration that the two protein colocalize. A previous publication reported AMPK localization to particulate clusters proximal to the nucleus [50]. The researchers believed this represented AMPK association with intracellular membranes. This observation could be lysosomes, as they too are located in distinct clusters proximal to the nucleus. I looked at the normal distribution of AMPK in cells by using fluorescent microscopy with anti-AMPKα antibody to observe endogenous AMPKα localization in HT-1080 cells. In addition, I stained the lysosomes with a red lysotracker dye, to see if AMPKα might colocalize with Rheb at the lysosomes. Under these conditions, we see that AMPKα appears to reside in the cytoplasm, but proximal to the nucleus overlapping with lysosomes (Figure 3.3.3, Top). Next, I overexpressed Rheb in the HT-1080 cells to see if this affected AMPKα localization. Under Rheb overexpression, we see an even stronger colocalization of AMPKα to the lysosome (Figure 3.3.3, Bottom). This finding reports that AMPK is observed at the lysosome, and suggests that Rheb is responsible for AMPK localization to the lysosomes.

Figure 3.3.3: Rheb-AMPKα Colocalize

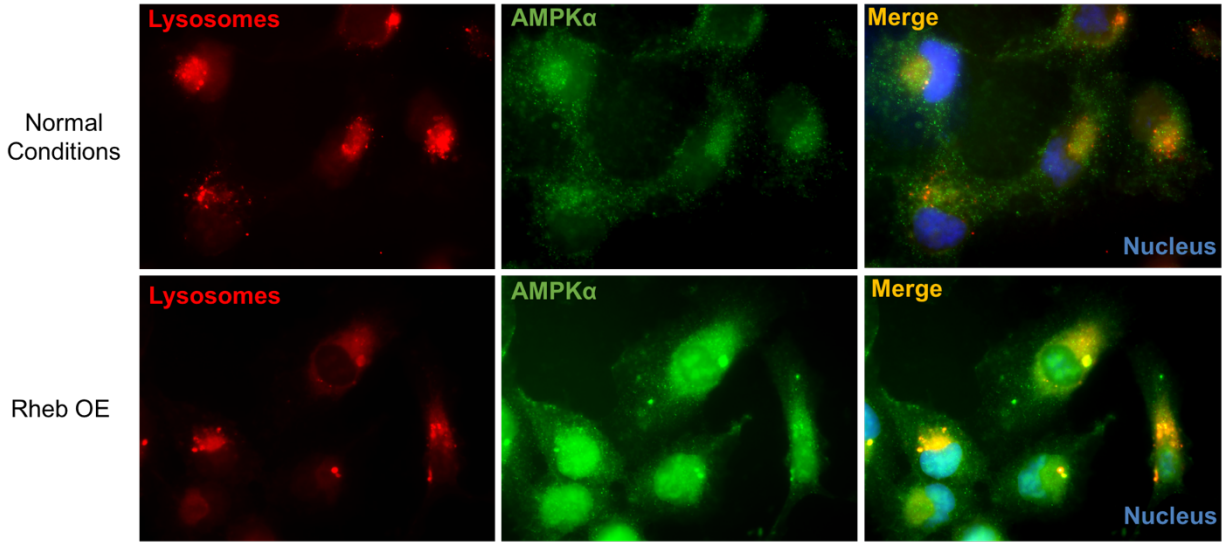

Top: Endogenous AMPKα (green) was imaged in HT-1080 cells stained with Lysotracker (red). Bottom: Rheb was overexpressed in HT-1080 cells stained with Lyostracker (red) and endogenous AMPKα (green) was imaged. Nucleus is stained in blue.

Rheb overexpression blocks phenformin-activation of AMPK

AMPK activity is increased under conditions where the cell is stressed, including conditions where nutrients are lacking, and there are high AMP/ATP levels inside the cell. A class of drugs called biguanides, specifically metformin and phenformin, have been previously shown to stimulate AMPK activity [51]. These drugs activate AMPK through an indirect mechanism; they inhibit complex I of the mitochondrial respiratory chain, which results in decreased ATP production and increased levels of AMP [52]. This results in activation of AMPK. Similarly, serum starvation is known to activate AMPK due to low growth factors and increased production of reactive oxygen species [53], [54]. Under serum starved conditions, AMPK becomes activated upon phosphorylation at Thr172 by LKB1 and CAMKK2 [55].

Using this knowledge, I developed an AMPK activation assay to test AMPK activity in cells. I grew cells under serum starved conditions in combination with Phenformin treatment (Figure 3.3.4A). As a read out for AMPK activation, I performed a western blot using an antibody against phosphorylated-AMPKα Thr172 (pAMPKα).

I performed the AMPK activation assay, detailed above, in HEK 293T cells. The overexpression of RHEB did not appear to affect phosphorylation of AMPKα, nor did transfection of an empty expression vector control (Lanes 1, 2, and 4 Figure 3.3.4B). As expected, in the presence of phenformin pAMPKα is greatly increased (Lane 3 Figure 3.3.4B). However, overexpression of RHEB greatly reduced the phosphorylation of AMPKα in the presence of phenformin (Lane 5 Figure 3.2.4B). The empty expression vector control did not affect pAMPKα levels in the presence of phenformin (Lane 6 Figure 3.2.4B). These results suggest Rheb prevents AMPK activation.

Figure 3.3.4: Rheb Inhibits AMPK Activation

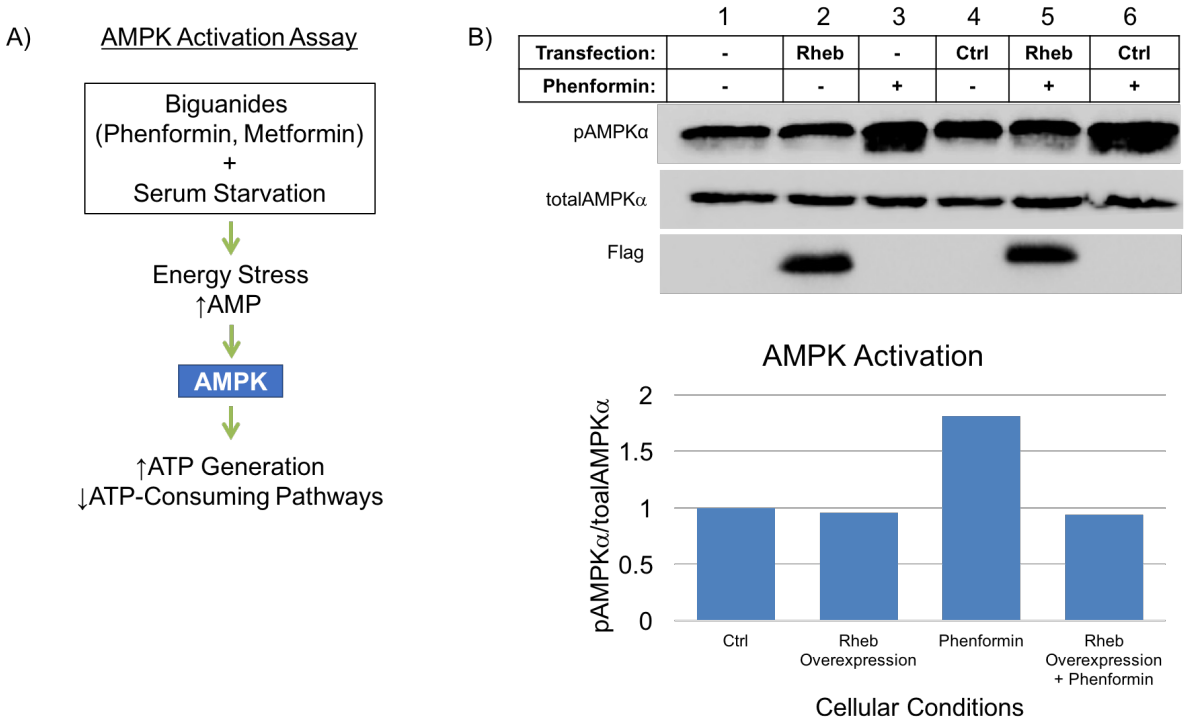

A) AMPK activation assay. Treatment of cells with a class of drugs known as biguanides in combination with serum starvation increases the energy stress (and AMP levels) in the cells, activating AMPK activity. B) Effect of Rheb overexpression on AMPK activation in response to phenformin treatment. HEK 293T cells transiently overexpressing FLAG-RHEB were treated with phenformin, cell lysates were collected, and phosphorylation levels of AMPKα were measured using western blot. Image J analysis was performed to quantitate levels of pAMPKα as a ratio to totalAMPKα. A bar graph is shown for lanes 1 (Ctrl), 2 (Rheb Overexpression), 3 (Phenformin), and 5 (Rheb Overexpression + Phenformin). Phosphorylated AMPK values were normalized to lane 1 (ctrl), which was set at 1.

3.4 BRAF

Another interesting RHEB binding protein I studied was the interaction with BRAF. This was obtained in the course of my characterization of Rheb cancer mutants. Therefore, this section is written in the order of results as I obtained them, with the BRAF-RHEB interaction explored in the second half of this section.

Analysis of cancer genomic databases reveal important alterations in Rheb

Advancements in sequencing technology have made it possible to sequence an enormous number of cancer patient samples in the last decade. Most of this data is readily available for researchers to access through public databases including TCGA, COSMIC, and others. I used the cBioPortal, a user-friendly data portal that combines the data from these cancer genomic databases, to analyze Rheb alterations in cancer [56], [57]. A number of genomic alterations in Rheb have been identified across a broad range of cancer types (Figure 3.4.1A). The most striking alteration is Rheb amplification. Most notably, in cancers where >100 samples have been analyzed, Rheb has high genomic amplification in 21.5% (23/107) of prostate, 10.3% (32/311) of ovarian, 3.9% (9/230) of lung and 3.8% (11/287) of melanoma cancers. A number of somatic mutations have also been identified in Rheb, including 51 missense mutations, and 9 truncating mutations (Figure 3.4.1B). Examination of the missense somatic point mutations in Rheb reveal a recurrent mutation at tyrosine 35 (Figure 3.4.1B). Further analysis of the point mutations at Y35 reveal a significant number of them are found in clear cell renal cell carcinoma (ccRCC), and the majority of mutations result in an asparagine substitution (Y35N) (Figure 3.4.1C).

A previous study attempting to identify new cancer driving mutations identified this Rheb Y35N mutation to be significant in ccRCC [19]. In this study the researchers analyzed somatic point mutations in 4,742 tumor-normal pairs and screened for new cancer genes that were not previously identified, contained more mutations than expected relative to background, clustered

within the gene, and were enriched in evolutionarily conserved sites. Rheb Y35N was identified as being significant in ccRCC due to these variables.

Mutation at tyrosine 35 is particularly interesting because it exists in the highly-conserved effector domain region of small GTPases, a region that facilitates interaction with downstream proteins and signaling activation. I hypothesized this mutation may alter Rheb signaling and have an observable effect on cells.

Figure 3.4.1: Rheb Mutations in Cancer

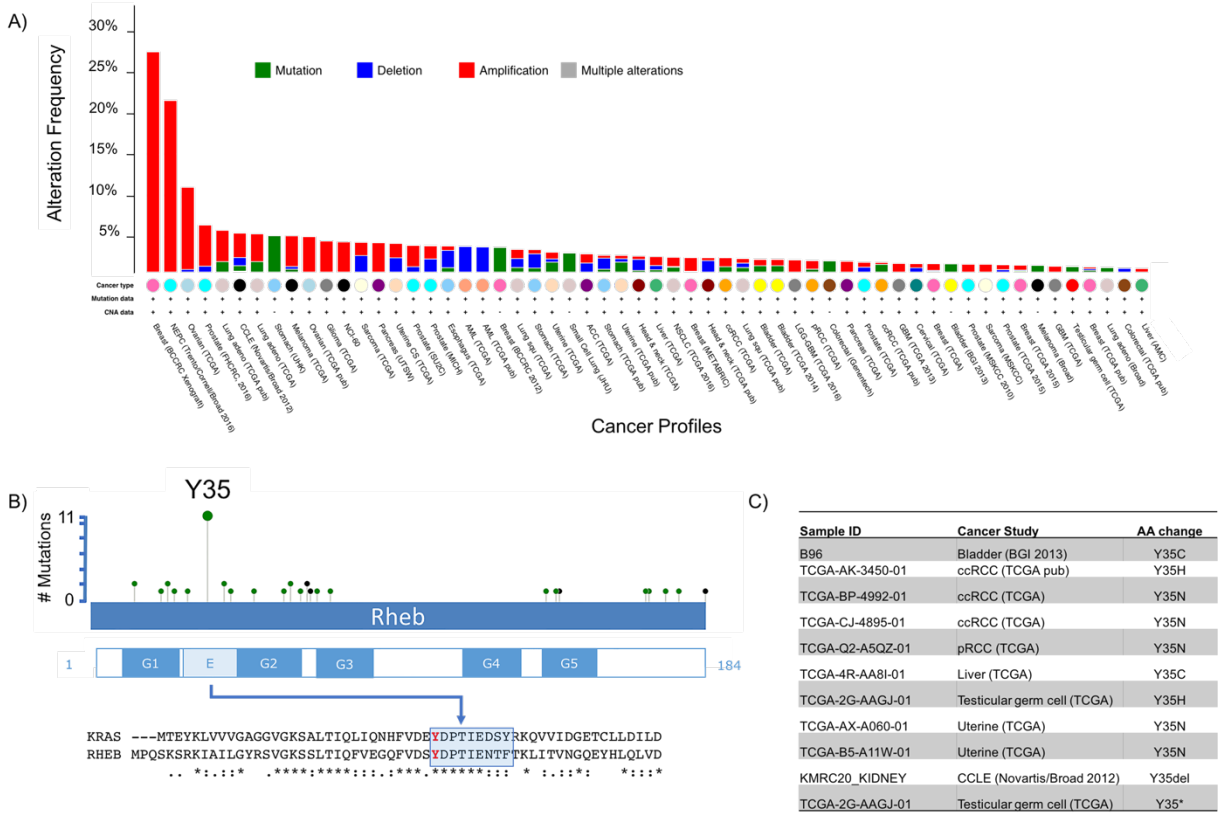

Sample ID	Cancer Study	AA change
B96	Bladder (BGI 2013)	Y35C
TCGA-AK-3450-01	ccRCC (TCGA pub)	Y35H
TCGA-BP-4992-01	ccRCC (TCGA)	Y35N
TCGA-CJ-4895-01	ccRCC (TCGA)	Y35N
TCGA-Q2-A5QZ-01	pRCC (TCGA)	Y35N
TCGA-4R-AA8I-01	Liver (TCGA)	Y35C
TCGA-2G-AAGJ-01	Testicular germ cell (TCGA)	Y35H
TCGA-AX-A060-01	Uterine (TCGA)	Y35N
TCGA-B5-A11W-01	Uterine (TCGA)	Y35N
KMRC20_KIDNEY	CCLE (Novartis/Broad 2012)	Y35del
TCGA-2G-AAGJ-01	Testicular germ cell (TCGA)	Y35*

A) Figure is adapted from the cBioPortal website [www.cbioportal.org]. Genomic alterations of Rheb in various cancer subtypes with the cancer sequencing dataset. B) Figure is also adapted from the cBioPortal website. Y35 locus contains the highest number of recurring somatic point mutations in Rheb. To show the importance of the Y35 location in respect to Rheb and other small GTPases, the first 60 amino acids of RHEB were aligned with KRAS, the effector domain is highlighted in blue. Y35 is indicated in Red. C) Table of the Y35 mutations, the cancer subtype, and the sample ID from the cBioPortal website.

Generation of Rheb Y35N expressing cell lines

To test the effect of Rheb Y35N mutation on cells, first I generated an NIH3T3 cell line stably expressing Rheb Y35N using lentiviral transduction gene delivery method. Specifically, I used a lentiviral transfer plasmid that drives expression of Rheb proteins under control of the CMV promoter. In addition, I generated NIH 3T3 cell lines expressing Rheb WT, and K-Ras G12V, a known cancer-transforming mutation found frequently in cancer. Western blot analysis showed all three cell lines had a 2-3-fold increase in RHEB or KRAS expression compared to control cell lines that were transduced with an empty expression vector (Figure 3.4.2A). Because I do not have a selectable marker in my lentiviral transfer plasmid, I performed the same western blot analysis several months later, after many rounds of passages and experiments. This was to ensure that the expression levels of my KRAS and RHEB mutants did not change over the course of experiments. I observed a similar 2-3 fold increase in RHEB and KRAS expression as I when I first measured their expression (Figure 3.4.2B).

Figure 3.4.2: Generation of NIH 3T3 Cell Lines Stably Expressing RHEB Y35N

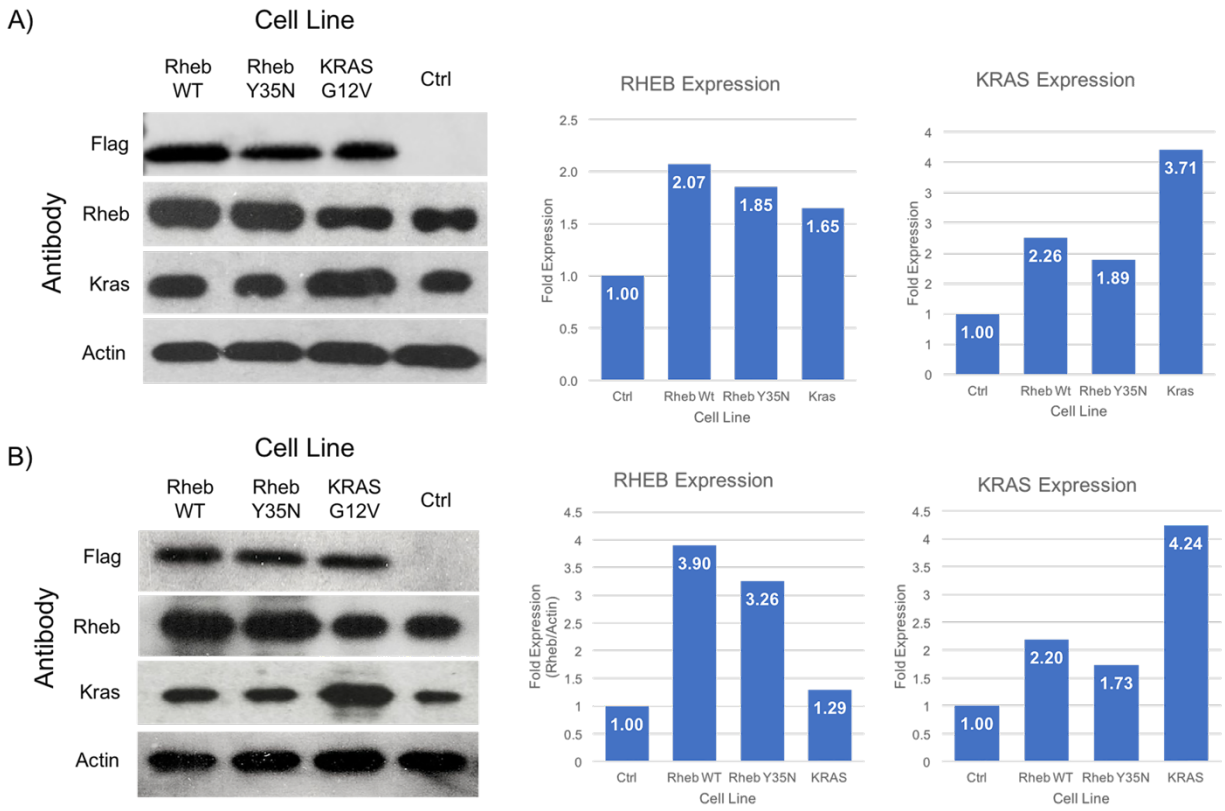

A) Western blot of FLAG, RHEB, KRAS, and ACTIN protein in total cell lysates collected from NIH-3T3 cell lines stably expressing RHEB WT, RHEB Y35N, KRAS G12V, or an empty vector expressing no protein (Ctrl). Fold expression for RHEB was calculated by identifying all band intensities using ImageJ analysis, then finding the ratio of RHEB/ACTIN for each sample. The Ctrl sample RHEB/ACTIN ratio was set at 1. All other samples' ratios were normalized to Ctrl. KRAS fold expression was calculated same as RHEB. B) Same analysis of RHEB and KRAS expression as in *A*, but after several months of growth, passages, and experiments.

Cancer cell transformation properties

Early genetic studies on cancer gene mutations used rodent fibroblast cell lines (NIH 3T3) to study mechanisms of malignant transformation [58]. NIH 3T3 cells were chosen in part because of their sensitivity to Ras mutant transformation and ease of transfection, and quickly became the gold-standard for use in biological assays for cancer transformation [59]. Transformation of normal cells into cancer cells is characterized by gaining the following attributes: reduced serum dependence, loss of density-dependent growth inhibition, and acquisition of anchorage-independent growth. The following sections will explain each of these attributes in more detail.

Rheb Y35N cell lines show increased growth under serum starvation

Fetal bovine serum (FBS) is usually added to cell culture media to provide essential growth factors required for cell proliferation. Media lacking FBS causes cells to grow at a much slower rate, or sometimes not at all. Transformed cancer cells are able to proliferate even without high levels of FBS, due to production of their own essential growth factors [60]. A common way to test cell cancer transformation, is to grow cells under serum starved conditions and then monitor their proliferation rates.

Under normal growth conditions, all cell lines showed similar growth rates (Figure 3.4.3A). However, under serum starved conditions, Rheb Y35N cells grew significantly better than Rheb WT cells (Figure 3.4.3B). While control cells died off, Rheb WT cells appeared to grow initially before tapering off around day 4 of no serum growth. Rheb Y35N cell lines appeared to grow strongly, with a similar growth curve as when grown under normal conditions. The ability of cells to grow in the absence of serum is indicative of transformed cancer cell lines, as we can see in the growth curve of KRAS G12V cell lines. Rheb Y35N cell lines appear to have a growth curve very similar to the KRAS G12V cell lines, indicating Rheb Y35N may transform cells into cancer-like cells.

Figure 3.4.3: Overexpression of RHEB Y35N Increases Cell Growth Under Serum Starvation

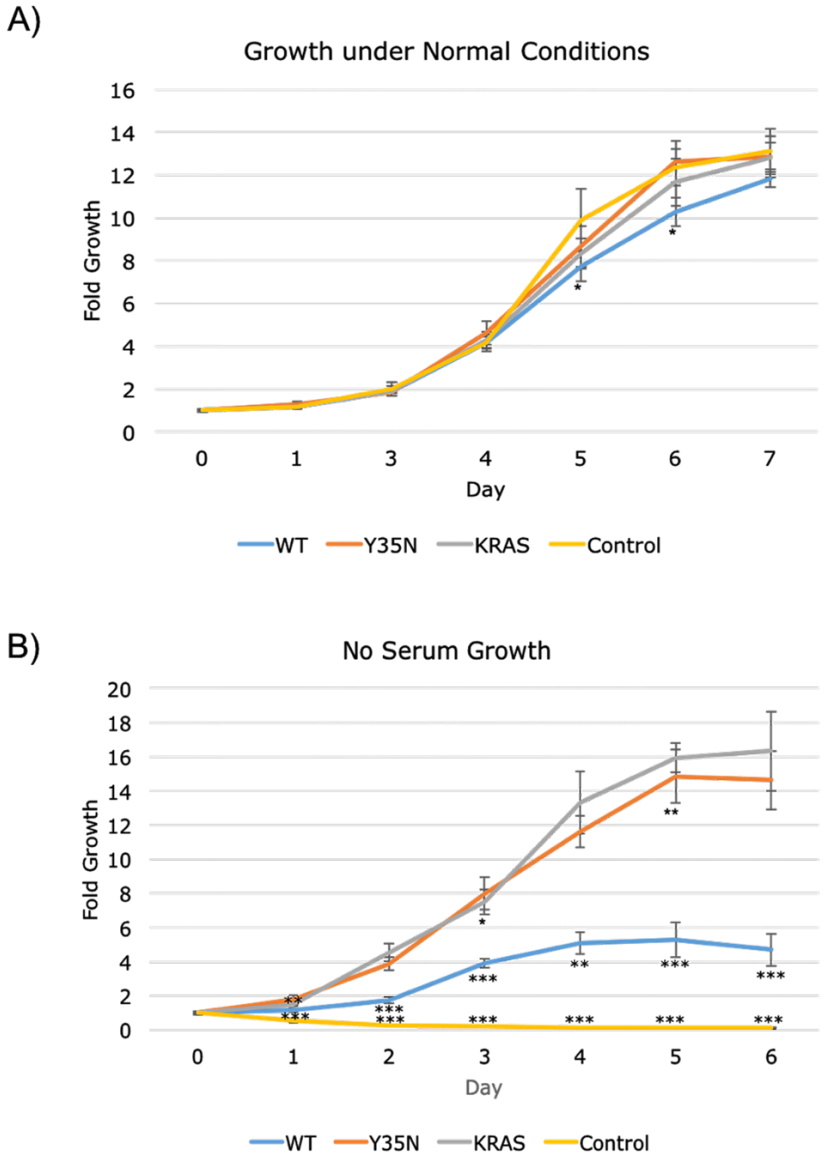

Growth curves of NIH 3T3 cell lines stably expressing RHEB WT, RHEB Y35N, or KRAS G12V grown in media containing 10% FBS (A), or serum-free media (B), for 7 days. Fold Growth was calculated as follows: (OD at day X) / (OD at day 0), where OD was read according to Cell Counting Kit-8 (Dojindo Mol. Tech.) protocol. Error bars are the standard deviation measured from 3 separate experiments, significance at each time point was calculated compared to KRAS values, *P<0.05, **P<0.01, ***P<0.001.

Rheb Y35N cell lines advance through the cell cycle under serum starvation

There are a series of cell cycle checkpoints to keep cells from growing uncontrollably, especially in conditions were nutrients are low. A common attribute of cancer cells is to ignore these cell cycle checkpoints and to continue advancing through the cell cycle. To measure this attribute in my cell lines, I stained DNA of the cells with propidium iodide (PI) and used flow cytometry to measure the percentage of cells in each stage of the cell cycle. Under normal conditions there was no significant differences between the RHEB Y35N, RHEB WT, KRAS G12V and control cell lines. Each cell line exhibited ~60% of cells in the G1 phase, ~17% in the S Phase, and ~23% in the G2 phase (Figure 3.4.4A).

However, cells grown in the absence of serum showed a drastically different cell cycle profile. RHEB WT and control cell lines showed a similar pattern, with significantly reduced percentages of cells in the S and G2 phase (Figure 3.4.4B). RHEB Y35N cell lines appeared un-phased by the absence of serum. The percentage of cells in the S and G2 phases was similar between serum starved and normal growth conditions (Figure 3.4.4B). Additionally, Rheb Y35N appeared similarly to KRAS G12V cell lines. This suggests that the Rheb Y35N mutation is promoting advancement through the cell cycle similar to oncogenic transformed cells.

Figure 3.4.4: RHEB Y35N Drives Cell Cycle Progression

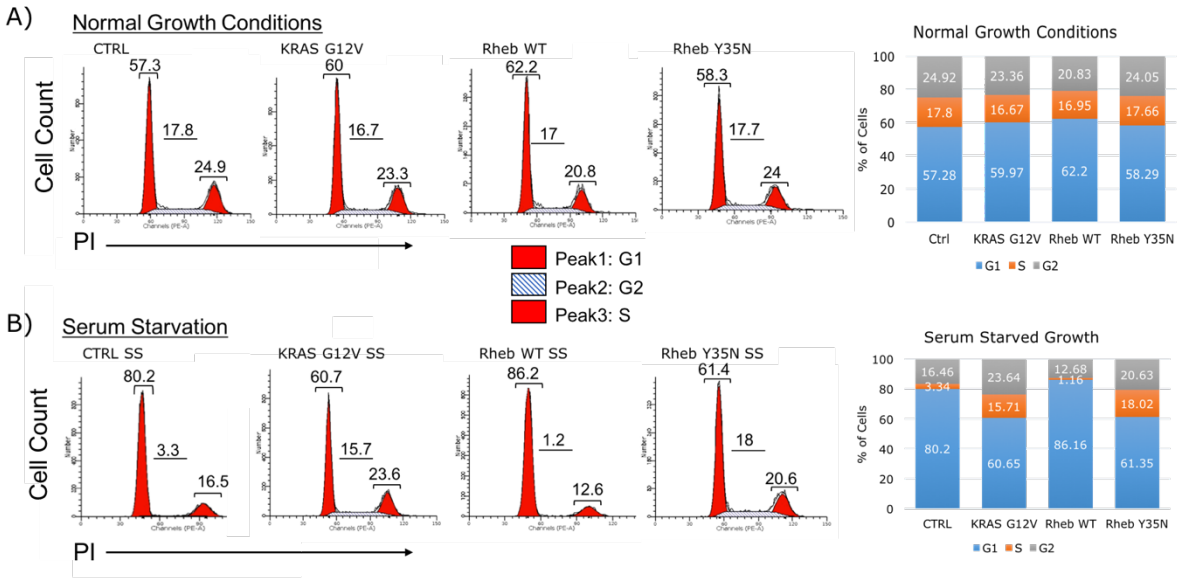

NIH 3T3 stably expressing cell lines were grown for 6 days with serum (A) or without serum (B). Cells were then fixed, treated with RNase A to remove RNA, and incubated with propidium iodide (PI) to dye DNA. Cells were grouped into cell cycle stage based on PI intensity measured using flow cytometry. The numbers above each bar represent percentage of cells in each phase. Graphs summarizing the percentages are shown to the right.

Rheb Y35N drives Foci Formation

Normal fibroblasts grown on cell culture plates will continue to grow and divide until they come into contact with neighboring cells and there is no more room for them to grow [61]. This phenomenon can be explained by transmembrane proteins that act as mechanotransducers to inhibit cell growth when they form intercellular contact junctions [62]. In cancer, these contact junctions are altered in such a way that cells continue to grow even when at high densities. The focus formation assay is a common way to measure the loss of density-dependent growth. Fibroblasts, transformed with an oncogenic mutant gene, are grown for several weeks past confluency, stained with crystal violet dye, and visualized under a microscope. The multicellular structures formed from this unimpeded growth are called foci. Using this assay, many researchers have shown Ras transformation of cells induces loss of density-dependent growth and promotes foci formation [59].

Performing the foci formation assay with the NIH 3T3 cell lines, I observed RHEB Y35N cells readily forming foci (Figure 3.4.5). The foci formed by RHEB Y35N cells lines were extremely similar in size and number to transformed KRAS G12V cancer cell lines. In addition, RHEB WT and control cells failed to form foci. This suggests that Rheb Y35N drives foci formation similar KRAS G12V.

Figure 3.4.5: RHEB Y35N Enables Foci Formation

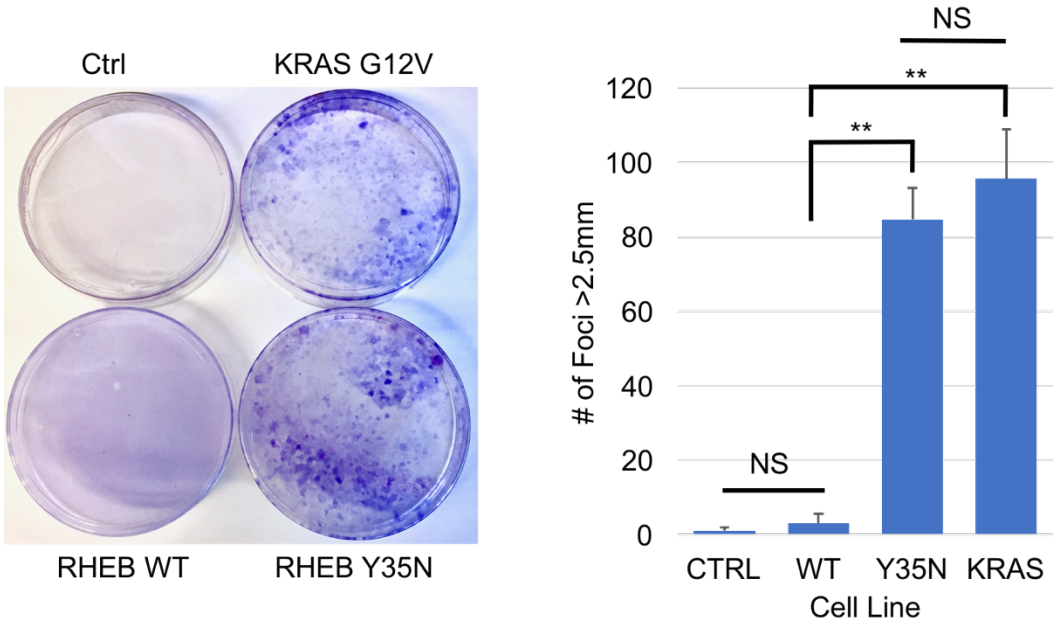

Foci Formation Assay. NIH 3T3 stably expressing cell lines were grown under low serum conditions for 3 weeks. *Left:* cells were fixed with methanol and stained with crystal violet dye for easy visualization. *Right*: Foci >2.5mm in diameter were counted. Error bars represent standard deviation from 3 separate experiments, *P<0.05, **P<0.01, ***P<0.001.

Rheb Y35N enables anchorage independent growth

Normal fibroblasts require a solid substratum to adhere in order to grow. However, transformed fibroblasts have the ability to grow in anchorage-independent environments, such as in liquid culture or when suspended in semisolid medium [63]. The mechanism behind cancer cells exhibiting anchorage independent growth is believed to be through several strategies, including: hyperactivation of cell survival and proliferation pathways, and alteration of ECM proteins to trick the cell into believing it is in the correct environment [64]. The most common assay to test anchorage independent growth is through the colony formation assay. In this assay, cells are suspended in a semi-solid media, and allow to grow for 3-4 weeks. Transformed cells will be able to divide and form colonies, which can be stained and easily visualized by eye.

I performed the colony formation assay with the NIH 3T3 cell lines using a semi-solid medium containing media and a low percentage of agar. After four weeks I observed Rheb Y35N expressing cell lines were able to grow and form colonies in suspension (Figure 3.4.6). They also grew in similar number to KRAS G12V expressing cells lines. In contrast, RHEB WT and control cell lines were unable to grow and form colonies in significant numbers. This suggests that RHEB Y35N confers the ability for anchorage independent growth similar to KRAS G12V expressing cell lines.

Figure 3.4.6: Rheb Y35N Enables Anchorage Independent Growth

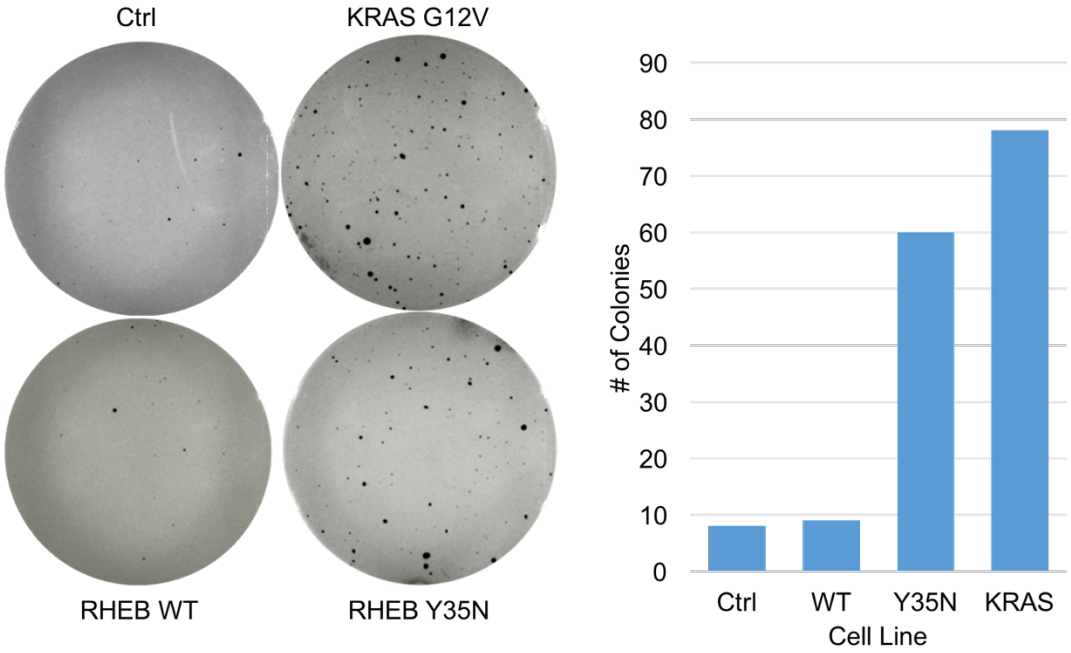

Soft Agar Colony Formation Assay. NIH 3T3 stably expressing cell lines were grown in Agar-Media suspension for 3 weeks. *Left:* Plates were incubated overnight with Nitroblue Tetrazolium Chloride (NBT) in order to visualize colonies on a gel imager. *Right:* Graph showing the number of colonies present.

RHEB Y35N Activates mTORC1 Similarly to RHEB WT

It appears Rheb Y35N confers cancer-like growth properties onto cells. To understand how this occurs I set out to characterize Rheb Y35N signaling in the cell, and identify how it differs from Rheb WT. The most obvious Rheb signaling pathway to look at first is mTORC1. mTORC1 activity can be quantified by measuring the phosphorylation levels of its downstream target S6. I grew the cell lines under normal and serum starved conditions, collected cell lysates, and performed western blot for phosphorylated and total S6 protein. In the absence of serum mTORC1 should be shut down and we should expect to see low levels of phosphorylated S6. However, in both the Rheb WT and Rheb Y35N cell lines we see a high level of phosphorylated S6 in the absence of serum (Figure 3.4.7A). This indicates that Rheb Y35N and Rheb WT activate mTORC1 at similar levels.

Next, I sought to determine if Rheb Y35N activation of mTORC1 contributes to the cancer-like growth phenotypes we observed in the previous studies. I treated cells with three different concentrations of rapamycin, a mTORC1 inhibitor, and measured the growth of cells after 48 hours. As expected, Rheb WT growth was greatly inhibited by increased rapamycin concentration (Figure 3.4.7B). However, Rheb Y35N was able to grow significantly more than Rheb WT, even at higher concentrations of rapamycin (Figure 3.4.7B).

To further test this observation, I tracked the growth curve of the cell lines treated with 20nM rapamycin over six days. I observed a large decrease in the growth curve of Rheb WT cells under rapamycin treatment, while Rheb Y35N cells appeared to be only slightly inhibited by rapamycin treatment (Figure 3.4.7C). These results suggest that while Rheb Y35N activates mTORC1 signaling similarly to Rheb WT, the cancer-growth phenotype we observe is not dependent on mTORC1 signaling.

Figure 3.4.7: RHEB Y35N Activates mTORC1 Similarly to RHEB WT

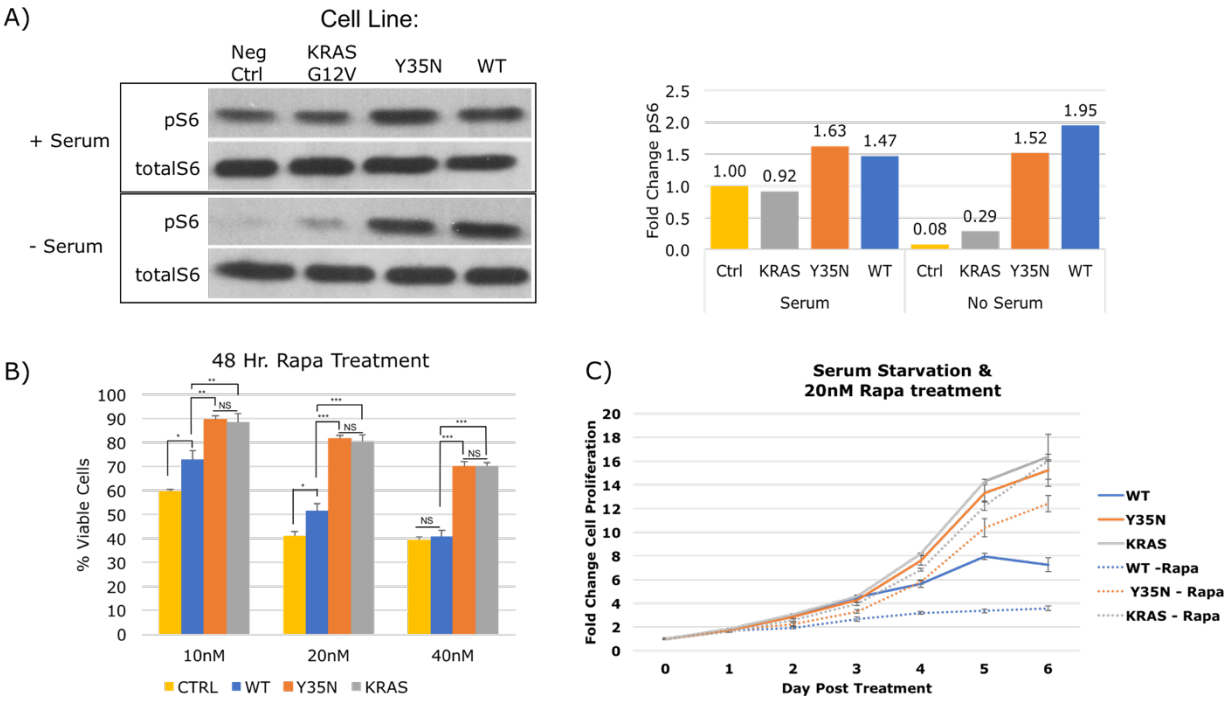

A) NIH 3T3 cell lines stably expressing RHEB WT, RHEB Y35N, KRAS G12V, or Ctrl were grown in the presence or absence of serum, and cell lysates were collected after 24 hours. Western blot was performed using antibodies for phosphorylated -S6, and total -S6. Fold expression for each protein (S6) was calculated as: (intensity of phosphorylated protein) / (intensity of total protein). All ratios were normalized to Ctrl under normal growth conditions. B) RHEB Y35N growth is not sensitive to mTORC1 inhibition. NIH 3T3 cell lines were treated with 3 different concentrations of mTORC1 inhibitor, Rapamycin, for 48 hours. % Viable Cells = (OD value of treated cells) / (OD value of non-treated cells) * 100. OD values were measured using Cell Counting Kit-8. C) RHEB Y35N cell lines are not sensitive to mTORC1 inhibition. NIH 3T3 cell lines were grown in serum-free conditions, with or without 20nM Rapamycin treatment. Growth was monitored using Cell Counting Kit-8 for 6 days.

Rheb Y35N Activates ERK Signaling

ERK is the major downstream signaling component of the RAS/RAF/MEK signaling pathway. Increased ERK signaling is the driving force behind active RAS mutant cancer transformation. Several studies have shown Rheb activates ERK signaling through various mechanisms. We sought to determine whether Rheb Y35N also has an effect on ERK signaling by measuring the phosphorylation of ERK protein. I grew the cell lines under normal and serum starved conditions, collected cell lysates, and performed western blot for phosphorylated and total ERK protein. In the absence of serum, RAS/RAF/MEK should be shut down and we should expect to see low levels of phosphorylated ERK. Our results show Rheb Y35N cell lines still contain high levels of phosphorylated ERK in the absence of serum. These levels were similar to those seen in KRAS G12V cells (Figure 3.4.8A). Rheb WT shows slightly elevated levels of phosphorylated ERK, but at much lower levels than Rheb Y35N or KRAS G12V cells. This could be due to increased KRAS expression in the RHEB WT NIH 3T3 cell lines (Figure 3.4.2).

Because RHEB Y35N displayed similar characteristics to KRAS G12V cell lines, I hypothesized that the observed cancer-like growth phenotypes in Rheb Y35N cell lines was due to activation of ERK signaling. To test this, I treated the cell lines with three different concentrations of U0126, a MEK inhibitor, and measured their growth after 48 hours. Rheb Y35N and KRAS G12V viability was greatly reduced by U0126 treatment at all three concentrations of (Figure 3.4.8B). However, Rheb WT viability was significantly greater at 1uM and 10uM U0126 treatment.

To further examine the effect of RAS/RAF/MEK inhibition on Rheb Y35N cells, I tracked the growth curve of the cell lines grown in the absence of serum and treated with 10uM U0126 over six days. I observed a large decrease in the growth curve of Rheb Y35N cells under U0126 treatment, while Rheb WT cells appeared to be only slightly inhibited by U0126 treatment (Figure 3.4.8C). These results suggest that unlike Rheb WT, Rheb Y35N activates RAS/RAF/MEK signaling and this is the reason for Rheb Y35N mediated cancer growth properties.

Figure 3.4.8: RHEB Y35N Activates ERK Signaling

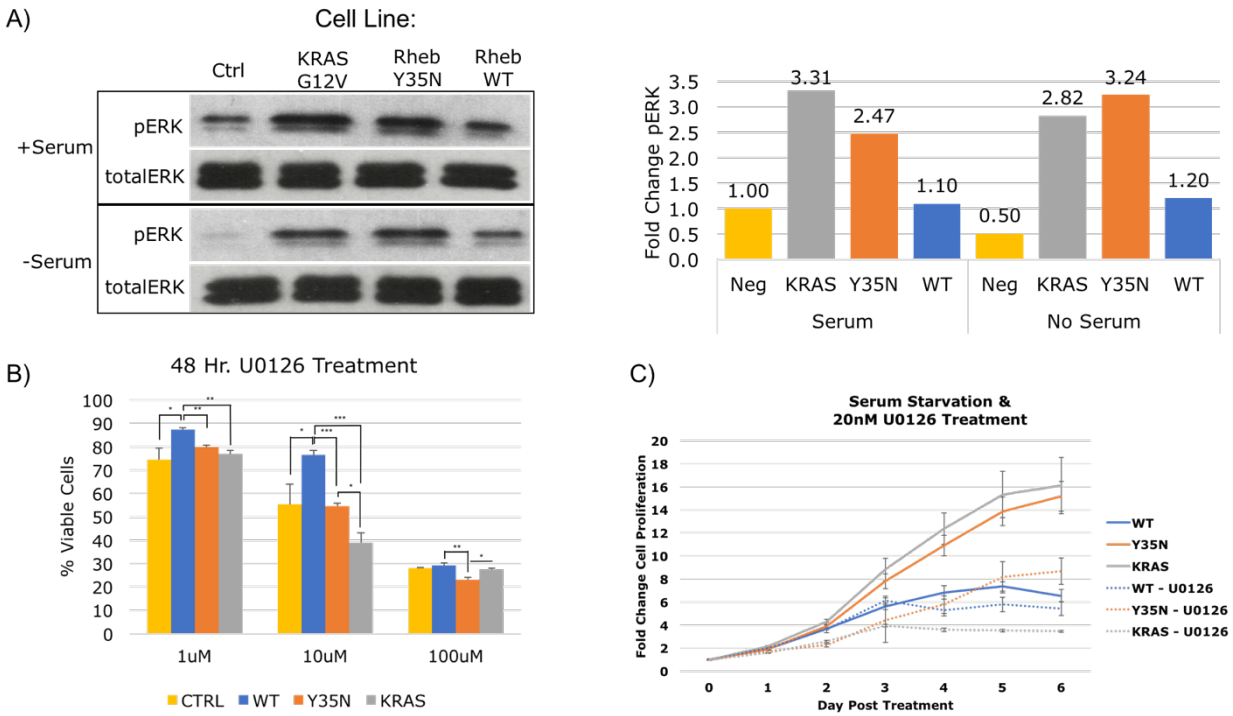

A) RHEB Y35N strongly activates mTORC1. NIH 3T3 cell lines stably expressing RHEB WT, RHEB Y35N, KRAS G12V, or Ctrl were grown in the presence or absence of serum, and cell lysates were collected after 24 hours. Western blot was performed using antibodies for phosphorylated -ERK, and total -ERK. Fold expression for each protein (S6 or ERK) was calculated as: (intensity of phosphorylated protein) / (intensity of total protein). All ratios were normalized to Ctrl under normal growth conditions. B) RHEB Y35N growth is sensitive to Erk inhibition. NIH 3T3 cell lines were treated with 3 different concentrations of MAPK inhibitor, U0126, for 48 hours. % Viable Cells = (OD value of treated cells) / (OD value of non-treated cells) * 100. OD values were measured using Cell Counting Kit-8. C) RHEB Y35N cell lines are sensitive to Erk inhibition. NIH 3T3 cell lines were grown in serum-free conditions, with or without 10uM U0126 treatment. Growth was monitored using Cell Counting Kit-8 for 6 days.

RHEB and ERK Signaling

Previous studies have reported that Rheb inhibits Raf signaling directly. Early *in vitro* studies show Rheb inhibits Raf mediated cancer transformation of cells, and interacts directly with Raf-1 (C-Raf), when mixed with insect cell lysates overexpressing Raf-1 [65], [66]. However, later studies in mammalian cells showed that while RHEB inhibits both BRAF and CRAF activity, RHEB only binds BRAF, and not CRAF [67]. Additional studies have confirmed that RHEB inhibits BRAF kinase activity independently of mTORC1 [68], [69]. The proposed mechanism is that Rheb binding to BRAF inhibits two events required for Raf activation; 1. RHEB prevents BRAF/CRAF hetero- and homo-dimerization, and 2. RHEB prevents BRAF association with RAS.

RHEB Knockdown Results in ERK Activation

Previous reports suggested that Rheb binds to and inhibits BRAF activity [67]–[69]. To test this, I looked at the levels of phosphorylated-ERK in the lysates of cells where RHEB is knocked out compared with cells where there is endogenous RHEB. Briefly, I generated Rheb knockdown cell lines by using lentiviral integration of RHEB shRNA into HEK 293T cells. I generated three separate cell lines expressing three different shRNA sequences. I found shRNA1 construct was the strongest at RHEB knockdown as evidenced by western blot showing decreased RHEB and decreased phosphorylated S6K, an indicator of mTORC1 shut down (Figure 3.4.9A). In this cell line I observed increased levels of phosphorylated-ERK compared with control cell lines expressing RHEB endogenously (Figure 3.4.9B). This suggests that RHEB WT inhibits Raf/Mek/Erk pathway in cells.

RHEB Overexpression Results in ERK Inhibition

We hypothesized that the RHEB Y35N mutant activates BRAF in cells through less effective binding, while RHEB WT binds BRAF stronger and inhibits BRAF signaling. We decided to see if the overexpression of RHEB WT in the RHEB Y35N stably expressing cell lines would

decrease Raf/Mek/Erk pathway. To achieve this, I transiently transfected Rheb WT into the RHEB Y35N expressing cell lines and monitored changes in levels of phosphorylated-ERK. I saw that expression of RHEB WT in RHEB Y35N cell lines resulted in a significant decrease of phosphorylated-ERK (Figure 3.4.9C). This suggests that RHEB Y35N activates, or at least does not inhibit, the Raf/Mek/Erk pathway.

Figure 3.4.9: RHEB Knockdown Results in ERK Activation, RHEB Overexpression Results in ERK Inhibition

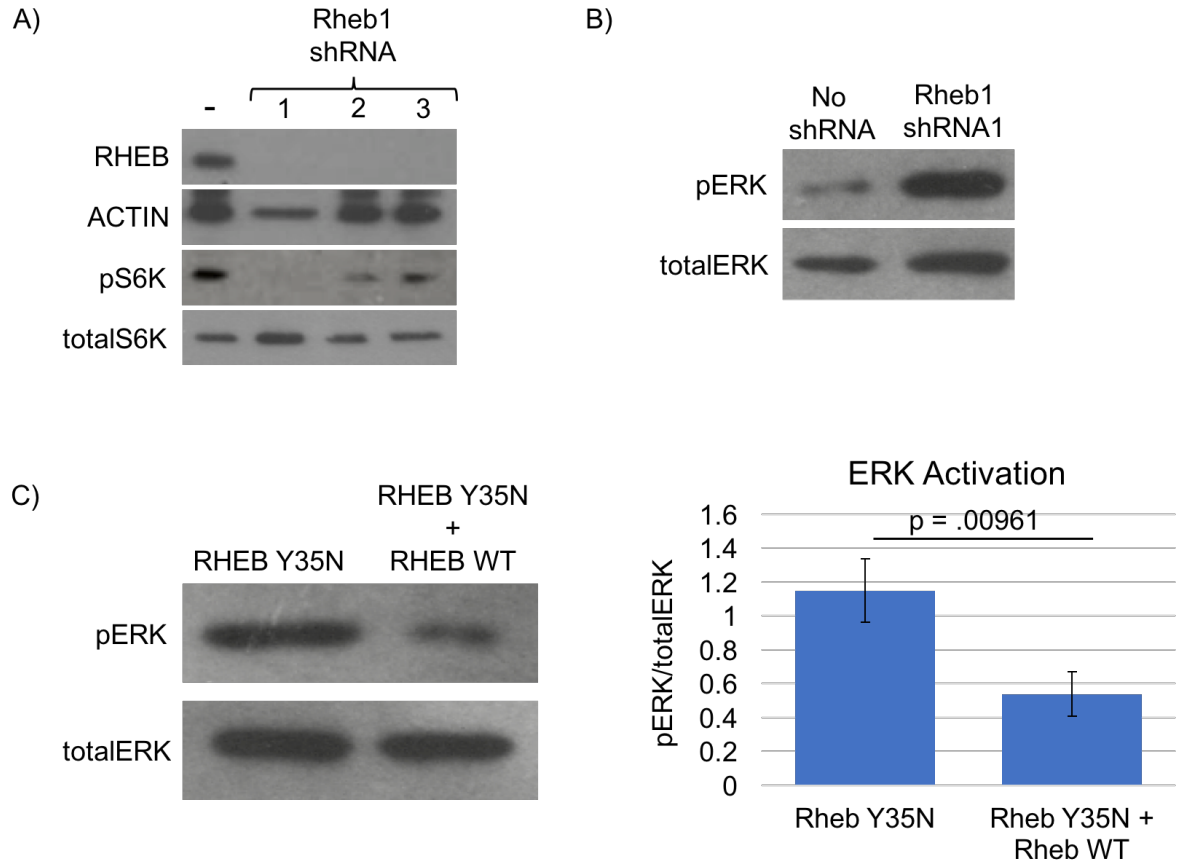

A) Three HEK 293T cell lines stably expressing different Rheb1 shRNA constructs were generated using lentiviral transduction. Western blots for RHEB protein are shown. To confirm a decrease in mTORC1 activity resulting from effective Rheb knockdown, western blot for phosphorylatedS6K (pS6K) is also shown. B) Western blot showing levels of phosphorylated-ERK (pERK) in Rheb knockdown cells versus control cells (No shRNA). The HEK 293T cell line expressing Rheb1 shRNA construct 1, from *A,* is shown. C) NIH 3T3 cell lines stably expressing Y35N were transiently transfected with plasmids to overexpress RHEB WT. *Left:* Western blot for phosphorylated-ERK (pERK) is shown. *Right:* Graph showing levels of pERK/totalERK in RHEB Y35N cell lines versus RHEB Y35N cells overexpressing RHEB WT. Numbers are from ImageJ analysis of western blot band intensities from three separate experiments.

RHEB binds BRAF and RHEB Y35N is less effective in binding B-Raf

To identify the mechanism of RHEB Y35N activation of ERK signaling, I first looked to see if RHEB Y35N binds RAF similar to RHEB WT. To accomplish this, I expressed FLAG-tagged RHEB WT or RHEB-Y35N in HEK293T cells, collected the cell lysates, and performed an immunoprecipitation using anti-FLAG antibody. Western blot analysis using BRAF and CRAF antibodies revealed that both RHEB WT and RHEB Y35N bind BRAF (Figure 3.4.10). Neither RHEB protein interacted with C-RAF. This result confirms an earlier report that Rheb WT binds BRAF and not CRAF. Interestingly, RHEB Y35N binds BRAF much less effectively than RHEB WT (Figure 3.4.10).

Figure 3.4.10: RHEB Y35N Binds BRAF Less Effectively than RHEB WT

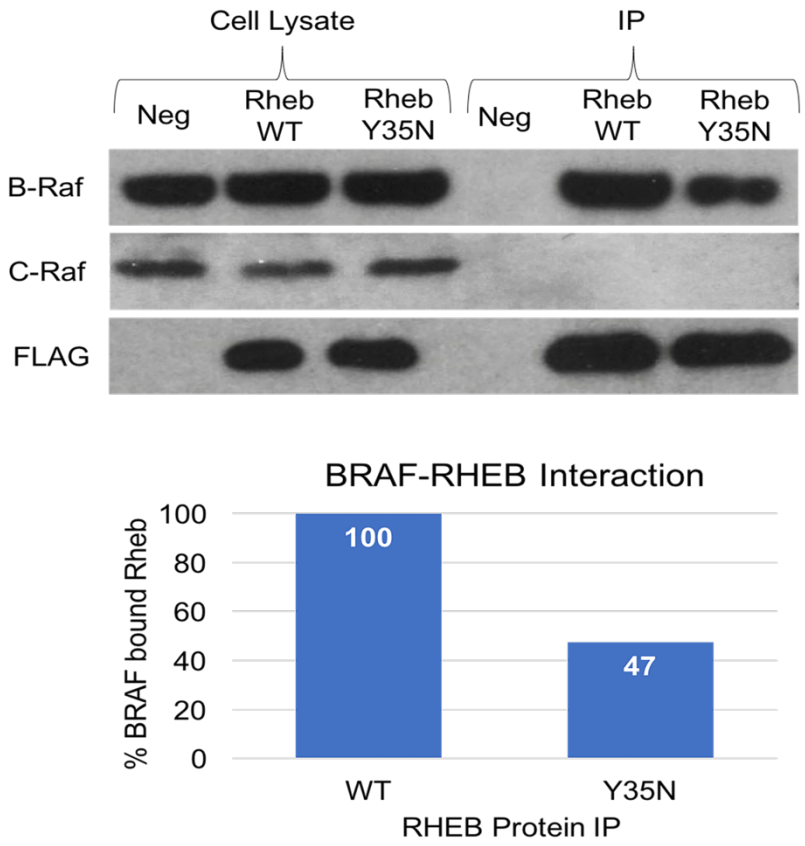

Top: Western blot for BRAF, CRAF, and FLAG is shown. HEK 293T cells were transfected with plasmids expressing FLAG-RHEB WT, FLAG-RHEB Y35N, or an empty plasmid expressing no protein (Neg). Cell Lysate was collected 48 hours post transfection, and an immunoprecipitation (IP) using anti-FLAG antibody was carried out. Bottom: Percentage of BRAF bound Rheb was calculated as a ratio of BRAF/FLAG western blot intensities. Where RHEB WT ratio was set at 100% and RHEB Y35N was normalized to RHEB WT. Results are from 3 separate experiments.

RHEB Y35N Does Not Interfere with BRAF/CRAF Dimerization in contrast to RHEB WT

Previous publications propose that RHEB WT binds BRAF and prevents BRAF/CRAF dimerization [67]. My results show RHEB Y35N binds BRAF less effectively than RHEB WT. Thus, it is possible RHEB Y35N allows more BRAF/CRAF dimerization than RHEB WT. To explore this hypothesis, I performed immunoprecipitation of BRAF in the cell lines stably expressing RHEB WT or RHEB Y35N. To observe BRAF/CRAF dimerization, I then performed a western blot for CRAF from my BRAF immunoprecipitated samples (Figure 3.4.11). I observed virtually no CRAF bands in the RHEB WT expressing cells, representing little BRAF/CRAF dimerization. However, I saw bands for CRAF in the RHEB Y35N expressing cells, suggesting that RHEB Y35N does not interfere with BRAF/CRAF dimerization (Figure 3.4.11).

The complete absence of CRAF bands in the RHEB WT lane is surprising. In these cell lines RHEB WT is overexpressed, so it is possible that overexpression of RHEB WT is strongly inhibiting BRAF/CRAF dimerization. RHEB Y35N overexpression in cells that also express endogenous levels of RHEB WT show the presence of a CRAF band. This suggests that endogenous levels of RHEB WT inhibit BRAF/CRAF dimerization at more medium levels than what we see with the overexpression of RHEB WT.

Figure 3.4.11: RHEB Y35N Does Not Interfere with BRAF/CRAF Dimerization

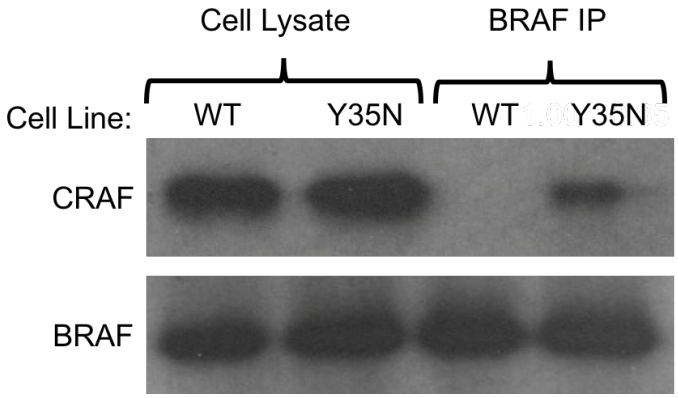

Cell lysates were collected from NIH 3T3 cell lines stably expressing RHEB WT or RHEB Y35N. Immunoprecipitation of endogenous BRAF was performed. Western blots against CRAF and BRAF are shown.

RHEB Y35N Binds AMPK and Inhibits AMPK Activity Similar to RHEB WT

While I was working on these experiments, a publication came out suggesting Rheb Y35N activates BRAF through the AMPK pathway [70]. AMPK is known to phosphorylate and inhibit BRAF, and a previous study has shown Rheb WT to bind and activate AMPK [71], [72]. The authors propose a mechanism in which Rheb Y35N outcompetes Rheb WT for AMPK binding, resulting in inhibition of AMPK signaling.

I performed several experiments to test RHEB Y35N effects on AMPK and my results differ from theirs in the following aspects. First, I performed an immunoprecipitation of RHEB Y35N, RHEB WT and RHEB T38A and looked at Y35N binding. I observed that RHEB Y35N bound AMPK less effectively than RHEB WT (Figure 3.4.12A). Additionally, I performed an AMPK activation assay in my NIH 3T3 cell lines and observed that RHEB Y35N and RHEB WT similarly inhibited AMPK activity (Figure 3.4.12B).

These results lead me to believe that ERK activation in Y35N cells is not primarily due to AMPK inhibition. It is possible that AMPK inhibition plays a minor role in BRAF activation, but the observation that RHEB WT and RHEB Y35N have similar effects on AMPK can't explain the large differences observed between WT and Y35N cell lines.

Figure 3.4.12: RHEB Y35N Binds AMPK and Inhibits AMPK Activity Similar to RHEB WT

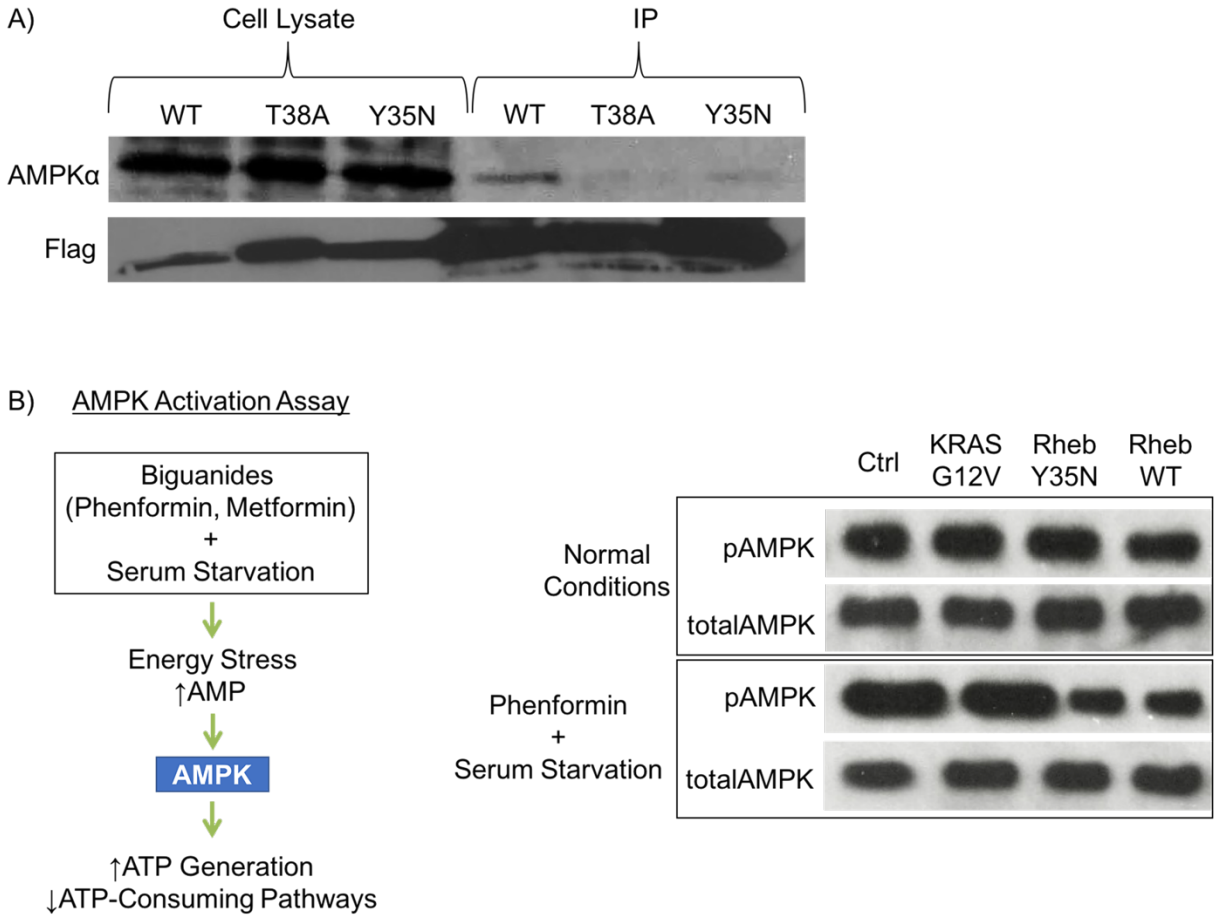

A) Rheb WT, T38A, and Y35N mutants were transiently transfected and expressed in HEK 293T cells, cell lysates were collected, and immunoprecipitation for each was carried out. These results show a Western blot for AMPKα and FLAG from those samples. B) Left: Overview of AMPK activation assay carried out in the NIH 3T3 cell lines stably expressing KRAS G12V, RHEB Y35N and RHEB WT. Right: western blot for phosphorylated AMPKα (pAMPK) and total AMPKα in cell lysates of NIH 3T3 cell lines stably expressing KRAS G12V, RHEB Y35N, and RHEB WT. Results from two different cellular conditions are shown, normal growth conditions of cells (top) and AMPK activation assay conditions (bottom).

Proposed model for RHEB Y35N activation of BRAF

These results suggest a model in which RHEB Y35N binds BRAF less effectively than RHEB WT. This reduced interaction allows for better BRAF/CRAF dimerization, leading to activation of ERK signaling (Figure 3.4.13). BRAF needs to be dimerized with itself or with CRAF for activation and downstream signaling of the RAF/MEK/ERK pathway [73]. It is suggested this is due to interaction with RAS dimers [74]–[76]. We propose that RHEB dimers block BRAF dimer formation by possibly interfering with RAS-BRAF binding. Overexpression of mutant RHEB Y35N dilutes the inhibitory effects of WT RHEB by forming WT-Y35N heterodimers that cannot efficiently bind BRAF. This allows for increased BRAF dimerization with Ras proteins.

*At the time of writing this thesis, I am in the process of preparing a manuscript for publication covering the results from this section **3.4 BRAF**.

Figure 3.4.13: Proposed Model for RHEB Y35N Activation of BRAF

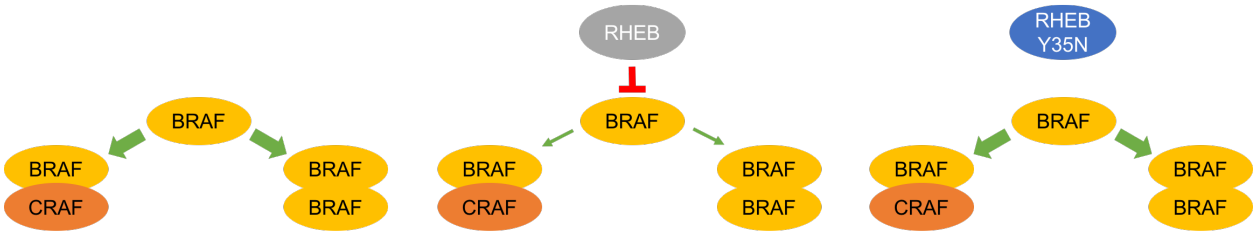

This is the proposed model for RHEB Y35N activation of RAF/MEK/ERK signaling. I propose a mechanism in which RHEB Y35N binds BRAF less effectively than RHEB WT, thereby freeing up BRAF/CRAF to form hetero- and homo-dimers and activate downstream signaling.

CHAPTER 4:

SUMMARY OF FINDINGS, SIGNIFICANCE, AND ALTERNATIVE APPROACHES

4.1 Summary

CAD

CAD is the protein responsible for carrying out the first three enzymatic steps of *de novo* pyrimidine nucleotide biosynthesis. I identified CAD as an effector protein for Rheb using a combination of techniques including mutant RHEB protein expression, immunoprecipitation, western blotting, and mass spectrometry. I showed that CAD interacted less effectively with the Rheb effector domain mutant (RHEB T38A) than with normal RHEB. I also demonstrated this interaction was dependent on RHEB-GTP loading. Additional experiments using size exclusion chromatography and non-denaturing protein separating gels, identified strong RHEB-CAD complexes around 520kDA, and 780kDa in size. I also found that RHEB binds CAD at an important UTP inhibitory region of the Carbamoyl-phosphate synthetase domain. I showed that RHEB stimulated CAD activity both *in vitro* and *in vivo,* but does not appear to desensitize CAD to regulation by UTP. Additionally, I observed RHEB and CAD colocalize at the lysosome. All of these experiments identify CAD as the first Rheb effector protein outside of mTORC1.

We have narrowed down the region of CAD where Rheb interacts. This Rheb-binding region is located in the CPSase domain and overlaps with a UTP and PRPP binding site that regulates CPSase activity [47]. UTP is end product of pyrimidine nucleotide biosynthesis and acts a negative feedback loop to inhibit CPSase activity. PRPP is a substrate required for UMP synthesis, and excess amounts of PRPP result in stimulation of CAD activity [45]. It would be interesting to further define this interface through co-crystallization and molecular modeling to identify mutations or small peptides that could alter this interaction. One possibility is that Rheb binding interferes with the binding of UTP and PRPP. However, my *in vitro* studies imply that CAD activity is still inhibited by UTP even in the presence of RHEB. We do not know if PRPP has an additive effect or no effect on RHEB-CAD binding and activation.

It has been reported that S6K phosphorylates and activates CAD, downstream of mTORC1 [39], [40]. The S6K binding site is located at Serine-1859, a large distance away from

the Rheb binding region we have identified. In addition, our *in vitro* experiments show RHEB can directly stimulate CAD activity. Thus, my findings suggest that there are two ways to activate CAD. Rheb can activate CAD through stimulation of mTORC1/S6K, and Rheb can directly stimulate CAD activity. In both cases, Rheb plays an important role in generating pyrimidine nucleotide biosynthesis in the cell.

The identification of RHEB-CAD complexes existing around 500kDa and 700kDa is interesting because previous experiments reported CAD to forms oligomers in cells, and is required for CAD activity [77]. Recent publications show that S6K phosphorylation of Serine-1859 on CAD promotes CAD oligomerization and activation [39]. My data shows possible CAD dimers and trimers in the presence of Rheb overexpression. It is possible Rheb promotes CAD oligomerization and activation. It is also possible there are other proteins in the RHEB-CAD complex to account for this size. However, after the samples were subjected to size exclusion chromatography, I did not see any other protein bands in the SDS-PAGE of RHEB-CAD fractions. Further experiments are needed to test if Rheb affects CAD oligomerization as a method for CAD activation.

Another important finding from my studies is Rheb affects cellular localization of CAD. Rheb has been shown previously to be crucial for the proper localization of TSC and mTORC1 to the lysosome, and that this localization is key for activation of mTORC1 signaling [31], [32]. We observed CAD localization change from primarily cytoplasmic to largely lysosomal, when Rheb was overexpressed in cells. Additionally, FTI treatment inhibiting Rheb localization to lysosomes, also caused CAD to return to cytoplasmic localization with little lysosomal overlap. This suggests that Rheb recruits CAD to lysosomes and may be important for CAD function. RHEB-CAD identification is an important stepping stone in uncovering RHEB's function in signal transduction in the cell. Since mTORC1 activation occurs on lysosomes, my results raise the possibility that both mTORC1 and CAD activation occurs on the lysosomal membrane. Studies have reported that amino acids accumulate in the lysosomes resulting in the activation of mTORC1 [78]. Thus it

is possible that CAD-lysosomal localization is important for CAD access to glutamine, the amino acid required for the first step in CAD enzymatic activity.

The RHEB-CAD interaction has important implications for cellular signaling. I showed that RHEB stimulated CAD activity resulting in increased pyrimidine nucleotide levels in the cell. Nucelotide biosynthesis has long been a target for anti-cancer and anti-viral medications, including antifolates and nucleoside analogs [79]. Relatively little is known about the signaling proteins controlling nucleotide synthesis, and no previous protein has been identified that directly regulates CAD activity. Thus, RHEB-CAD interaction is extremely interesting, and provides an opportunity as a potential therapeutic target.

AMPK

AMPK is an important energy-sensing protein-complex responsible for the regulation of many diverse signaling pathways in the cell. AMPK becomes activated when the cell becomes stressed (usually through high ratio of AMP/ATP). AMPK activates catabolic pathways to generate more energy for the cell, and shuts down energy consuming pathways. I have shown that RHEB interacts with the AMPKα subunit in an effector domain dependent manner. In addition, I have shown that AMPKα interaction is specific to RHEB among other small GTPases, and that AMPKα appears to colocalize with RHEB on the lysosomes. I also report evidence that RHEB inhibits AMPKα phosphorylation/activation in cells under high stress. These results suggest Rheb signaling controls another important energy sensing pathway in the cell, outside of mTORC1.

Studies have shown that AMPK inhibits mTORC1 activity through the phosphorylation of one of its subunits, RAPTOR, and through phosphorylation and activation of TSC [80], [81]. mTORC1 induces cell proliferation which uses considerable cellular energy, when that energy becomes diminished AMPK becomes activated and shuts down mTORC1. My results suggest a feedback loop, where RHEB inhibits AMPK resulting in decreased TSC2 activation, and increased

Rheb signaling. My results show that Rheb overexpression inhibits AMPK activation even when cells are stressed. This suggests that in conditions where RHEB is overexpressed or overactive, RHEB could shut down AMPK and promote cellular growth through increased activation of signaling pathways downstream of Rheb.

A previous publication reported Rheb activates AMPK [72]. However, my results show that overexpression of Rheb inhibits AMPK activation in response to phenformin treatment. There are a few major differences between my experiments and theirs. Firstly, we used very different cell lines. In their experiments, they used a TSC2+/+ cell line, that is also p53-/-. When this cell line was generated with the purpose of TSC2 knockout only, it was discovered that the cells did not grow without p53 also being knocked out [82], [83]. In order to generate a control cell line, they therefore added back TSC2, but kept p53 knocked out. It could be that the absence of p53 in these cells alters RHEB's ability to inhibit AMPK, thus resulting in what appears to be activation of AMPK. Second, we subjected the cells to different treatments. I put the cells under great stress by combining serum starvation and phenformin treatment to strongly activate AMPK. It may be that Rheb inhibition of AMPK can only be detected when there is a strong need for AMPK activation. This would be the case in proliferating tumor cells that are vastly outgrowing their nutrient-depleted surroundings.

Little is known about AMPK localization, and whether it changes based on activation. My results suggest AMPK lysosomal localization is dependent on RHEB, because overexpression of RHEB protein results in further accumulation of AMPK on lysosomes. Previous experiments have shown Rheb affects mTORC1 activity by keeping it at the lysosomal surface, and is required for TSC mediated signaling [32], [33]. My previous results with RHEB-CAD show a similar alteration in CAD localization in response to RHEB overexpression. These experiments suggest RHEB is responsible for localization of mTORC1, AMPK, and CAD to the lysosomal membrane where crucial signaling pathways are controlled.

Another important finding is that RHEB binds only to the AMPKα subunit, and not the β or γ subunits. It is possible Rheb disrupts the AMPK complex by binding the α subunit and preventing β or γ subunits from binding, or sequestering the α subunit away from the β and γ subunits. I believe this could be the mechanism for Rheb mediated inhibition of AMPK, but further experiments are needed to test this hypothesis.

BRAF

Another downstream effector I studied is BRAF. Past experiments have revealed that RHEB binds to and inhibits BRAF activity [67]–[69]. In those publications, it was revealed that RHEB interaction with BRAF inhibits BRAF from binding H-RAS or dimerizing with CRAF, both events that stimulate activation of Raf signaling. My experiments confirm the binding of RHEB to BRAF and not CRAF. Interestingly, this RHEB-BRAF interaction is altered in the RHEB Y35N mutant. My results show that RHEB Y35N binds BRAF at much lower levels than RHEB WT. We also see a significant increase in ERK signaling in RHEB Y35N compared with RHEB WT. From these results, combined with the previous publications on RHEB-BRAF interaction, I propose a mechanism where RHEB Y35N transforms cells through less effective binding of BRAF resulting in activation of BRAF and increased Raf/Mek/Erk signaling. In support of this idea, my results show that RHEB Y35N expressing cells are significantly more sensitive to ERK inhibition than RHEB WT expressing cell lines. Additionally, the RHEB Y35N mutant does not appear to affect mTORC1 or AMPK any differently than RHEB WT. This suggests the transformative abilities of Y35N stem mainly from activation of the Raf/Mek/Erk pathway.

While I was working on these experiments, a publication came out suggesting Rheb Y35N activates BRAF through the AMPK pathway [70]. In this paper, the authors propose a mechanism in which the RHEB Y35N mutant outcompetes RHEB WT for AMPK binding, resulting in inhibition of AMPK signaling. My results show that RHEB Y35N binds AMPK less effectively than RHEB

WT, and that RHEB Y35N and RHEB WT affect AMPK similarly. The authors point to previous studies where RHEB WT has been shown to bind and activate AMPK [72]. My results differ, in that they show both RHEB WT and RHEB Y35N inhibit AMPK activation under cellular stress. This leads me to believe that activation of Raf/MEK/Erk signaling in RHEB Y35N expressing cells is not primarily due to AMPK. It is possible that AMPK inhibition plays a role, but the observation that RHEB WT and RHEB Y35N both inhibit AMPK at similar levels, does not justify why there are such great differences between WT and Y35N cell lines.

The RHEB-BRAF interaction is an important addition to our understanding of Rheb signaling. It is interesting that RHEB WT inhibition of BRAF has not received more attention since its initial reports in the late 1990s to early 2000s. It may be that RHEB WT inhibition of BRAF signaling is only moderate in comparison to other controls of RAF signaling, or only relevant under certain conditions (i.e. serum starvation or certain cancers). The Y35N mutation appears to have a strong phenotypic effect on fibroblast cells, conferring attributes commonly seen in transformed cancer cells and similar to the effect KRAS G12V has on cells. Rheb, the Y35N mutation, and cancer are discussed further in section 4.3.

4.2 Multiple Downstream Effectors

The significant findings of my work have dramatically expanded our view of Rheb signaling. I have reported the identification of new Rheb-effector protein interactions that control multiple downstream signaling pathways. This includes Rheb interaction with mTORC1, CAD, AMPK, and BRAF (Figure 4.1). In addition, I present evidence that Rheb alters the signaling properties of each of these proteins. This work is of great biological significance, as all of these proteins control important singling pathways that have been linked to cancer and disease, and are therapeutic targets for these disorders.

Aberrant Rheb/mTORC1 signaling has been linked to proliferative diseases including cancer and tumor formation [37]. These diseases often arise from improper nutrient sensing and over activation or inappropriate inhibition of key signaling pathways in the cell. My results have demonstrated Rheb controls the signaling of many of these pathways. Quickly dividing cells require increased nucleotide pools in order to keep up with DNA synthesis for cell division. Rheb stimulation of CAD represents one method DNA synthesis could be increased in these cells, and is a potential therapeutic target for diseases with overactive Rheb. Additionally, AMPK is known to act as a tumor suppressor to shut down cell growth in times of low nutrients. My results show that Rheb prevents AMPK activation in the cell upon energy stress. Inhibition of AMPK also leads to further activation of RHEB/mTORC1 signaling through decreased phosphorylation and decreased activation of TSC. Thus, the RHEB-AMPK and RHEB-mTORC1 interactions may play a key role in supporting tumor growth.

My results, and previous publications, have presented evidence that RHEB inhibits BRAF signaling. The reason for this is unclear, as BRAF and mTORC1 promote similar pathways resulting in increased cellular growth and proliferation. It may be that BRAF and mTORC1 pathways compete for the same energy pool, so by inhibiting BRAF, Rheb is strengthening mTORC1 signaling. Interestingly, I show that a reoccurring cancer mutation in Rheb, RHEB Y35N, exhibits altered BRAF interaction that results in the activation of Raf/Mek/Erk signaling. In

addition, RHEB Y35N activated mTORC1 and inhibited AMPK similarly to RHEB WT. Through this combination of signaling pathway alterations we see that RHEB Y35N transforms cells similar to a KRAS G12V mutant. This is of extreme biological significance, as Rheb mutations in the right cellular context might drive cancer formation. Further studies *in vivo* would confirm the importance of Rheb mutations in cancer formation. Additionally, it would be interesting to see if Rheb Y35N, or other cancer mutations, affect the other Rheb signaling pathways presented in this dissertation.

Presence of multiple downstream effectors is a common feature of the Ras superfamily GTPases. For example, Ras activates Raf, PI3K, RalGDS, Rin1 and PKC. Ras mutations that selectively activate these downstream effectors have been identified and have been shown to be valuable in dissecting Ras functions [60]. Similar mutations may be generated for Rheb. I believe the RHEB Y35N mutation represents one such mutation, as RHEB Y35N exhibited different BRAF binding and signaling properties than RHEB WT, but both were similar at activating mTORC1 and inhibiting AMPK. Further analysis of Rheb mutants could help uncover additional Rheb signaling pathways in the cell.

Future studies on Rheb signaling should further define the conditions in which RHEB affects these effectors. One method my results suggest, is that RHEB may influence effector activation through changes in localization. It appears Rheb localization at the lysosome is crucial for activation of mTORC1, and my results show localization of CAD and AMPK to the lysosomes. This suggests RHEB controls signaling at the lysosomal membrane. Rheb signaling of specific pathways may also be dependent on the genetic background of the cell, and the specific signals the cell is receiving. AMPK, CAD, mTORC1, and BRAF are regulating my numerous different upstream pathways, and RHEB may play a central role in integrating those upstream signals.

Figure 4.1: A Proposed Model for Rheb Downstream Signaling

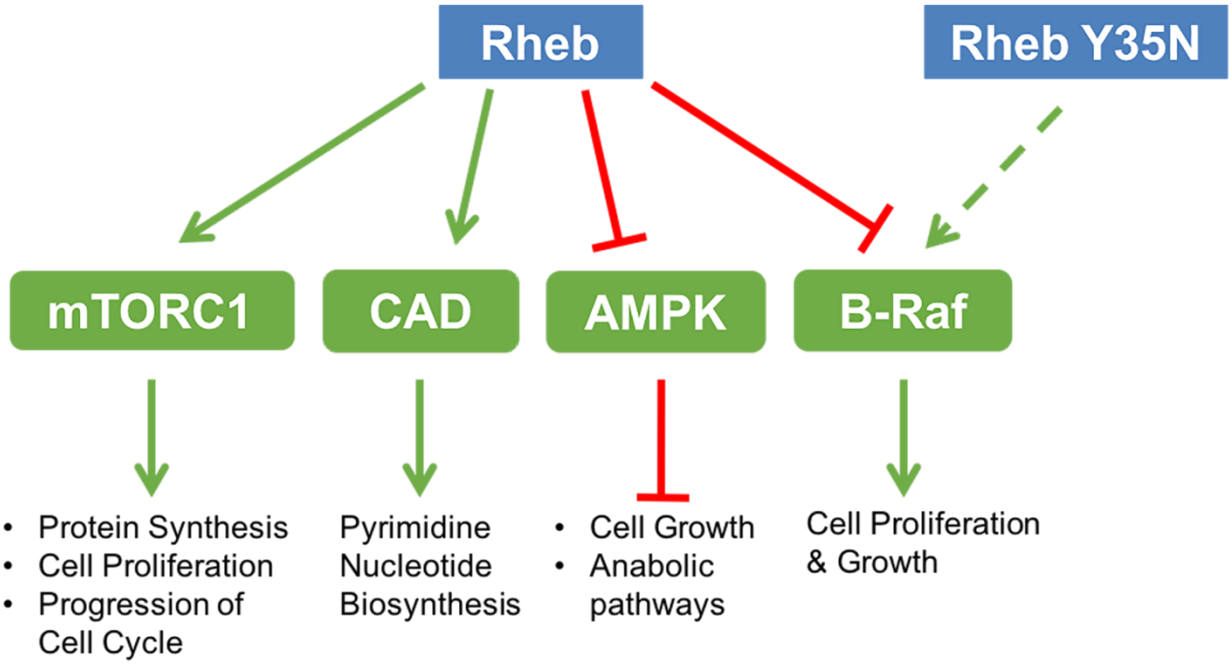

I have demonstrated that Rheb binds directly and activates mTORC1 signaling pathway to increase protein synthesis, cell proliferation and promote progression of the cell cycle. I have also revealed that Rheb binds CAD and stimulates pyrimidine nucleotide biosynthesis. I have shown Rheb binds AMPK and inhibits AMPK activity. Finally, I have shown that Rheb binds B-RAF, but that a reoccurring cancer mutation, Y35N, activates B-RAF resulting in cancer transformation of fibroblast cells.

4.3 Rheb Y35N Mutation and Cancer

Analysis of cancer genome databases uncovered an important Rheb mutation, Rheb Y35N. I showed that mouse embryonic fibroblasts stably expressing the RHEB Y35N mutant developed characteristics phenotypic of cancer cells, including: growth in the absence of serum, advancement through the cell cycle, anchorage-independent growth, and multilayer growth. The Y35N mutation was shown to not only stimulate mTORC1 activity, but also activate ERK. Additionally, it was shown that Y35N cancer growth was dependent on the activation of ERK signaling.

These results show a fascinating result, that a point mutation in Rheb can confer cancer-like properties onto cells. Point mutations at tyrosine 35 in Rheb are relatively rare, occurring in only 9 samples out of thousands that have been sequenced at TCGA. However, while many common cancer gene mutations have been identified (KRAS, EGFR, VHL, etc.), the majority of cancers are caused by genes that occur at frequencies <20%. Recently, researchers at MIT attempted to identify new cancer genes by looking for three factors: 1. genes that harbored point mutations in a significant pattern in cancer, 2. genes that have high mutational burden relative to background, and 3. clustering of mutations within evolutionary conserved sites [19]. These researchers identified 33 “novel” genes, one of which was the Rheb Y35N mutation. This mutation was found to be significant in clear cell renal cell carcinoma (ccRcc). This shows the importance of studying point mutations in proteins like Rheb, that are known to control crucial signaling pathways, regardless of how rare those mutations appear to occur.

Future experiments should focus on studying the effect RHEB Y35N has on the other Rheb signaling pathways identified in this dissertation. My results suggest see that Rheb Y35N stimulates mTORC1 and AMPK activity similar to Rheb WT, but its effect on CAD activity remains to be explored. Additionally, it remains unclear as to why this mutation is found significantly in kidney carcinoma. Perhaps the cellular environment and signaling of kidney cells is key for Rheb Y35N to drive cancer transformation. Clear cell renal cell carcinoma (ccRCC) appears to be

dependent on overactive VEGF receptor, a tyrosine kinase that transmits through several pathways including the Raf/Mek/Erk pathway [84]. Approved treatments for ccRCC target the Raf pathway, including sunitinib, a VEGFR inhibitor, and sorafenib, a RAF inhibitor [85], [86]. Thus, it is not surprising that RHEB Y35N may act through the BRAF pathway to transform cells, specifically in ccRcc. In fact, studies using mTORC1 inhibitors in combination with VEGFR inhibitors have shown therapeutic benefits in a subset of patients [87]. It may be that in patients suffering from ccRCC and carrying the RHEB Y35N mutation, should be targeted with a combination of RAF and mTOR inhibitors, as my results show RHEB Y35N strongly activates both pathways.

It would also be interesting to explore other Rheb point mutations found in cancer. While point mutations at tyrosine 35 are the most common, there are other 39 other point mutations that have been identified in cancer. Several interesting ones include mutations near the effector domain (V32 and E40), mutations at sites where previous studies identified Rheb activating mutations (S16 and G63), and mutations at a site where previous studies identified a dominant negative Rheb mutation (D60).

4.4 Alternative Approaches

In this dissertation, my approach to identify new Rheb effector proteins involved using expressing Rheb effector domain mutants, performing immunoprecipitation of Rheb proteins, and observing co-localization of proteins in the cell. In this section I would like to discuss alternative approaches that could be carried out in the future to identify new Rheb effectors and Rheb regulated signaling pathways.

Chemical Crosslinking

Another method would be to use chemical crosslinking to identify Rheb-protein interactions. The basic idea behind this method is that if you can add photoactivatable groups into proteins, you can use light to generate chemical crosslinking between your protein of interest and its interacting proteins. The protein of interest can then be immunoprecipitated, and interacting proteins can be identified using mass spectrometry analysis [88]. There are several advantages to this method over the method I performed. First, the chemical crosslinking would glue together the proteins in a strong complex. Knowing this, more rigorous washing could be performed during the immunoprecipitation, and thus lowering the potential number of proteins identified in your IP. Second, the addition of a photoactivatable group with a short crosslinker arm would ensure that only proteins in extremely close proximity of the protein of interest would become crosslinked upon photo activation. Third, because the timing of the crosslinking reaction can be controlled through light, one could potentially attempt the crosslinking procedure under various conditions to identify differences in protein-protein interactions.

Of course, there are several drawbacks to this method as well. Photoactivatable groups are added to proteins through the incorporation of unnatural amino acids. In order to accomplish this you must express your protein containing amber codons at sites where you want incorporation, suppressor tRNAs that recognize the amber codons, engineered tRNA synthetases

that will load the unnatural amino acids onto the suppressor tRNAs, and addition of the unnatural amino acids themselves [89]. This can be a time consuming and difficult procedure, although a powerful tool once successful.

BioID

BioID is another way to identify potential candidate protein interactions [90]. This method involves the use of a prokaryotic biotin ligase, BirA, that has been mutated to promote promiscuous biotinylation [91]–[93]. This mutant BirA can be fused to your protein of interest, and will add biotin to primary amines of adjacent interacting proteins. Biotinylated proteins can be easily isolated from cells and identified using mass spectrometry. The advantage of this approach is the ability to identify weak interactions that might otherwise be washed away during the immunoprecipitation steps. In addition, this method can be temporally induced through the use of an inducible promoter. The disadvantage of this procedure is the requirement of fusing biotin ligase to your protein of interest. In the case of Rheb, this would require fusing to the N-terminus, as the C-terminus is required for posttranslational modification and proper localization to lysosomal membranes. Additionally, the biotinylated proteins identified might not be truly interacting with the protein of interest and just be in close proximity, as the promiscuous BirA can biotinylate proteins within a 10 to 20 nm distance [93]. Also, false negatives may be produced if interacting proteins lack primary amines to be biotinylated.

Metabolomics

One method that could be performed is metabolomic analysis of cellular pathways in the cell. Metabolomic profiling using mass spectrometry is a powerful “omics” tool that is gaining traction as a new high throughput method of identifying the alteration of many pathways in the cell. This method can be used to take a snapshot of metabolites at a given time point, or combined with radio-labeled metabolites to measure flux through certain pathways. However, there are

limitations to this approach. The metabolome is extremely sensitive to environmental and genetic factors, and obtaining repeatable results requires rigorous attention to detail I order to replicate experimental conditions. Additionally, metabolomics analysis requires the use of NMR or mass spectrometry machines and along with analysis software to identify the metabolites. As is the problem with all omics methodologies that return lots of data, unless you have in depth-knowledge on a specific pathway you are interested in, it can be difficult to tease out which pathways are truly being effected. However, the software and statistical analysis packages are continuously being improved making these analyses easier for researchers to understand.

CHAPTER 5:

MATERIALS AND METHODS

Cell culture and transfection

HEK293T and HeLa cells were maintained in Dulbecco's modified Eagle's medium (DMEM) supplemented with 10% (vol/vol) fetal bovine serum and 1% (vol/vol) penicillin/ streptomycin. Cells were cultured at 37ºC in a 5% CO_2 incubator. Transfection was carried out using Lipofectamine 2000 (Invitrogen) according to the manufacturer's instructions.

FLAG Immunoprecipitation

HEK293T cells expressing FLAG tagged Rheb -WT, -T38A, -Q64L, H-Ras, RalA, Rac1, or GFP (control) were immunoprecipitated using anti-FLAG M2 affinity gel (Sigma). Briefly, the cells were lysed with lysis buffer (50mM HEPES pH 7.4, 150mM NaCl, 0.4% CHAPS, 1X Complete EDTA-free protease inhibitor cocktail (Roche), 1mM Na3VO4), 150 mM NaCl, 25 mM MgCl2), and the supernatant was cleared of cellular debris using centrifugation (16,000 × g for 10 min). Cleared supernatant was mixed with anti-FLAG M2 magnetic beads (Sigma) for affinity purification. The beads were collected, washed four times with lysis buffer. The remaining bound proteins were eluted three times with lysis buffer containing 62ug/mL of 3X FLAG peptide. Eluted proteins were concentrated using Amicon Ultra 0.5-ml centrifugal filters NMWL 10K (EMD Millipore, Billerica, MA).

Identification of CAD using Mass Spectrometry

After concentration, protein samples were subjected to SDS-PAGE and stained with SilverQuest silver staining kit (Invitrogen) according to the manufacturer's instructions. Protein bands were then excised from the silver-stained gel, in-gel-digested with trypsin, and subjected to nano-liquid chromatography-electrospray ionization mass spectrometry analysis using a DiNa nano-LC system (KYA Technologies) with an L-column 2 octyldecyl silane (0.05 mm by 100 mm, 3 µm; CERI) coupled to a QStar Elite hybrid LC-MS/MS system (AB Sciex). Protein identification was performed using Protein Pilot Version 3.0 software (AB Sciex) with default parameters.

Western blotting & Antibodies

The amount of total protein concentration in cleared lysate was determined by Bio-Rad protein assay. Equal protein extracts from various samples were separated by electrophoresis on SDS-PAGE gel, or NativePAGE gel (Life Technologies), and then transferred to a nitrocellulose membrane (GE Healthcare). The membrane was blocked in Tris-buffered saline containing 0.05% Tween20 and 5% bovine serum albumin, then probed with primary antibodies followed by secondary antibodies (Horseradish peroxidase (HRP)-conjugated). The blot was incubated in Pierce ECL Western Blotting Substrate solution (Thermo Scientific). Protein bands from peroxidase activities to chemiluminescent substrates were developed and detected on films.

Antibodies were purchased from the following companies: anti-CAD from Bethyl Laboratories, anti-Halo antibodies from Promega, anti-LAMP2 antibody from Abcam, anti-FLAG from Sigma, anti-Rheb from Cell Signaling, anti-Myc from, anti-TSC2 from Cell Signaling, and anti-mTOR from Cell Signaling, anti-FLAG from Sigma, anti-RHEB, -RAS, -Actin, -totalS6, -phosphoS6, -totalERK, -phosphoERK, -BRAF, and -CRAF all from Cell Signaling Technology.

Size Exclusion Chromatography

I used a 5mL column packed with Sephacryl S-300 high resolution resin (GE). Prior to loading samples, I washed the column with 20 mL of Elution Buffer (10mM HEPES pH 7.4, 150mM NaCl, 0.4% CHAPS). I loaded protein samples (prepared as in *Flag Immunoprecipitation* section) onto the size exclusion column and let gravity run the samples through the column. I collected 36 fractions, 250uL volume for each fraction (total of 9mL), and subjected them to SDS-PAGE followed by silver stain or western blot.

CPSase activity assay

Endogenous CAD was immunoprecipitated from HEK293T cells using anti-CAD antibody by the immunoprecipitation method described above. Rabbit IgG was used as a control. The products were mixed in the buffer containing 100 mM Tris-HCl (pH 8.0), 100 mMKCl, 3.2.2 mM glutamine, 17.5 mM aspartate, 3 mM ATP, 1 mM DTT, 7.5% dimethyl sulfoxide, 10% glycerol, and 5 mM MgCl2. The reaction was initiated by the addition of 1 mM 14C-labeled sodium bicarbonate (40–60 mCi/mmol, PerkinElmer Life Sciences) to a final concentration of 5 mM. The reaction was quenched after 60 min of incubation at 37 °C by the addition of trichloroacetic acid (TCA) to a final concentration of 20%. The samples were heated for 1 h at 95 °C, and then powdered dry ice was added to the tubes to eliminate excess CO2. Carbon 14-labeled metabolites were counted by a liquid scintillation counter.

Metabolic Profile Analysis

I followed a standard protocol used by the UCLA Metabolomics Core Facility they have previously published [43], [44]. To summarize, cells were cultured for 24 hr and rinsed with ice-cold 150 mM NH_4AcO (pH 7.3), followed by addition of 400 µl cold methanol and 400 µl cold water. Cells were scraped off and transferred to an Eppendorf tube, and 10 nmol norvaline as well as 400 µl chloroform were added to each sample. For the metabolite extraction, samples were vortexed for 5 min on ice and spun down, and the aqueous layer was transferred into a glass vial and dried. Metabolites were resuspended in 70% ACN, and a 5-µl sample was loaded onto a Phenomenex Luna 3u NH2 100A (150 × 2.0 mm) column. The chromatographic separation was performed on an UltiMate 3000RSLC (Thermo Scientific) with mobile phases A (5 mM NH_4AcO [pH 9.9]) and B (ACN) and a flow rate of 300 µl/ min. The gradient ran from 15% A to 95% A over 18 min, 9 min isocratic at 95% A, and re-equilibration for 7 min. Metabolite detection was achieved with a Thermo Scientific Q Exactive mass spectrometer run in polarity switching mode (+3.0 kV / −2.25 kV). TraceFinder 3.1 (Thermo Scientific) was used to quantify metabolites as the area under the curve using retention time and accurate mass measurements (≤3 ppm). Relative amounts of

metabolites were calculated by summing up all isotopomers of a given metabolite and normalized to the internal standard and cell number.

Immunofluorescent microscopy

Cells plated on 15-mm coverslips were immunostained with 5 μM HaloTag TMR Ligand (Promega) for 30 min according to the manufacturer's instructions. Cells were then fixed in PBS containing 1% formaldehyde for 15 min. For lysosome-associated membrane protein 2 (LAMP2) staining, cells were permeabilized in PBS containing 0.1% Triton X-100 for 15 min, incubated with anti-LAMP2 antibody overnight, and stained with fluorescently conjugated secondary antibodies for 1 h. The cells were mounted in Vectashield mounting medium (Vector Laboratories). Fluorescence images were obtained using an Olympus IX71 microscope equipped with a Hamamatsu ORCA-Flash 4.0 CCD monochrome camera (Hamamatsu Photonics).

Generation of Lentivirus and Reagents

Stably expressing cell lines were generated using lentiviral transduction method. The *Rheb* and *KRAS G12V* genes were amplified from pcDNA.3 plasmid vectors already containing *Flag-Rheb* or *Flag-KrasG12V* using PCR kit, and using primers containing EcoRI and BamHI restriction enzyme cut sites. My amplified products were ligated into the lentiviral transfer plasmid pCCL-c-MCS, after it was digested with EcoRI and BamHI, using ligase. The Rheb Y35N mutation was generated using Quickchange Lighting Site-Directed Mutagenesis Kit (Agilent).

Lentivirus was produced by transfecting the lentiviral transfer plasmid, the packaging plasmid (pCMV-R8.9) and the envelope plasmid (pMDG-VSVG) into HEK 293T cells using Lipofectamine 2000 (ThermoFisher). The media was collected 48 hours later and filtered through a 0.45 um filter. Lentiviral media was stored at -80ºC until ready for use.

Cell culture and Generation of Stably Expressing Cell Lines

NIH 3T3 cells were maintained in Dulbecco's modified Eagle's medium (DMEM) supplemented with 10% (vol/vol) fetal bovine serum and 1% (vol/vol) penicillin/ streptomycin. Cells were cultured at 37ºC in a 5% CO_2 incubator. NIH 3T3 cells were grown until 90% confluency before adding a mixture of 50% normal media, 50% lentiviral media, and 8ug/mL polybrene. Cells were incubated for 48 hours before being passaged and grown in normal media. Expression of transduced proteins were monitored via Western blot using anti-FLAG antibodies.

Growth Curve Assay

Cells were grown under normal conditions (DMEM containing 10% FBS) or serum starved (DMEM without FBS) and measured at given timepoints using the Cell Counting Kit-8 (Dojindo Molecular Technologies, Inc.) according to manufacturer's instructions. Briefly, cells were grown in 96 well plates, 10ul of CCK-8 dye was added to each well containing 100ul of cell media, cells were incubated for 1 hour, and then readings were obtained in triplicates using a Spectramax Plus 384 spectrophotometer (Molecular Devices) at O.D. 450nm.

Cell Cycle Analysis

NIH 3T3 cell lines were trypsinized, washed, and suspended in PBS. Cells were fixed for 1 hour at 4ºC in 70% ethanol. After fixation, cells were washed of ethanol and suspended in 500ul of PBS. 20ul of RNAase A (10mg/mL stock) and 25ul of propidium iodide (1mg/mL stock) solutions were added and the cells were incubated at 37ºC for 30min. Cells were analyzed by flow cytometry at the UCLA Flow Cytometry Core [Flow cytometry was performed in the UCLA Jonsson Comprehensive Cancer Center (JCCC) and Center for AIDS Research Flow Cytometry Core Facility that is supported by National Institutes of Health awards P30 CA016042 and 5P30 AI028697, and by the JCCC, the UCLA AIDS Institute, and the David Geffen School of Medicine at UCLA].

Foci Formation

NIH 3T3 cell lines were grown under normal growth conditions for 3 weeks, fresh media was added every 2-3 days. Cells were visualized with crystal violet staining method. Briefly, cells were fixed with ice-cold methanol for 10min on ice. Methanol was removed and the cells were incubated in 0.5% crystal violet solution (0.5g crystal violet in 100ml of 25% methanol solution) for 5min at room temperature. Cells were rinsed with H_2O until no more color came off in the rinse. For quantification, only those foci that were > than 2.5mm in diameter were counted.

Soft Agar Colony Formation Assay

To generate a semi-solid media growth surface for my cells, first I made 1% and 0.6% (mass/vol) agar-media solutions. I generated a 0.5% base-layer-matrix by heating up the 1% agar solution until dissolved, and mixing with normal growth media in a 50:50 ratio. I layered the solution onto a cell culture plate and let solidify in the cell incubator for 1 hour. I heated up the 0.6% agar solution until dissolved, and placed in 37 ºC H_2O bath to bring down to cell temperature. I trypsinized and suspended NIH 3T3 cell lines in normal media and 0.6% agar solution in a 50:50 ratio (now a 0.3% agar-media-cell solution). I layered this on top of the 0.5% solidified base-layer-matrix. Cells were grown in incubator as normal for 3-4 weeks, with small amount of normal media added 1x/week to prevent the gels from drying out. Cells were incubated with Nitro Blue Tetrazolium dye 1mg/ml stock (tablets purchased from Sigma) overnight at 37 ºC. Colonies were visualized using BioRad Imager and counted by eye.

Immunoprecipitation

HEK293T cells expressing FLAG tagged Rheb -WT, or -Y35N were immunoprecipitated using anti-FLAG M2 affinity gel (Sigma). Briefly, the cells were lysed with lysis buffer (50mM HEPES pH 7.4, 150mM NaCl, 0.4% CHAPS, 1X Complete EDTA-free protease inhibitor cocktail (Roche), 1mM Na3VO4), 150 mM NaCl, 25 mM MgCl2), and the supernatant was cleared of

cellular debris using centrifugation (16,000 × g for 10 min). Cleared supernatant was mixed with anti-FLAG M2 magnetic beads (Sigma) for affinity purification. The beads were collected, washed four times with lysis buffer. The remaining bound proteins were eluted three times with lysis buffer containing 62ug/mL of 3X FLAG peptide. Eluted proteins were concentrated using Amicon Ultra 0.5-ml centrifugal filters NMWL 10K (EMD Millipore, Billerica, MA).

REFERENCES

[1] K. Yamagata, L. K. Sanders, W. E. Kaufmannn, W. Yee, C. A. Barnes, D. Nathans, and W. F. Paul, “Rheb, a Growth Factor- and Synaptic Activity-Regulated Gene, Encodes a Novel Ras-related Protein,” *J. Biol. Chem.*, vol. 269, no. 23, pp. 16333–16339, Jun. 1994.

[2] J. J. Heard, V. Fong, S. Z. Bathaie, and F. Tamanoi, “Recent progress in the study of the Rheb family GTPases.,” *Cell. Signal.*, vol. 26, no. 9, pp. 1950–1957, May 2014.

[3] K. Saito, Y. Araki, K. Kontani, H. Nishina, and T. Katada, “Novel role of the small GTPase Rheb: its implication in endocytic pathway independent of the activation of mammalian target of rapamycin.,” *J. Biochem.*, vol. 137, no. 3, pp. 423–30, Mar. 2005.

[4] Y. Li, K. Inoki, and K.-L. Guan, “Biochemical and functional characterizations of small GTPase Rheb and TSC2 GAP activity.,” *Mol. Cell. Biol.*, vol. 24, no. 18, pp. 7965–75, Sep. 2004.

[5] Y. Yu, S. Li, X. Xu, Y. Li, K. Guan, E. Arnold, and J. Ding, “Structural basis for the unique biological function of small GTPase RHEB.,” *J. Biol. Chem.*, vol. 280, no. 17, pp. 17093–100, Apr. 2005.

[6] M. T. Mazhab-Jafari, C. B. Marshall, N. Ishiyama, J. Ho, V. Di Palma, V. Stambolic, and M. Ikura, “An autoinhibited noncanonical mechanism of GTP hydrolysis by Rheb maintains mTORC1 homeostasis.,” *Structure*, vol. 20, no. 9, pp. 1528–39, Sep. 2012.

[7] P. H. Patel, N. Thapar, L. Guo, M. Martinez, J. Maris, C.-L. Gau, J. a Lengyel, and F. Tamanoi, “Drosophila Rheb GTPase is required for cell cycle progression and cell growth.,” *J. Cell Sci.*, vol. 116, no. 17, pp. 3601–10, Sep. 2003.

[8] L. J. Saucedo, X. Gao, D. A. Chiarelli, L. Li, D. Pan, and B. A. Edgar, “Rheb promotes cell growth as a component of the insulin/TOR signalling network,” *Nat. Cell Biol.*, vol. 5, no. 6, pp. 566–571, Jun. 2003.

[9] D. C. Fingar and J. Blenis, “Target of rapamycin (TOR): an integrator of nutrient and growth factor signals and coordinator of cell growth and cell cycle progression.,” *Oncogene*, vol. 23, no. 18, pp. 3151–71, Apr. 2004.

[10] A. F. Castro, J. F. Rebhun, G. J. Clark, and L. A. Quilliam, “Rheb binds tuberous sclerosis complex 2 (TSC2) and promotes S6 kinase activation in a rapamycin- and farnesylation-dependent manner.,” *J. Biol. Chem.*, vol. 278, no. 35, pp. 32493–6, Aug. 2003.

[11] K. Inoki, Y. Li, T. Xu, and K.-L. Guan, “Rheb GTPase is a direct target of TSC2 GAP activity and regulates mTOR signaling.,” *Genes Dev.*, vol. 17, no. 15, pp. 1829–34, Aug. 2003.

[12] The European Chromosome 16 Tuberous Sclerosis Consortium, “Identification and characterization of the tuberous sclerosis gene on chromosome 16,” *Cell*, vol. 75, no. 7, pp. 1305–1315, Dec. 1993.

[13] A. D. Beggs, A. R. Latchford, H. F. A. Vasen, G. Moslein, A. Alonso, and S. Aretz, “PeutzeJeghers syndrome: a systematic review and recommendations for management.”

[14] K. Inoki and K.-L. Guan, “Tuberous sclerosis complex, implication from a rare genetic disease to common cancer treatment,” *Hum. Mol. Genet.*, vol. 18, no. 1, pp. 94–100, Apr. 2009.

[15] E. P. Henske, F. X. McCormack, F. McCormack, B. Kinder, K. Seyama, M. Nishimura, and D. Kwiatkowski, “Lymphangioleiomyomatosis - a wolf in sheep’s clothing.,” *J. Clin. Invest.*, vol. 122, no. 11, pp. 3807–16, Nov. 2012.

[16] J. J. Bissler, J. C. Kingswood, E. Radzikowska, B. A. Zonnenberg, M. Frost, E. Belousova, M. Sauter, N. Nonomura, S. Brakemeier, P. J. de Vries, V. H. Whittemore, D. Chen, T. Sahmoud, G. Shah, J. Lincy, D. Lebwohl, and K. Budde, “Everolimus for angiomyolipoma associated with tuberous sclerosis complex or sporadic lymphangioleiomyomatosis (EXIST-2): a multicentre, randomised, double-blind, placebo-controlled trial,” *Lancet*, vol. 381, no. 9869, pp. 817–824, Mar. 2013.

[17] F. X. McCormack, Y. Inoue, J. Moss, L. G. Singer, C. Strange, K. Nakata, A. F. Barker, J. T. Chapman, M. L. Brantly, J. M. Stocks, K. K. Brown, J. P. Lynch, H. J. Goldberg, L. R. Young, B. W. Kinder, G. P. Downey, E. J. Sullivan, T. V. Colby, R. T. McKay, M. M. Cohen, L. Korbee, A. M. Taveira-DaSilva, H.-S. Lee, J. P. Krischer, B. C. Trapnell, National Institutes of Health Rare Lung Diseases Consortium, and MILES Trial Group, “Efficacy and Safety of Sirolimus in Lymphangioleiomyomatosis,” *N. Engl. J. Med.*, vol. 364, no. 17, pp. 1595–1606, Apr. 2011.

[18] Z. H. Lu, M. B. Shvartsman, A. Y. Lee, J. M. Shao, M. M. Murray, R. D. Kladney, D. Fan, S. Krajewski, G. G. Chiang, G. B. Mills, and J. M. Arbeit, “Mammalian target of rapamycin activator RHEB is frequently overexpressed in human carcinomas and is critical and sufficient for skin epithelial carcinogenesis.,” *Cancer Res.*, vol. 70, no. 8, pp. 3287–98, Apr. 2010.

[19] M. S. Lawrence, P. Stojanov, C. H. Mermel, J. T. Robinson, L. a Garraway, T. R. Golub, M. Meyerson, S. B. Gabriel, E. S. Lander, and G. Getz, “Discovery and saturation analysis of cancer genes across 21 tumour types.,” *Nature*, vol. 505, no. 7484, pp. 495–501, Jan. 2014.

[20] M. T. Mazhab-Jafari, C. B. Marshall, J. Ho, N. Ishiyama, V. Stambolic, and M. Ikura, “Structure-guided mutation of the conserved G3-box glycine in Rheb generates a constitutively activated regulator of mTOR.,” *J. Biol. Chem.*, vol. 289, no. 18, pp. 12195–12201, May 2014.

[21] B. C. Grabiner, V. Nardi, K. Birsoy, R. Possemato, K. Shen, S. Sinha, A. Jordan, A. H. Beck, and D. M. Sabatini, “A diverse array of cancer-associated mTOR mutations are hyperactivating and can predict rapamycin sensitivity.,” *Cancer Discov.*, vol. 4, no. 5, pp. 554–563, May 2014.

[22] J. Urano, M. J. Comiso, L. Guo, P.-J. Aspuria, R. Deniskin, A. P. Tabancay, J. Kato-Stankiewicz, and F. Tamanoi, “Identification of novel single amino acid changes that result in hyperactivation of the unique GTPase, Rheb, in fission yeast.,” *Mol. Microbiol.*, vol. 58, no. 4, pp. 1074–86, Nov. 2005.

[23] T. Sato, A. Nakashima, L. Guo, and F. Tamanoi, “Specific activation of mTORC1 by Rheb

G-protein in vitro involves enhanced recruitment of its substrate protein.," *J. Biol. Chem.*, vol. 284, no. 19, pp. 12783–91, May 2009.

[24] A. P. Tabancay, C.-L. Gau, I. M. P. Machado, E. J. Uhlmann, D. H. Gutmann, L. Guo, and F. Tamanoi, "Identification of dominant negative mutants of Rheb GTPase and their use to implicate the involvement of human Rheb in the activation of p70S6K.," *J. Biol. Chem.*, vol. 278, no. 41, pp. 39921–30, Oct. 2003.

[25] L. Yan, G. M. Findlay, R. Jones, J. Procter, Y. Cao, and R. F. Lamb, "Hyperactivation of mammalian target of rapamycin (mTOR) signaling by a gain-of-function mutant of the Rheb GTPase.," *J. Biol. Chem.*, vol. 281, no. 29, pp. 19793–7, Jul. 2006.

[26] X. Long, Y. Lin, S. Ortiz-Vega, K. Yonezawa, and J. Avruch, "Rheb binds and regulates the mTOR kinase.," *Curr. Biol.*, vol. 15, no. 8, pp. 702–13, Apr. 2005.

[27] X. Long, Y. Lin, S. Ortiz-Vega, S. Busch, and J. Avruch, "The Rheb switch 2 segment is critical for signaling to target of rapamycin complex 1.," *J. Biol. Chem.*, vol. 282, no. 25, pp. 18542–51, Jun. 2007.

[28] A. Hanker, N. Mitin, R. S. Wilder, E. P. Henske, F. Tamanoi, a D. Cox, and C. J. Der, "Differential requirement of CAAX-mediated posttranslational processing for Rheb localization and signaling.," *Oncogene*, vol. 29, no. 3, pp. 380–91, Jan. 2010.

[29] K. Takahashi, M. Nakagawa, S. G. Young, and S. Yamanaka, "Differential membrane localization of ERas and Rheb, two Ras-related proteins involved in the phosphatidylinositol 3-kinase/mTOR pathway.," *J. Biol. Chem.*, vol. 280, no. 38, pp. 32768–74, Sep. 2005.

[30] J. F. Hancock, H. Paterson, and C. J. Marshall, "A polybasic domain or palmitoylation is required in addition to the CAAX motif to localize p21ras to the plasma membrane.," *Cell*, vol. 63, no. 1, pp. 133–9, Oct. 1990.

[31] Y. Sancak, L. Bar-Peled, R. Zoncu, A. L. Markhard, S. Nada, and D. M. Sabatini, "Ragulator-Rag complex targets mTORC1 to the lysosomal surface and is necessary for its activation by amino acids.," *Cell*, vol. 141, no. 2, pp. 290–303, Apr. 2010.

[32] S. Menon, C. C. Dibble, G. Talbott, G. Hoxhaj, A. J. Valvezan, H. Takahashi, L. C. Cantley, and B. D. Manning, "Spatial Control of the TSC Complex Integrates Insulin and Nutrient Regulation of mTORC1 at the Lysosome," *Cell*, vol. 156, no. 4, pp. 771–785, Feb. 2014.

[33] C. Demetriades, N. Doumpas, and A. A. Teleman, "Regulation of TORC1 in Response to Amino Acid Starvation via Lysosomal Recruitment of TSC2," *Cell*, vol. 156, no. 4, pp. 786–799, Feb. 2014.

[34] M. Patel and J.-F. Côté, "Ras GTPases' interaction with effector domains: Breaking the families' barrier.," *Commun. Integr. Biol.*, vol. 6, no. 4, pp. e24298-1–9, Jul. 2013.

[35] I. R. Vetter and A. Wittinghofer, "The Guanine Nucleotide-Binding Switch in Three Dimensions," *Science.*, vol. 294, no. 5545, pp. 1299–1304, Nov. 2001.

[36] K. Wennerberg, K. L. Rossman, and C. J. Der, “The Ras superfamily at a glance.,” *J. Cell Sci.*, vol. 118, no. Pt 5, pp. 843–6, Mar. 2005.

[37] M. Laplante and D. M. Sabatini, “mTOR signaling in growth control and disease.,” *Cell*, vol. 149, no. 2, pp. 274–93, Apr. 2012.

[38] X. Long, Y. Lin, S. Ortiz-Vega, K. Yonezawa, and J. Avruch, “Rheb binds and regulates the mTOR kinase.,” *Curr. Biol.*, vol. 15, no. 8, pp. 702–13, Apr. 2005.

[39] A. M. Robitaille, S. Christen, M. Shimobayashi, M. Cornu, L. L. Fava, S. Moes, C. Prescianotto-Baschong, U. Sauer, P. Jenoe, and M. N. Hall, “Quantitative phosphoproteomics reveal mTORC1 activates de novo pyrimidine synthesis.,” *Science*, vol. 339, no. 6125, pp. 1320–3, Mar. 2013.

[40] I. Ben-Sahra, J. J. Howell, J. M. Asara, and B. D. Manning, “Stimulation of de novo pyrimidine synthesis by growth signaling through mTOR and S6K1.,” *Science*, vol. 339, no. 6125, pp. 1323–8, Mar. 2013.

[41] H. Iwahana, M. Fujimura, S. Ii, M. Kondo, M. Moritani, Y. Takahashi, T. Yamaoka, K. Yoshimoto, and M. Itakura, “Molecular cloning of a human cDNA encoding a trifunctional enzyme of carbamoyl-phosphate synthetase-aspartate transcarbamoylase-dihydroorotase in de Novo pyrimidine synthesis.,” *Biochem. Biophys. Res. Commun.*, vol. 219, no. 1, pp. 249–55, Feb. 1996.

[42] P. F. Coleman, D. P. Suttle, and G. R. Stark, “Purification from hamster cells of the multifunctional protein that initiates de novo synthesis of pyrimidine nucleotides.,” *J. Biol. Chem.*, vol. 252, no. 18, pp. 6379–85, Sep. 1977.

[43] F. D. Sigoillot, D. H. Kotsis, E. M. Masko, M. Bame, D. R. Evans, and H. I. G. Evans, “Protein kinase C modulates the up-regulation of the pyrimidine biosynthetic complex, CAD, by MAP kinase.,” *Front. Biosci.*, vol. 12, pp. 3892–8, May 2007.

[44] F. D. Sigoillot, D. R. Evans, and H. I. Guy, “Growth-dependent regulation of mammalian pyrimidine biosynthesis by the protein kinase A and MAPK signaling cascades.,” *J. Biol. Chem.*, vol. 277, no. 18, pp. 15745–51, May 2002.

[45] M. E. Jones, “Pyrimidine Nucleotide Biosynthesis in Animals: Genes, Enzymes, and Regulation of UMP Biosynthesis,” *Annu. Rev. Biochem.*, vol. 49, no. 1, pp. 253–279, Jun. 1980.

[46] H. Schägger and G. von Jagow, “Blue native electrophoresis for isolation of membrane protein complexes in enzymatically active form.,” *Anal. Biochem.*, vol. 199, no. 2, pp. 223–31, Dec. 1991.

[47] X. Liu, H. I. Guy, and D. R. Evans, “Identification of the regulatory domain of the mammalian multifunctional protein CAD by the construction of an Escherichia coli hamster hybrid carbamyl-phosphate synthetase,” *J. Biol. Chem.*, vol. 269, no. 44, pp. 27747–27755, Nov. 1994.

[48] T. Sato, H. Akasu, W. Shimono, C. Matsu, Y. Fujiwara, Y. Shibagaki, J. J. Heard, F. Tamanoi, and S. Hattori, “Rheb protein binds CAD (carbamoyl-phosphate synthetase 2,

aspartate transcarbamoylase, and dihydroorotase) protein in a GTP- and effector domain-dependent manner and influences its cellular localization and carbamoyl-phosphate synthetase (CPSase) activity," *J. Biol. Chem.*, vol. 290, no. 2, pp. 1096–105, Jan. 2015.

[49] D. G. Hardie, F. A. Ross, and S. A. Hawley, "AMPK: a nutrient and energy sensor that maintains energy homeostasis," *Nat. Rev. Mol. Cell Biol.*, vol. 13, no. 4, pp. 251–262, Mar. 2012.

[50] J. S. Oakhill, Z.-P. Chen, J. W. Scott, R. Steel, L. A. Castelli, N. Ling, S. L. Macaulay, and B. E. Kemp, "Beta-Subunit myristoylation is the gatekeeper for initiating metabolic stress sensing by AMP-activated protein kinase (AMPK)," *Proc. Natl. Acad. Sci.*, vol. 107, no. 45, pp. 19237–19241, Nov. 2010.

[51] G. Zhou, R. Myers, Y. Li, Y. Chen, X. Shen, J. Fenyk-Melody, M. Wu, J. Ventre, T. Doebber, N. Fujii, N. Musi, M. F. Hirshman, L. J. Goodyear, and D. E. Moller, "Role of AMP-activated protein kinase in mechanism of metformin action.," *J. Clin. Invest.*, vol. 108, no. 8, pp. 1167–74, Oct. 2001.

[52] D. G. Hardie, "Neither LKB1 Nor AMPK Are the Direct Targets of Metformin," *Gastroenterology*, vol. 131, no. 3, p. 973, Sep. 2006.

[53] R. J. Shaw, M. Kosmatka, N. Bardeesy, R. L. Hurley, L. A. Witters, R. A. DePinho, and L. C. Cantley, "The tumor suppressor LKB1 kinase directly activates AMP-activated kinase and regulates apoptosis in response to energy stress.," *Proc. Natl. Acad. Sci. U. S. A.*, vol. 101, no. 10, pp. 3329–35, Mar. 2004.

[54] C.-A. Wu, Y. Chao, S.-G. Shiah, and W.-W. Lin, "Nutrient deprivation induces the Warburg effect through ROS/AMPK-dependent activation of pyruvate dehydrogenase kinase," *Biochim. Biophys. Acta - Mol. Cell Res.*, vol. 1833, no. 5, pp. 1147–1156, May 2013.

[55] D. B. Shackelford and R. J. Shaw, "The LKB1-AMPK pathway: metabolism and growth control in tumour suppression.," *Nat. Rev. Cancer*, vol. 9, no. 8, pp. 563–75, Aug. 2009.

[56] E. Cerami, J. Gao, U. Dogrusoz, B. E. Gross, S. O. Sumer, B. A. Aksoy, A. Jacobsen, C. J. Byrne, M. L. Heuer, E. Larsson, Y. Antipin, B. Reva, A. P. Goldberg, C. Sander, and N. Schultz, "The cBio cancer genomics portal: an open platform for exploring multidimensional cancer genomics data.," *Cancer Discov.*, vol. 2, no. 5, pp. 401–4, May 2012.

[57] J. Gao, B. A. Aksoy, U. Dogrusoz, G. Dresdner, B. Gross, S. O. Sumer, Y. Sun, A. Jacobsen, R. Sinha, E. Larsson, E. Cerami, C. Sander, and N. Schultz, "Integrative analysis of complex cancer genomics and clinical profiles using the cBioPortal.," *Sci. Signal.*, vol. 6, no. 269, pp. 1–19, Apr. 2013.

[58] R. A. Weinberg, "Use of Transfection to Analyze Genetic Information and Malignant Transformation," *Biochim. Biophys. Acta*, vol. 651, pp. 25–35, Feb. 1981.

[59] G. J. Clark, A. D. Cox, S. M. Graham, and C. J. Der, "Biological assays for Ras transformation.," *Methods Enzymol.*, vol. 255, pp. 395–412, 1995.

[60] M. A. White, C. Nicolette, A. Minden, A. Polverino, L. Van Aelst, M. Karin, and M. H. Wigler, “Multiple Ras Functions Can Contribute to Mammalian Cell Transformation,” *Cell*, vol. 80, pp. 533–541, Feb. 1995.

[61] M. Abercrombie, “Contact inhibition in tissue culture,” *In Vitro*, vol. 6, no. 2, pp. 128–142, Sep. 1970.

[62] U. Cavallaro, B. Schaffhauser, and G. Christofori, “Cadherins and the tumour progression: is it all in a switch?,” *Cancer Lett.*, vol. 176, no. 2, pp. 123–128, Feb. 2002.

[63] E. J. Stanbridge and J. Wilkinson, “Analysis of malignancy in human cells: malignant and transformed phenotypes are under separate genetic control.,” *Proc. Natl. Acad. Sci. U. S. A.*, vol. 75, no. 3, pp. 1466–9, Mar. 1978.

[64] M. C. Guadamillas, A. Cerezo, and M. A. del Pozo, “Overcoming anoikis – pathways to anchorage-independent growth in cancer,” *J. Cell Sci.*, vol. 124, no. 19, pp. 3189–97, Oct. 2011.

[65] W. M. Yee and P. F. Worley, “Rheb interacts with Raf-1 kinase and may function to integrate growth factor- and protein kinase A-dependent signals.,” *Mol. Cell. Biol.*, vol. 17, no. 2, pp. 921–33, Feb. 1997.

[66] J. C. Clark, M. S. Kinch, K. Rogers-Graham, S. M. Sebti, A. D. Hamilton, and C. J. Der, “The Ras-related Protein Rheb Is Farnesylated and Antagonizes Ras Signaling and Transformation,” *J. Biol. Chem.*, vol. 272, no. 16, pp. 10608–10615, Apr. 1997.

[67] M. Karbowniczek, G. P. Robertson, and E. P. Henske, “Rheb inhibits C-raf activity and B-raf/C-raf heterodimerization.,” *J. Biol. Chem.*, vol. 281, no. 35, pp. 25447–56, Sep. 2006.

[68] M. Karbowniczek, T. Cash, M. Cheung, G. P. Robertson, A. Astrinidis, and E. P. Henske, “Regulation of B-Raf kinase activity by tuberin and Rheb is mammalian target of rapamycin (mTOR)-independent.,” *J. Biol. Chem.*, vol. 279, no. 29, pp. 29930–7, Jul. 2004.

[69] E. Im, F. C. von Lintig, J. Chen, S. Zhuang, W. Qui, S. Chowdhury, P. F. Worley, G. R. Boss, and R. B. Pilz, “Rheb is in a high activation state and inhibits B-Raf kinase in mammalian cells.,” *Oncogene*, vol. 21, no. 41, pp. 6356–6365, Sep. 2002.

[70] Y. Wang, X. Hong, J. Wang, Y. Yin, Y. Zhang, Y. Zhou, H. Piao, Z. Liang, L. Zhang, G. Li, G. Xu, D. J. Kwiatkowski, and Y. Liu, “Inhibition of MAPK pathway is essential for suppressing Rheb-Y35N driven tumor growth,” *Oncogene*, vol. 36, no. 6, pp. 756–765, Feb. 2017.

[71] C.-H. Shen, P. Yuan, R. Perez-Lorenzo, Y. Zhang, S. X. Lee, Y. Ou, J. M. Asara, L. C. Cantley, and B. Zheng, “Phosphorylation of BRAF by AMPK Impairs BRAF-KSR1 Association and Cell Proliferation,” *Mol. Cell*, vol. 52, no. 2, pp. 161–172, Oct. 2013.

[72] M. D. Lacher, R. Pincheira, Z. Zhu, B. Camoretti-Mercado, M. Matli, R. S. Warren, and a F. Castro, “Rheb activates AMPK and reduces p27Kip1 levels in Tsc2-null cells via mTORC1-independent mechanisms: implications for cell proliferation and

tumorigenesis.," *Oncogene*, vol. 29, no. 50, pp. 6543–56, Dec. 2010.

[73] A. K. Freeman, D. A. Ritt, and D. K. Morrison, "The importance of Raf dimerization in cell signaling.," *Small GTPases*, vol. 4, no. 3, pp. 180–5, 2013.

[74] C. K. Weber, J. R. Slupsky, H. A. Kalmes, and U. R. Rapp, "Active Ras induces heterodimerization of cRaf and BRaf.," *Cancer Res.*, vol. 61, no. 9, pp. 3595–8, May 2001.

[75] X. Nan, T. M. Tamgüney, E. A. Collisson, L.-J. Lin, C. Pitt, J. Galeas, S. Lewis, J. W. Gray, F. McCormick, and S. Chu, "Ras-GTP dimers activate the Mitogen-Activated Protein Kinase (MAPK) pathway," *Proc. Natl. Acad. Sci.*, vol. 112, no. 26, pp. 7996–8001, Jun. 2015.

[76] K. Inouye, S. Mizutani, H. Koide, and Y. Kaziro, "Formation of the Ras dimer is essential for Raf-1 activation.," *J. Biol. Chem.*, vol. 275, no. 6, pp. 3737–40, Feb. 2000.

[77] L. Lee, R. E. Kelly, S. C. Pastra-Landis, and D. R. Evans, "Oligomeric structure of the multifunctional protein CAD that initiates pyrimidine biosynthesis in mammalian cells.," *Proc. Natl. Acad. Sci. U. S. A.*, vol. 82, no. 20, pp. 6802–6, Oct. 1985.

[78] R. Zoncu, L. Bar-Peled, A. Efeyan, S. Wang, Y. Sancak, and D. M. Sabatini, "mTORC1 Senses Lysosomal Amino Acids Through an Inside-Out Mechanism That Requires the Vacuolar H+-ATPase," *Science.*, vol. 334, no. 6056, pp. 678–683, Nov. 2011.

[79] M. G. Vander Heiden, "Targeting cancer metabolism: a therapeutic window opens," *Nat. Rev. Drug Discov.*, vol. 10, no. 9, pp. 671–684, Aug. 2011.

[80] D. M. Gwinn, D. B. Shackelford, D. F. Egan, M. M. Mihaylova, A. Mery, D. S. Vasquez, B. E. Turk, and R. J. Shaw, "AMPK phosphorylation of raptor mediates a metabolic checkpoint.," *Mol. Cell*, vol. 30, no. 2, pp. 214–26, Apr. 2008.

[81] K. Inoki, T. Zhu, and K.-L. Guan, "TSC2 mediates cellular energy response to control cell growth and survival.," *Cell*, vol. 115, no. 5, pp. 577–90, Nov. 2003.

[82] D. J. Kwiatkowski, H. Zhang, J. L. Bandura, K. M. Heiberger, M. Glogauer, N. el-Hashemite, and H. Onda, "A mouse model of TSC1 reveals sex-dependent lethality from liver hemangiomas, and up-regulation of p70S6 kinase activity in Tsc1 null cells.," *Hum. Mol. Genet.*, vol. 11, no. 5, pp. 525–34, Mar. 2002.

[83] H. Zhang, G. Cicchetti, H. Onda, H. B. Koon, K. Asrican, N. Bajraszewski, F. Vazquez, C. L. Carpenter, and D. J. Kwiatkowski, "Loss of Tsc1/Tsc2 activates mTOR and disrupts PI3K-Akt signaling through downregulation of PDGFR," *J. Clin. Invest.*, vol. 112, no. 8, pp. 1223–1233, Oct. 2003.

[84] W. M. Stadler, "Targeted agents for the treatment of advanced renal cell carcinoma," *Cancer*, vol. 104, no. 11, pp. 2323–2333, Dec. 2005.

[85] J. A. Gollob, "Sorafenib: Scientific Rationales for Single-Agent and Combination Therapy in Clear-Cell Renal Cell Carcinoma," *Clin. Genitourin. Cancer*, vol. 4, no. 3, pp. 167–174, Dec. 2005.

[86] C. Kollmannsberger, D. Soulieres, R. Wong, A. Scalera, R. Gaspo, and G. Bjarnason, “Sunitinib therapy for metastatic renal cell carcinoma: recommendations for management of side effects.,” *Can. Urol. Assoc. J.*, vol. 1, no. 2 Suppl, pp. S41-54, Jun. 2007.

[87] C. Battelli and D. C. Cho, “mTOR inhibitors in renal cell carcinoma.,” *Therapy*, vol. 8, no. 4, pp. 359–367, Jul. 2011.

[88] M. Suchanek, A. Radzikowska, and C. Thiele, “Photo-leucine and photo-methionine allow identification of protein-protein interactions in living cells,” *Nat. Methods*, vol. 2, no. 4, pp. 261–268, Apr. 2005.

[89] K. Sakamoto, A. Hayashi, A. Sakamoto, D. Kiga, H. Nakayama, A. Soma, T. Kobayashi, M. Kitabatake, K. Takio, K. Saito, M. Shirouzu, I. Hirao, and S. Yokoyama, “Site-specific incorporation of an unnatural amino acid into proteins in mammalian cells,” *Nucleic Acids Res.*, vol. 30, no. 21, pp. 4692–4699, Nov. 2002.

[90] K. J. Roux, D. I. Kim, and B. Burke, “BioID: A Screen for Protein-Protein Interactions,” *Curr. Protoc. Protein Sci*, vol. 74, no. Unit 19.23, pp. 1–19, Nov. 2013.

[91] E. Choi-Rhee, H. Schulman, and J. E. Cronan, “Promiscuous protein biotinylation by Escherichia coli biotin protein ligase,” *Protein Sci.*, vol. 13, no. 11, pp. 3043–3050, Dec. 2008.

[92] J. E. Cronan, “Targeted and proximity-dependent promiscuous protein biotinylation by a mutant Escherichia coli biotin protein ligase.,” *J. Nutr. Biochem.*, vol. 16, no. 7, pp. 416–8, Jul. 2005.

[93] K. J. Roux, D. I. Kim, M. Raida, and B. Burke, “A promiscuous biotin ligase fusion protein identifies proximal and interacting proteins in mammalian cells.,” *J. Cell Biol.*, vol. 196, no. 6, pp. 801–10, Mar. 2012.